

SATELLITE-BASED RADAR FOR FLOOD MONITORING IN BANGLADESH



Bangladesh Flood Action Plan
Ministry of Water Resources
Flood Plan Coordination Organization (FPCO)

Prepared by:
Geographic Information System
FAP 19

PA-ABW-809

BANGLADESH FLOOD ACTION PLAN

**SATELLITE-BASED RADAR FOR
FLOOD MONITORING IN BANGLADESH**

GEOGRAPHIC INFORMATION SYSTEM (FAP 19)

Prepared for

The Flood Plan Coordination Organization (FPCO)
of the
Ministry of Water Resources

June 1995

 **ISPAN**

IRRIGATION SUPPORT PROJECT FOR ASIA AND THE NEAR EAST

Sponsored by the U.S. Agency for International Development



IRRIGATION SUPPORT PROJECT FOR ASIA
AND THE NEAR EAST

ISPAN Technical Support Center
Suite 300
1611 North Kent Street
Arlington, Virginia 22209-2111
USA
Phone: (703) 247-8730
FAX: (703) 243-9004

TABLE OF CONTENTS

TABLE OF CONTENTS	i
LIST OF FIGURES	iii
LIST OF TABLES	iv
ACKNOWLEDGMENTS	v
LIST OF ACRONYMS	vi
SUMMARY	vii
CHAPTER 1 INTRODUCTION	1-1
1.1 Institutional Setting	1-1
1.2 Rationale	1-1
1.3 Goal and Objectives	1-3
1.4 Organization of the Document	1-3
CHAPTER 2 SYNTHETIC APERTURE RADAR (SAR)—BASIC CONCEPTS AND SATELLITE SYSTEMS	2-1
2.1 Radar Remote Sensing Concepts	2-1
2.2 Radar System Configuration	2-2
2.3 Target Parameters	2-3
2.4 Satellite SAR Systems	2-4
2.4.1 ERS-1 and ERS-2	2-4
2.4.2 JERS-1	2-5
2.4.3 Shuttle Imaging Radar, SIR-C	2-5
2.4.4 ALMAZ	2-6
2.4.5 RADARSAT	2-6
CHAPTER 3 REVIEW OF RADAR PROJECTS RELEVANT TO NATURAL RESOURCES IN BANGLADESH	3-1
3.1 Flooded Environments	3-1
3.2 Coastal and Marine Environments	3-2
3.3 General Land Use	3-4
CHAPTER 4 CONSIDERATIONS FOR RADAR PROJECT IMPLEMENTATION IN BANGLADESH	4-1
4.1 Project Design	4-1
4.2 Technology Transfer Issues	4-2
4.3 SAR Application Potential in Bangladesh	4-3
4.3.1 Monsoon Season Flood Mapping and Monitoring	4-5
4.3.2 Coastal Zone Monitoring	4-6

4.3.3	Land Use Monitoring	4-7
4.3.4	Earth Sciences	4-7
CHAPTER 5 APPLICATION STUDY USING RADAR IMAGERY FOR FLOOD MONITORING		
	MONITORING	5-1
5.1	Approach	5-1
5.1.1	Study and Test Areas	5-1
5.2	Data Sets	5-2
5.2.1	ERS-1 SAR Data	5-2
5.2.2	Other Satellite Remote Sensing Data	5-4
5.2.3	Topographic Map Information and Digital Elevation Model Data	5-4
5.2.4	MIKE 11 Flood Model	5-4
5.3	Ground Reference Data	5-4
5.3.1	Data Collection Strategies	5-5
5.3.2	Descriptive Parameters	5-5
5.4	SAR Image Processing and GIS Data Integration	5-5
5.4.1	Strategy and Tools	5-5
5.4.2	Geo-referencing and Resampling	5-6
5.4.3	Filtering, Scaling, Stretching	5-9
5.4.4	Image Classification	5-11
5.5	SAR Image Processing: Assessment of Results	5-12
5.5.1	Flood Maps	5-12
5.5.2	Assessment of SAR Classification Results	5-15
5.5.3	Ground Reference Data	5-21
5.6	Assessment and Use of the SAR Flood Map	5-23
5.6.1	Comparing SAR with Flood Model Results	5-23
5.6.2	Change Detection	5-24
5.6.3	Comparing Classification with Land-Type Map	5-24
5.6.4	Multi-temporal Display and Analysis	5-24
5.6.5	Merger of SAR Image with Landsat TM	5-25
CHAPTER 6 CONCLUSIONS AND RECOMMENDATIONS		
6.1	SAR Technology	6-1
6.2	Application for Flood Monitoring	6-1
6.3	Awareness and Institutional Needs	6-2
REFERENCES CITED		R-1
OTHER REFERENCES		R-7
APPENDIX A Ground Reference Information and Accuracy Assessment of Classification		
APPENDIX B Classification for Monsoon Season Radar Ground Reference Information		

LIST OF FIGURES

Figure 1.1	Coverage of ERS-1 SAR Image Frames Used in this Study	1-2
Figure 1.2	ERS-1 SAR Image Central Bangladesh, July 24, 1993	1-5
Figure 1.3	ERS-1 SAR Image of Central Bangladesh, August 28,1993	1-7
Figure 1.4	SAR Image Interpretation Keys (A-F) of Some Major Physiographic Features on the Central Bangladesh SAR Image	1-9
Figure 1.5	ERS-1 SAR Image of the Sylhet Region Acquired on May 28,1993	1-13
Figure 1.6	SAR Image Interpretation Keys (A-C) of Some Major Physiographic Features in Sylhet Area of Northeastern Bangladesh	1-15
Figure 1.7	Photographs Illustrating Typical Flood Conditions and Land Use in the Floodplains of Bangladesh	1-17
Figure 2.1	Radio Detection and Ranging (RADAR)	2-1
Figure 2.2	Synthetic Aperture Radar Imaging the Earth's Surface	2-2
Figure 2.3	Various Radar Reflection Types	2-4
Figure 2.4	RADARSAT SAR Operation Modes	2-7
Figure 5.1	ERS-1 SAR Subscene of the Tangail Test Area, July 24,1993	5-2
Figure 5.2	Schematic Profile of a Typical Landscape in Bangladesh	5-3
Figure 5.3	Flow Chart of SAR Image Processing Procedure	5-6
Figure 5.4	Series of SAR Images Showing the Effects of Resampling and Filtering, and a Landsat image of the Same Area	5-7
Figure 5.5	Histograms of SAR Data At Various Steps of Processing	5-10
Figure 5.6	Assessment of Radar Image Classification Using Topographic Maps	5-13
Figure 5.7	Results of ERS-1 SAR Classification for Central Bangladesh Scene of July 24, 1993	5-17
Figure 5.8	Results of ERS-1 SAR Classification for Central Bangladesh Scene of August 28, 1993	5-19
Figure 5.9	Radar Image Signatures Expected For Various Land, Water, and Vegetation Features	5-22
Figure 5.10	Comparison of Results from the Flood Management Model and SAR Image Classification for July 24, 1993	5-27
Figure 5.11	Comparison of Results from the Flood Management Model and SAR Image Classification for August 28, 1993	5-29
Figure 5.12	Comparison of SAR Classification Results with Flooded Areas Predicted by the Flood Management Model	5-31
Figure 5.13	Change Detection Map of Different Flood Levels in July and August, 1993	5-33
Figure 5.14	Multi-temporal ERS-1 SAR Data Set and Change Detection Map	5-35
Figure 5.15	Merger of Radar Classification Results with Landsat TM Data	5-37

LIST OF TABLES

Table 2.1	Summary of the Main Satellite SAR Systems and the Operating Parameters	2-5
Table 4.1	Areas of SAR Application Potential in Bangladesh	4-4
Table 4.2	Flexibility of RADARSAT SAR System	4-6
Table 5.1	Assessment of SAR filters Used in this Study	5-11
Table 5.2	Accuracy Assessment of Classification of SAR image - 24 July 1993	5-16
Table 5.3	Accuracy Assessment of Classification of SAR image - 28 August 1993	5-16
Table 5.4	Comparison of SAR Classification with Land Type	5-25

ACKNOWLEDGMENTS

This report is the result of a collaborative effort undertaken during 1993-95 by several organizations and individuals in Bangladesh and led by a team from the Geographic Information System (FAP 19) project with the support of the Flood Plan Coordination Organization (FPCO). The FAP 19 project leaders were Iffat Huque and Ahmadul Hassan. The project was designed and managed by Timothy Martin, FAP 19 Team Leader.

In addition to the FAP 19 team, the extensive field data collection exercise was conducted with the support of the Fisheries Study (FAP 17), Bangladesh Space Research and Remote Sensing Organization (SPARRSO), the Tangail Compartmentalization Pilot Project (FAP 20), the Flood Management Model (FAP 25) project and the Surface Water Modelling Center (SWMC). The following persons from those organizations were instrumental in the data collection exercise: Dr. Munir Ahmed, Mohammad Shawkat Ali, Khondokar Masudul Hasan, Kirk Kuykendal, Bob Pengel, and Dr. Dewan Abdul Qadir.

The support of the ISPAN Chief of Party, Dr. Keith Pitman and Darrell Deppert is recognized, as well as inputs from many other FAP 19 staff and consultants, including: Shamsuddin Ahmed, Dr. Tom Chidley, Michael Emch, Thomas (Jay) Hart, Mostafa Kamal, Nasreen Islam Khan, Syed Iqbal Khosru, and Dr. Mike Pooley. The administrative staff of ISPAN are also acknowledged for their support throughout the course of the study.

The report was written by Dirk Werle, Iffat Huque, Timothy Martin, Brian Tittley and Ahmadul Hassan. Abdul Malik Faruq assisted in preparation of images and graphics. Editorial services were provided by Carol Jones and report production was assisted through the efforts of Qazi Salimullah and Shaila Faruq Sinha.

Digital radar data was acquired and preprocessed through a special effort of the Thailand Remote Sensing Center and the European Space Agency.

LIST OF ACRONYMS

AVIIRR	Advanced Very High Resolution Radiometer
BWDB	Bangladesh Water Development Board
CCT	Computer Compatible Tape
CPP	Compartmentalization Pilot Project
DEM	Digital Elevation Model
DN	Digital Number
EMS	Electromagnetic Spectrum
ERS-1	European Remote Sensing Satellite -1
SEA	European Space Agency
FAP	Flood Action Plan
FMM	Flood Management Model
FPCO	Flood Plan Coordinating Organization
GIS	Geographic Information System
GPS	Global Positioning System
ISPAN	Irrigation Support Project for Asia and the Near East
JPL	Jet Propulsion Laboratory
LUM	Lower Upper Middle
MAP	Maximum A Posteriori
MPO	Master Plan Organization
MSS	Multispectral Scanner
NASA	National Aeronautic and Space Administration (USA)
NOAA	National Oceanographic and Atmospheric Administration (USA)
RAR	Real Aperture Radar
RMS	Root Mean Square
SAR	Synthetic Aperture Radar
SD	Standard Deviation
SPARRSO	Space Research and Remote Sensing Organization
TM	Thematic Mapper
USAID	United States Agency for International Development
VIR	Visual and Infrared

SUMMARY

Within the framework of the Flood Action Plan (FAP) program, the Government of Bangladesh has assigned the United States Agency for International Development (USAID)-sponsored FAP 19 Geographic Information System (GIS) project a supporting role for providing leadership in the development, application and institutionalization of GIS technology in Bangladesh. In order to organize, process and interpret spatial information for resource management and environmental monitoring, GIS relies on up-to-date remote sensing data as a source. This FAP 19 project examines how satellite-based radar remote sensing can be used for mapping and monitoring floods in Bangladesh.

Remote sensing offers measuring techniques, including imaging radar, to obtain data that can be used for monitoring the environment. To provide useful information products, it is essential to combine information derived from the synoptic view afforded by remote sensing from space with data from field surveys, in situ point measurements and numerical models. This can be achieved by remote sensing with GIS as an enabling technology.

Radar remote sensing using airborne or space borne synthetic aperture radar (SAR) sensors has received little attention in Bangladesh. In comparison, optical remote sensing technology has been used worldwide for more than two decades and institutionalized in Bangladesh since 1980 at the Space Research and Remote Sensing Organization (SPARRSO). Landsat Multispectral Scanner (MSS) and Thematic Mapper (TM), SPOT, and Advanced Very High Resolution Radiometer (AVHRR) data have been used to assess natural resources, and weather satellites have been used operationally to monitor the atmospheric environment. As a com-

pliment to these applications, recent advancement in SAR technology now offers high-resolution imaging capability and an opportunity to "see" through cloud cover and acquire data during both day and night. This operational advantage can be fully exploited during the monsoon season to monitor dynamic environmental *processes*, and to map the *results* of these processes, as has previously been demonstrated using optical sensors.

A review of current literature on SAR application development in tropical environments shows that imaging radar can provide valuable information for identifying flooded areas, coastal and marine features, and land use characteristics. The findings confirm that SAR application potential exists in situations where optical remote sensing is either impossible or severely restricted because of environmental conditions. Primary application potential exists in situations where SAR data can provide information that other remote sensing tools cannot, including the following application areas:

- mapping and monitoring of storm surges, river floods, excessive rain and flash floods;
- stream flow dynamics of major river systems;
- soil moisture assessment; and
- coastal and marine wind-wave fields.

Secondary application potential exists where SAR data adds value to information derived from a primary remote sensing data source. Candidate application areas include crop assessment, forest inventory, infrastructure mapping, terrain analysis and disaster damage assessment. In these areas, the

synergistic value of several remote sensing methods may be exploited.

Satellite SAR data are currently available in a variety of formats from experimental sensor systems on board the European radar satellite ERS-1 and the Japanese radar satellite JERS-1. Limited archival SAR data also are available from the Russian ALMAZ and SIR-B missions of the United States. Data continuity is assured over the next decade since the ERS-2 and the Canadian RADARSAT missions are scheduled for launch in 1995. Based on the SAR system parameters of these missions, a number of them appear capable of at least partially fulfilling essential data requirements in Bangladesh. For example, the RADARSAT SAR data stream will allow relatively frequent observations at various levels of spatial detail; coverage for the entire area of Bangladesh will be available at 50 m to 100 m resolution, while for regional investigations, 10 m to 25 m resolution.

The capability to incorporate SAR data into flood monitoring activities, land use analysis, and coastal zone management will require substantial technical and logistical support, training, and technology transfer to one or more Bangladesh institutions. As a first step in developing this technology, FAP 19 investigated digital image processing and GIS integration methods for analysis of ERS-1 SAR imagery and developed ground reference data and modelling techniques. The project demonstrated the potential of the ERS-1 SAR for delineating flooded areas during the persistent cloud cover of the monsoon flood season. When used in conjunction with large-scale topographic and elevation data, satellite SAR was able to provide additional information about localized flooding conditions.

ERS-1 SAR scenes of Central Bangladesh were used to map the flood extent for dates in July and August, 1993. The SAR delineation of flooded and nonflooded areas compared favorably with ground information collected simultaneously to the radar data; the overall agreement was over 80 percent. Agreement was greatest for open water surfaces,

nonflooded settlements, homesteads, and for certain crops. Difficulties were encountered in the classification of crop canopies that were partially flooded.

The SAR processing procedure developed in this study relied on digital analysis techniques including density slicing and GIS processing. These options were implemented using PC-based SAR image analysis and GIS software. They should be viewed as the first step in understanding the interaction between satellite SAR and the unique environmental conditions of Bangladesh. The extensive ground reference data collected proved essential for interpreting and analyzing the radar images.

In addition to the classification of several individual ERS-1 images, this project explored various means for increasing the utility of the radar data. For example, multi-temporal data were used for creating a map showing changes in extent of flooding and for assessing the dynamics of hydrology, cropping patterns and agronomic practices.

Other exercises included an assessment of classified radar imagery and the results of a hydrodynamic mathematical model, the Flood Management Model (FMM), which revealed that the two approaches to flood mapping and monitoring can be quite complementary. It appears that classified SAR imagery can be especially useful for verifying FMM results. The radar classification also compared favorably with the most detailed landtype (flood depth) maps of Bangladesh, which were produced by FAP 19 on another project through integration of soil classification maps with a digital elevation model. Finally, a classified radar image was combined with Landsat TM data of the same area, acquired five months later in the dry season. Examination of the resulting composite image suggests that such a presentation is valuable for interpreting the radar image and provides an understanding of complex land use practices, which vary greatly between the dry season and the monsoon flood period.

This FAP 19 radar project, which began in 1993, is the first to explore the potential of satellite-based

SAR for applications in natural resource assessment and environmental monitoring in Bangladesh. It is concluded that satellite radar technology, especially when combined with GIS, mathematical modelling and other techniques, has enormous potential for understanding, monitoring and predicting changes in the complex hydrology of Bangladesh's floodplains.

This study has made an important first step in exploring the use of satellite-based SAR technology. Much has been learned about the potential applications; however, as noted elsewhere in this report, there are shortcomings to this study which follow-on projects could address. In order to optimize SAR data acquisition and the information that can be retrieved by SAR image analysis, future projects should consider environmental factors such as crop calendars, flood cycles, atmospheric and ground surface conditions. A well designed, comprehensive ground data collection program should be orchestrated. In addition, radar-specific factors such as SAR system parameters, satellite orbit parameters, and SAR data product availability, should be considered. This is particularly important when considering the new radar satellites, scheduled for launch in late 1995, and the possibilities for developing operational use of SAR data from these sources.

Information on the application potential for SAR technology in Bangladesh is generally sparse and, the capability to incorporate SAR data into flood monitoring activities, land use analysis, and coastal zone management is limited in Bangladesh. Achievement of this capability will require substantial technical and logistical support, training, and overall strengthening of one or more Bangladesh institutions.

CHAPTER 1

INTRODUCTION

1.1 Institutional Setting

Natural resource assessment and monitoring requires collecting, processing, and analyzing data from a variety of sources and at a variety of spatial and temporal scales. In Bangladesh, government departments and agencies, in cooperation with international donor organizations, operate in, and cope with, a natural environment in which dynamic and rapidly changing conditions require frequent monitoring activities in order to make sound environmental management decisions.

Modern remote sensing techniques have been applied to geographical research, flood monitoring, and natural resource assessment in Bangladesh for more than two decades (ESCAP/SPARRSO, 1989). The government has embraced the use of this technology by establishing the Bangladesh Space Research and Remote Sensing Organization (SPARRSO), while the Flood Action Plan (FAP) has addressed principles of remote sensing for use in water resources planning and management under FAP 19, the Geographic Information System (GIS) project.

The FAP 19 project is coordinated by the Flood Plan Coordination Organization (FPCO) of the Ministry of Water Resources and is funded by the United States Agency for International Development (USAID) and implemented by the Irrigation Support Project for Asia and the Near East (ISPAN). In addition to its main project focus within the FAP, the FAP 19 team has provided leadership in the development, application, and institutionalization of GIS technology in Bangla-

desh. In order to organize, process, and interpret spatial information for resource management and environmental monitoring, GIS relies on up-to-date remote sensing data.

1.2 Rationale

The principal satellites used for remote sensing projects in Bangladesh are geostationary weather satellites and the sun-synchronous, near-polar orbiting Landsat, SPOT, and NOAA satellites. A common characteristic of all of the sensors on-board these satellites is that they operate in the visible and infrared (VIR) portion of the electromagnetic spectrum (EMS). Use of the microwave, or radar, region of the EMS remains largely unexplored in Bangladesh.

With the obvious exception of weather satellite monitoring, remote sensing investigations carried out in Bangladesh have required cloud-free weather conditions. The acquisition of useful VIR data sets, therefore, has been mostly restricted to the dry season between November and May. Change-detection studies have used data sets collected before and after the monsoon season to avoid the cloud cover that predominates from May to October. These remote sensing investigations were able to analyze the *results* of environmental change, but they were not able to record the extent of flooding, let alone the actual *processes* that govern change as a result of monsoon floods. Consequently, flooding during the monsoon season is not well documented in Bangladesh. There is a critical need to determine not only *where* the flooding actually occurs, but

also to better understand the processes that determine the morphology of Bangladesh's rivers and extensive floodplains.

This study of radar applications is part of the FAP 19 effort to provide decision makers with useful techniques as well as timely and accurate information that will improve their ability to monitor flood conditions in Bangladesh. From a technological point of view, radar, and more specifically Synthetic Aperture Radar (SAR), is a fairly new and sophisticated tool which requires user-specific systems development and training. Yet, when used in an operational setting on a regular basis, SAR can be a most unique and valuable tool for monitoring highly dynamic environmental phenomena and events despite cloud cover, rainfall, or darkness.

In conjunction with other data sources, radar also could be used in Bangladesh for assessing river morphology, agriculture, land resources, or oceanographic and coastal zone phenomena associated with the development and impact of cyclones. The advent of modern imaging radar technology and the launch of several high-resolution radar remote sensing satellite systems provides an opportunity to assess its application potential.

The launch of the European Space Agency's ERS-1 radar satellite in 1991 presented such an opportunity. FAP 19 acquired four ERS-1 SAR images for the radar project (Figure 1.1). Two of the images were acquired for an area around the confluence of the Ganges and Brahmaputra/Jamuna rivers in central Bangladesh during the monsoon flood season on July 24, 1993, and August 28, 1993 (Figure 1.2 and 1.3). The other ERS-1 images were acquired in May, 1993, over the Sylhet area of northeastern Bangladesh (Figure 1.5).

A series of 10-km by 10-km subscenes show different features at a spatial resolution of 25 meters; six subscenes are part of the central Bangladesh region (Figure 1.4 A-F), and three

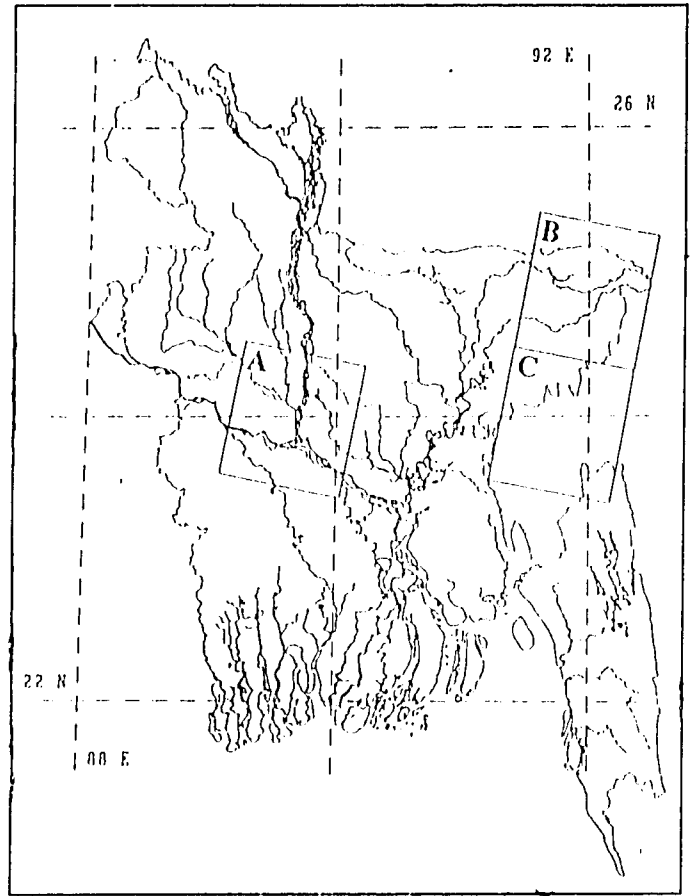


Figure 1.1: Coverage of ERS-1 SAR image frames used in this study.

A: Central Bangladesh scene
B and C: Sylhet scenes

subscenes are part of the Sylhet region (Figure 1.6 A-C). A set of ground reference photographs provides further illustration (Figure 1.7, A-F).

The ERS-1 SAR images document three important advantages when considering the application of SAR by itself or in conjunction with other remote sensing techniques:

- Capability of satellite radar remote sensing to acquire *high-resolution* data for a *variety of applications*.
- Capability to acquire data on a regular basis over *large areas* for monitoring purposes.
- Operational capability to capture a reliable stream of data *despite cloud cover*.

1.3 Goal and Objectives

The primary goal of this radar application study is to explore the potential of satellite radar over the floodplains in Bangladesh during the monsoon season when other sensors are hindered by cloud cover. The results and experience gained from this work may contribute to the establishment of a more rigorous flood monitoring program.

In pursuing this goal, the following specific objectives were established to address key requirements for radar remote sensing work in Bangladesh:

- To provide conceptual background and orientation of radar remote sensing technology to potential users in Bangladesh.
- To review radar application studies that are relevant to users and environmental settings in Bangladesh.
- To conduct an initial study of flood mapping applications using satellite radar imagery, and using FAP 19 image processing and GIS hardware and software tools.
- To conduct a SAR image classification exercise using a set of ground reference observations collected at the time of SAR data acquisition.
- To assess and evaluate the results of the radar application review and the SAR study within the context of actual information requirements in Bangladesh.

1.4 Organization of the Document

Chapter 2 provides an overview of basic radar concepts, systems, and target parameters; it also contains a description of commonly used satellite-based SAR systems. Chapter 3 contains a literature review of international SAR project results that pertain to resource issues in Bangladesh. Chapter 4 considers the use of SAR technology in Bangladesh in areas such as project design, technology transfer, and evaluation of SAR application potential. Chapter 5 contains the core of this report: the analysis of ERS-1 satellite SAR data for the FAP

19 flood monitoring exercise. The chapter includes a presentation of the study approach, a description of selected study sites and the ground reference program, a technical description of the image processing and data integration procedures, and an assessment of the flood mapping results. Conclusions and recommendations are found in Chapter 6, which is followed by a list of references.

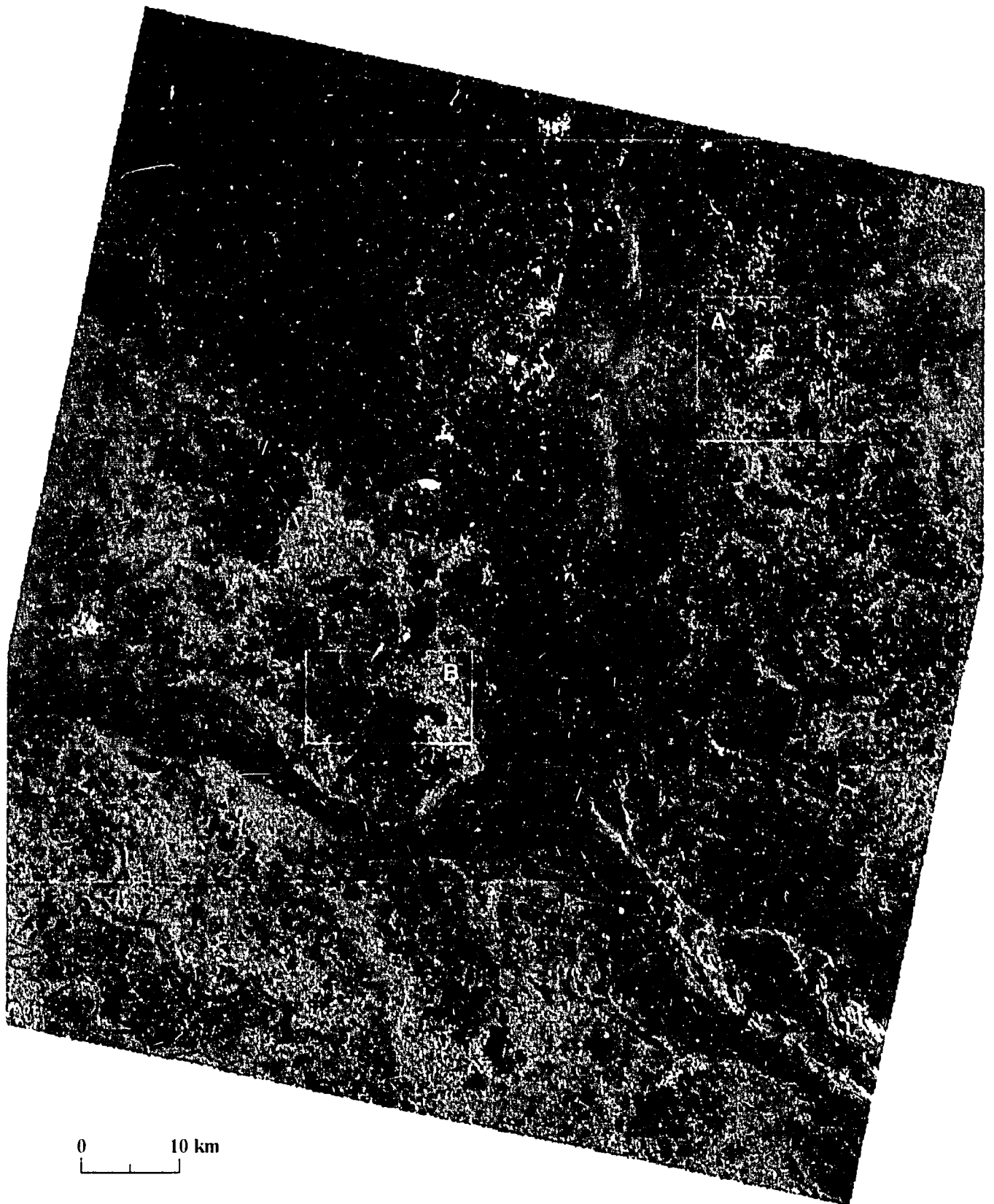


Figure 1.2: ERS-1 SAR Image of Central Bangladesh, July 24, 1993. Full scene. 100 km by 100 km. 8-bit. MAP filtered. Boxes refer to locations of subscenes used during SAR image processing; Box A refers to Figure 5.1 and Box B to Figure 5.14.

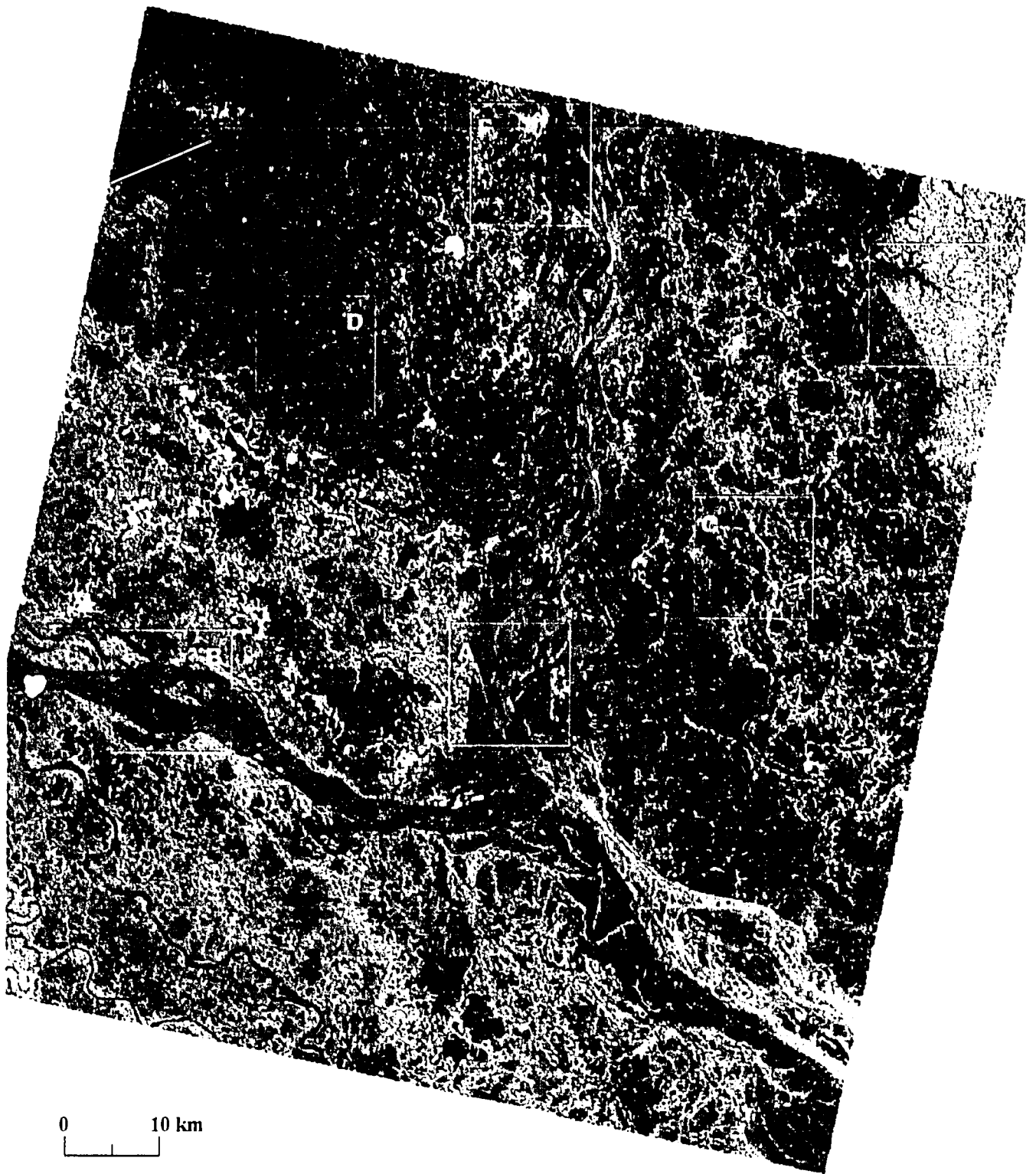


Figure 1.3: ERS-1 SAR Image of Central Bangladesh, August 28, 1993. Full scene, 100 km by 100 km, 8-bit, MAP filtered. The boxes refer to locations of annotated subscenes shown in Figure 1.4



Subscene A: Braided pattern of the Jamuna River during monsoon; light-grey radar signatures indicate areas of high river flow and the river banks and edges of chars (mid-channel islands). Other features of note include bright corner reflections of a series of power line pylons in the lower part of the image and the linear signature of the Brahmaputra Right Embankment that clearly separates flooded and nonflooded areas in the left of the image.

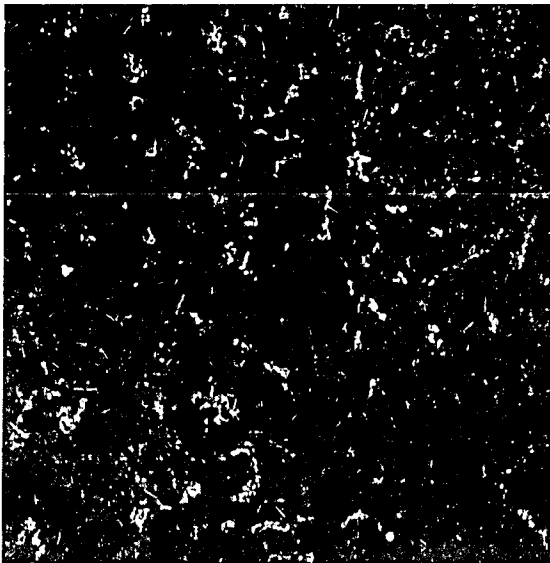


Subscene B: The Ganges River in dark grey image tone gives less indication of stream flow dynamics than the Jamuna image in subscene A. Note the partially submerged chars and diaras (fluvial accretion in and along the river, respectively). The floodplain supports flooded crops in shallower basins and nonflooded crops on lower ridges and levees.

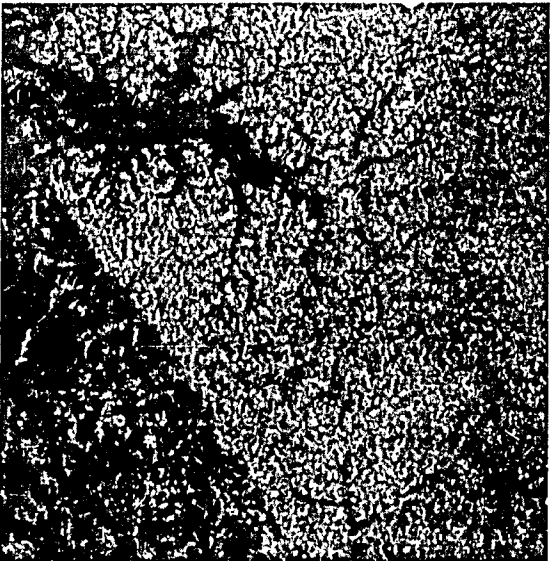


Subscene C: Jamuna-Old Dhaleshwari floodplain with extensive areas of flooded and nonflooded terrain shown as dark grey and medium-grey radar signatures, respectively. The dense pattern of settlements and homestead forest appears radar-bright and light grey; it is associated with slightly higher elevations along the rivers and remnants of older levees.

Figure 1.4: SAR Image Interpretation Keys (A-F) of Some Major Physiographic Features on the Central Bangladesh SAR Image. Prominent land crop and flood scape elements are readily detected in this August radar scene.



Subscene D: Lower Atrai basin with almost level relief that floods deeply, and often quickly, during the monsoon. Extensive surfaces of open water appear radar-dark. Deep-flooding makes long-stemmed, floating *paddy*, a prominent crop. Homesteads on raised mounds and elongated ridges (medium to light grey) dot the flood scape. Note also nonflooded, linear features of the transportation network.



Subscene E: Pleistocene upland terrain (5-15m elevation, nonflooded) of the Madhupur Tract is represented in the variegated medium-grey image tones. There is a distinct, almost linear, boundary between the upland tract and the lower lying floodplain (medium to dark grey). The dendritic drainage pattern has shaped small valleys, or *bairis*, in which *boro* (dry season paddy) is cultivated.



Subscene F: Major settlements and towns give radar-bright signatures that occasionally may be confused with very strong radar return from certain flooded vegetation. Shown here is the town of Sirajganj on the west bank of the Jamuna River. The town's distinct roads and urban center act as corner reflectors. Drainage features within the floodplain are distinct.

Figure 1.4: (Continued)

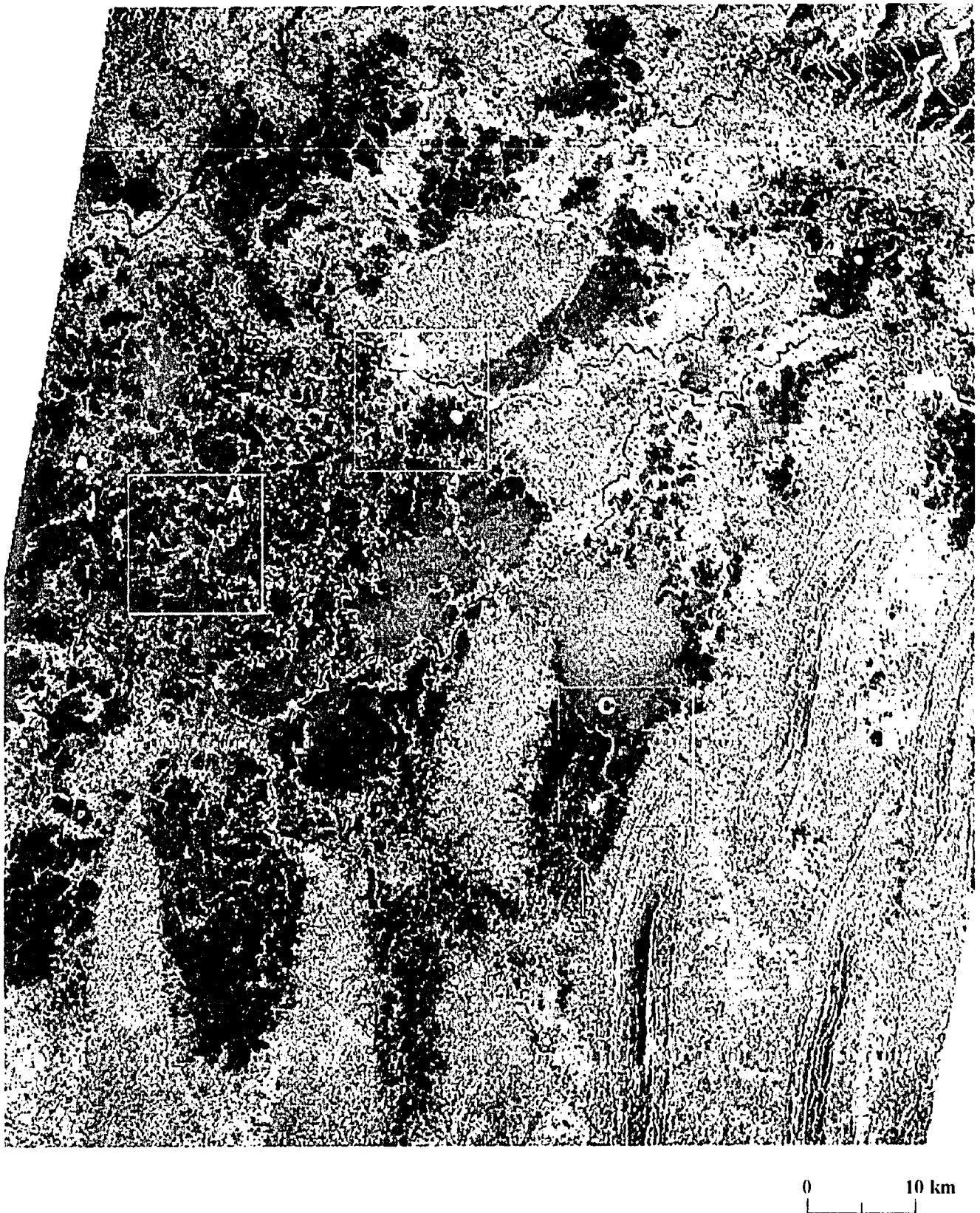
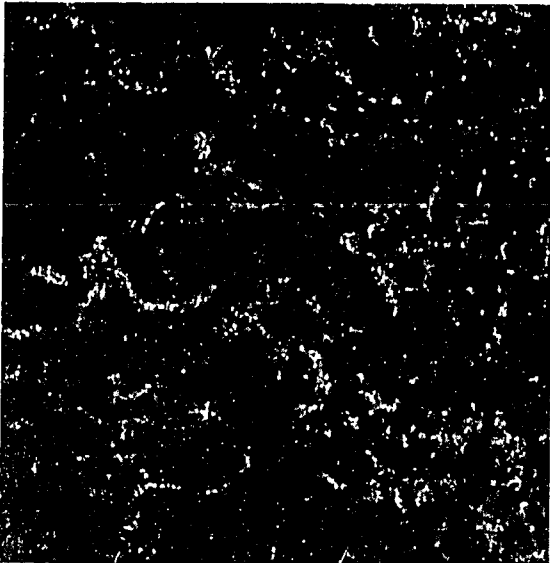


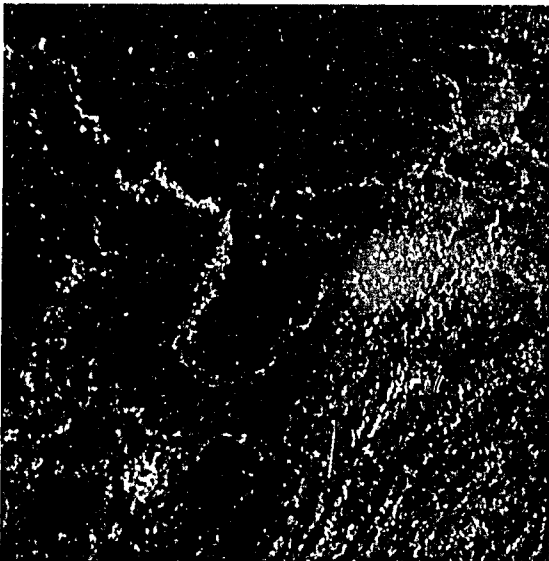
Figure 1.5: ERS-1 SAR Image of the Sylhet Region, May 28, 1993. The image is subset from two frames and includes an area of about 100 km by 100 km, 8-bit, MAP filtered. The boxes refer to locations of annotated subscenes shown in Figure 1.6.



Subscene A: The central basin is a low lying area with a succession of *beels* and *haors*, river cut-offs, scours and long levees known as *kandha*. The shallow, flooded terrain appears radar dark; cultivated areas appear in medium to dark grey tone, and settlements and homestead forest are marked by radar-bright and light grey tone.



Subscene B: The city of Sylhet is characterized by a cluster of radar corner reflections between the Surma River in the south and a small, 40 m high hillock, or *tila*, to the east. The floodplain to the south of the Surma River is characterized by medium and dark grey radar signatures of mostly flooded land interspersed with settlements.



Subscene C: The central Sylhet lowlands of the *haor* basin are mostly flooded during the monsoon season, and are marked by radar dark and dark grey signatures. *Aman* and *boro* are the main crops. Note the higher elevation natural rivers levees entering the depression from the 40 to 60 m high *tila* ranges in the right of the image.

Figure 1.6: SAR Image Interpretation Keys (A-C) of Some Major Physiographic Features in Sylhet Area of Northeastern Bangladesh. Prominent land, crop, and flood scape elements are readily detected and cultivation associations are indicated in this May radar image (see Figure 1.5 for location).

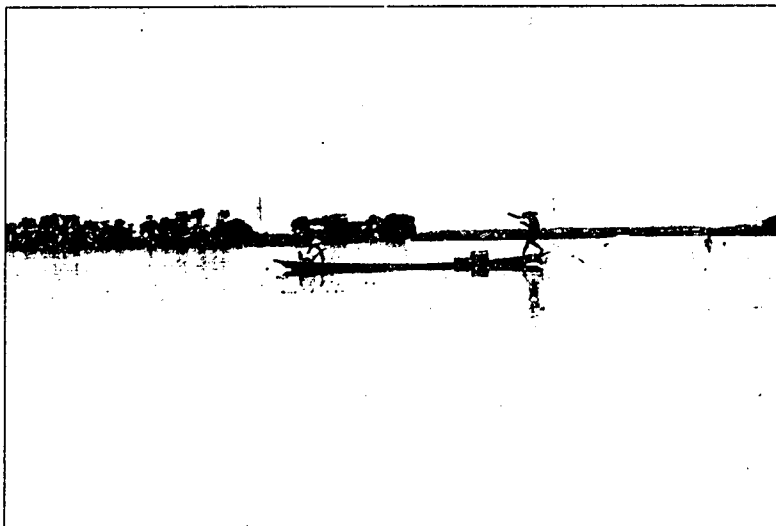


Photo A: Flooding along the Jamuna River July, 1993. Note settlements on the levee in the background.

Photo B: Rice paddy in various stages of cultivation and growth in less flood-prone terrain, near Sirajganj in July, 1993. Note homestead forest and settlements on higher ground.



Photo C: Flooded sugarcane in the Tangail area in July, 1993. Given limited radar penetration capability, the SAR image signature of these conditions may represent a source of confusion when classifying flooded and nonflooded terrain.

Figure 1.7: Photographs Illustrating Typical Flood Conditions and Land Use in the Floodplains of Bangladesh. Photos A to F were taken during a ground reference program that was carried out in parallel to ERS-1 SAR data acquisition on July 24, 1993, and August 28, 1993.



Photo D: Extensive flooding along the Dhaleshwari River in August, 1993. Agricultural fields are largely submerged. Note the accumulation of water hyacinth in the foreground.

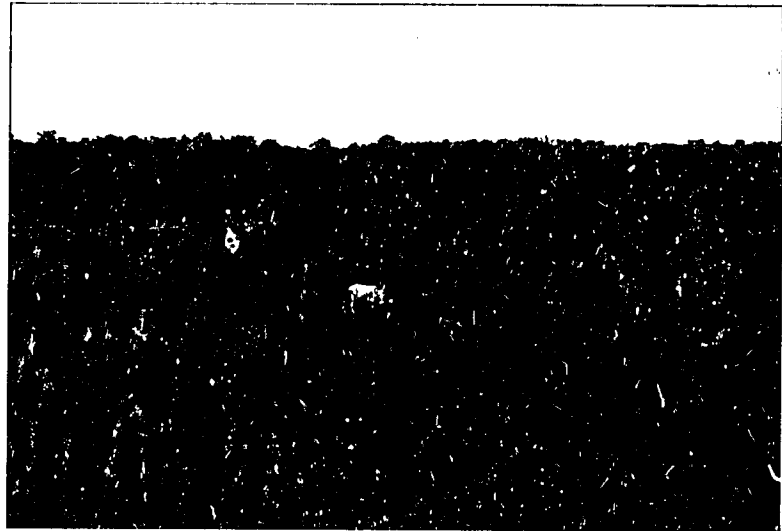


Photo E: Newly transplanted *aman* paddy in less flood-prone terrain, near Sirajganj, August, 1993. Note sugarcane fields in the middle background and homestead forest and settlements on higher ground.

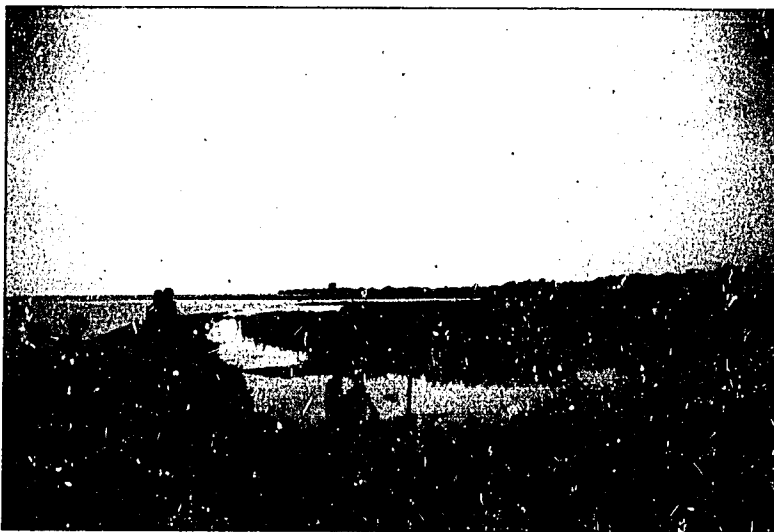


Photo F: An embankment in the extensively flooded, lower Atrai basin, August, 1993. Note the water hyacinth in the foreground and deep water *aman* paddy in the middle.

Figure 1.7: (Continued)

CHAPTER 2

SYNTHETIC APERTURE RADAR (SAR)— BASIC CONCEPTS AND SATELLITE SYSTEMS

The basic concepts of imaging radar must be understood before evaluating the technology. This chapter emphasizes SAR, its operating parameters, and the characteristics of its interaction with ground targets. The discussion provides important background information for assessing the advantages and limitations of modern radar technology in resource and environmental analyses. The chapter concludes with a review of different satellite-based SAR missions.

2.1 Radar Remote Sensing Concepts

Radar stands for *radio detection and ranging*, which is the most concise description of the principle and performance of a radar. A radar instrument transmits microwave (*radio*) signals, receives the portion of the signal reflected by the target (called backscatter), and simultaneously measures the intensity and time delay of the return signals. *Detection* is the sensing of the reflected energy, and *ranging* is the measuring of the time elapsed since transmission (Figure 2.1). An in-depth overview, including a detailed description of imaging radar systems, theory, SAR processing principles, and analysis procedures can be found in several textbooks, including Ulaby, *et al.* (1981-1986), Leberl (1990), and Curlander and McDonough (1991).

Most imaging radars used for Earth observation and mapping are side-looking systems. A two-dimensional imaging plane is produced by transmitting pulses orthogonal to the flight, or

orbital, path. In this manner, continuous strips of the Earth's surface are "illuminated." The scanning concept of the imaging radar is different from that employed by remote sensing optical scanners. Since the microwave pulses of an imaging radar travel at the speed of light, radar image resolution is independent of angular resolution. Furthermore, imaging radars achieve across-track resolution by measuring the relative time delay of each echoed component of a pulse.

The governing factor for the across-track, or *range*, resolution of an imaging radar is the length of the radiated pulse. Along-track, or *azimuth*, resolution is determined by the width of the radiated radar beam, which, in turn, is limited by the physical size of the antenna, or aperture, hence the term *real aperture radar* (RAR). The along-

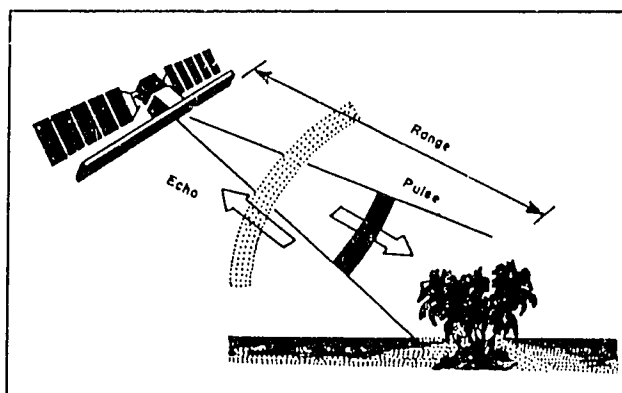


Figure 2.1: Radio Detection and Ranging (RADAR). A RADAR system has three primary functions: (1) it transmits microwave energy (pulse) signals toward the scene, (2) it receives the portion of the backscattered energy from the scene (echo), and (3) it observes the strength and the time delay (range) of the return signal. (Source: Raney, 1994)

track resolution of an RAR cannot be improved substantially over a wide swath because it progressively decreases farther down-range. The weakness of an RAR could be overcome if the amplitude and phase of the received signal could be recorded and memorized for successive radar scan lines (Figure 2.2). In such a case, the data could be processed as if these scan lines had been collected by a large aperture. This led to the concept of SAR.

The generation of a synthetic array for high azimuth image resolution can be explained in the following way. A radar antenna transmits pulses in a fan-shaped beam pattern at regular intervals along the flight path. While illuminated, the target reflects a series of microwave pulses emitted by the radar. The radar receiver records this entire array of the amplitude and phase of the target's return signals and keeps it in memory for later processing. From the target's perspective, the synthetic array is longer for more distant targets and shorter for those nearer the antenna. Thus, the effective length of the synthetic array is directly proportional to the distance, or range, of the target to the radar. Since the resolution is proportional to the length of the antenna, yet inversely proportional to the range, these two effects compensate each other. As a

result, the resolution of a SAR image in the azimuth direction remains the same across the track. The SAR technique lends itself well to obtaining high resolution imagery over great distances.

2.2 Radar System Configuration

An imaging radar in its most basic form consists of a transmitter, an antenna designed for both transmitting and receiving microwave energy, a receiver, and a data processing and recording unit.

The *transmitter* generates a microwave pulse of short duration (on the order of microseconds). The ability of a radar to distinguish and resolve closely spaced objects largely depends on the pulse length. The signal is then transmitted by way of an antenna.

The *antenna* fulfills two functions: it directs the microwave signal toward the target and it receives the returned portion of the transmitted signal. The design and form of the antenna determines the beam width and the width of the illuminated ground surface.

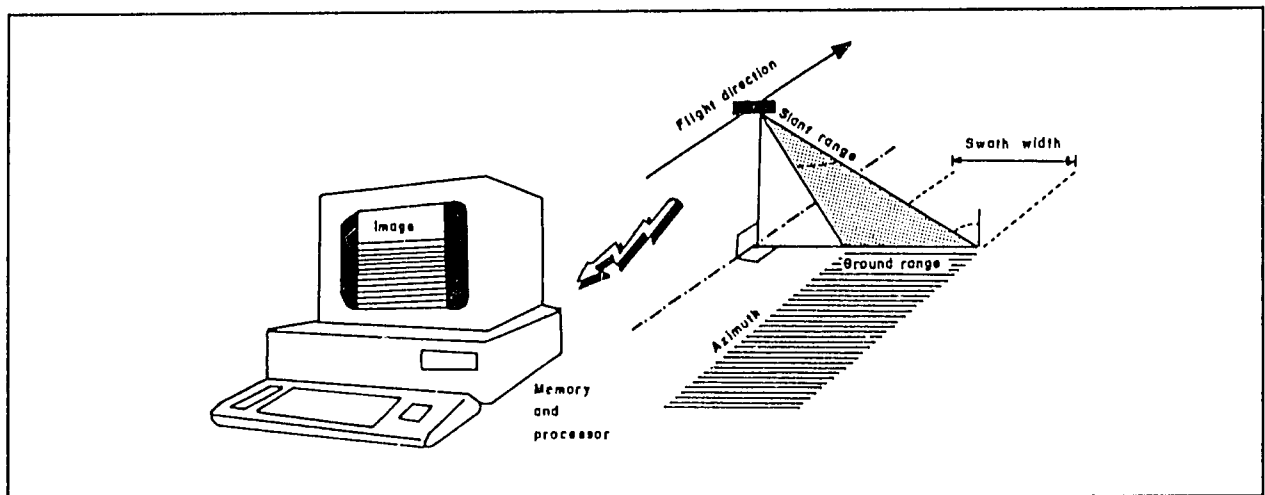


Figure 2.2: Synthetic Aperture Radar Imaging the Earth's Surface. The perspective is oblique down and to one side of the orbital plane. The slant range is the line of sight between the radar and each reflecting element on the surface. Most users require images to represent distance on the ground, referred to as ground range. The geometric conversion from slant range to ground range is accomplished by SAR processors. (Source: Raney, 1994)

The *receiver* measures the strength of the returned signal and relates the receiving time to the transmission time in order to determine the range distance of an object relative to the radar. Since the returned signal is always much weaker than the transmitted signal (due to the scattering processes and partial reflection or absorption), a low-noise amplifier is used to increase the signal strength. Signal correction routines also may be applied to compensate for the radar viewing geometry.

The *SAR signal processor* performs several computational tasks: it produces a record of the optimum signal return, reduces undesirable signal artifacts or effects related to the radar viewing geometry, suppresses noise, and eventually produces a digital output tape for further digital SAR image analysis and image output. SAR processors can generate images with varying degrees of radiometric and geometric sophistication, as well as image noise ("speckle").

The *radar imaging parameters* that need to be considered include wavelength, polarization, and radar look direction and incidence angle.

Wavelength is an important system parameter in understanding the interaction between the radar signal and the target. Radar remote sensing uses the microwave region of the EMS, which extends from .3 GHz to 300 GHz, or in terms of wavelength, from 1 m to 1 mm. The most common imaging radars operate at wavelengths ranging from 65 cm to 3 cm. There is a widely accepted naming convention for radar bands: X-band is centered on the 3 cm wavelength, C-band on 5 cm, S-band on 10 cm, L-band on 23 cm, and P-band on the 60 cm wavelength. The ability of radar to penetrate soil or vegetation also depends on the wavelength (but also on incidence angle, polarization, and moisture conditions). Longer wavelengths penetrate deeper than shorter ones.

Radar energy can be transmitted and received in vertical and horizontal *polarization* states. As with wavelength, there is a naming convention for polarization: C-HV, for instance, stands for

horizontal transmit polarity at the C-band wavelength and vertical receive polarity. HH and VV are like-polarized signals and HV and VH are cross-polarized signals. Upon hitting a target, the radar energy may be depolarized.

Radar viewing geometry consists of *look-direction* and *incidence angle*. Look-direction is the direction in which the radar beam is pointed. The aspect and orientation of features illuminated by the radar relative to the look-direction influences the strength of the signal returned. Features parallel to the look direction, such as a fence line, may not return an appreciable amount of radar energy, whereas the same feature at other orientations, particularly perpendicular to the look direction, may return strong signals. The angle at which the radar energy is incident to a surface or target varies across the image swath. Typically, the range of incidence angles over a 100 km-wide image swath is fairly small for satellite sensors, on the order of five to six degrees.

2.3 Target Parameters

The strength or weakness of radar return from the earth's surface depends upon so-called *target parameters*: surface roughness or smoothness, moisture, and point targets such as corner reflectors.

Radar is sensitive to *roughness and smoothness* of surfaces. Sensitivity varies according to the choice of radar imaging parameters. For instance, a grass surface may appear smooth at L-band but rough at X-band. Calm water surfaces also are smooth relative to commonly used radar wavelengths, and radar energy is reflected from them, as from a mirror. This results in little radar return and dark signatures on the radar image (Figure 2.3). Other surfaces, such as a recently plowed field with topographic variations as small as 15 cm, appear rough at X-band (3 cm) because the radar energy is scattered diffusely upon incident, thus returning an appreciable amount of energy back to the receiver.

The electrical properties of targets also can have an important influence on the intensity of the radar return. The presence of *moisture* in the soil or in vegetation can significantly increase radar reflectivity as the moisture level of the target increases. The multiple reflections of so-called *point targets*, or corner reflectors, provide strong radar returns for image analysis. Settlements usually are formidable concentrations of corner reflectors, and their location and extent is generally marked by bright signatures on radar images (Figure 2.3).

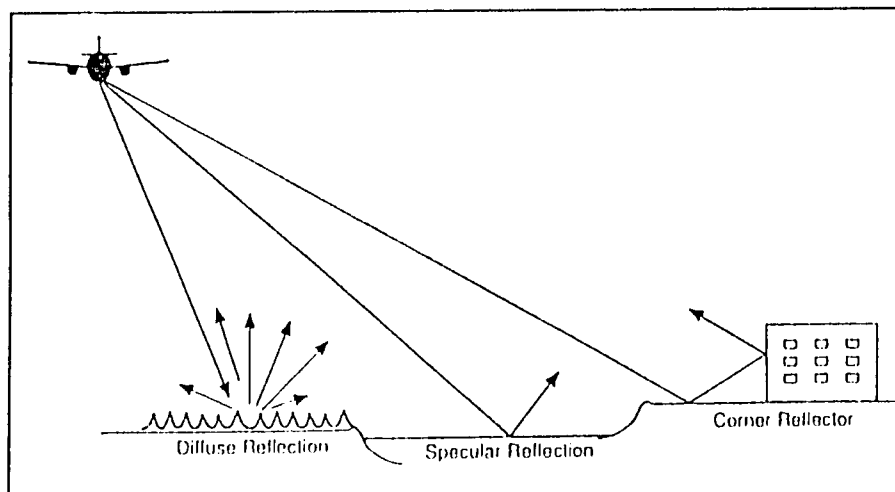


Figure 2.3: Various Radar Reflection Types. Specular and diffuse reflectance are the products of surface roughness. Horizontal, smooth surfaces, for example, a calm water surface or a paved highway, reflect nearly all incident energy away from the radar in a mirror-like, or specular, fashion. Radar energy incident upon a rough surface, for example, a vegetation surface, is scattered in many directions and is called diffuse reflectance. Corner reflectors return most of the incident radar energy. (Source: Raney, 1994)

In addition to the *surface* scattering mechanisms described above, some targets may exhibit volume scattering effects. Volume scattering involves scattering elements within a medium, for example leaves, branches or twigs within a forest canopy. This type of scattering can also occur in a layer of very dry soil, sand or ice. The intensity of the volume scattering depends on the physical properties of the volume and its scattering elements and the characteristics of the radar (wavelength, polarization and incidence angle). In many cases volume scattering and surface scattering

mechanisms combine resulting in a process of multiple scattering.

2.4 Satellite SAR Systems

Several spaceborne SAR missions are in operation, and others are scheduled to be launched in 1995. These include the European ERS-1 (1991) and ERS-2 (1995) missions, the Japanese JERS-1 mission (1992), the Canadian RADARSAT mission (1995), the Russian ALMAZ-1 (planned) mission, and the American Space Shuttle SIR-C mission (1994/95). In principle, these systems acquire SAR imagery with a spatial resolution on the order of 10 m to 100 m, which matches flood data requirements at the local, regional, and national level in Bangladesh. With the exception of SIR-C, all the SAR systems are capable of global data acquisition, and coverage of Bangladesh can be achieved with a revisit period of several days to several weeks (Li & Raney 1991, Raney, *et al.* 1990, and Werle 1992). The

main SAR system and operating parameters are summarized in Table 2.1 and discussed in the following sections.

2.4.1 ERS-1 and ERS-2

In 1991, the European Space Agency (ESA) launched ERS-1. ERS-2, with a SAR system identical to the one on ERS-1, will be launched in 1995. The ERS-1 payload includes a single-frequency C-band SAR with vertical transmit and receive polarization (C-VV). The fixed radar viewing geometry over the 100 km-wide image

Table 2.1 Summary of the Main Satellite SAR System and Operating Parameters

	ERS-1/ERS-2	JERS-1	SIR-C	ALMAZ	RADARSAT
Country	Europe/SEA	Japan	USA	Russia	Canada
Launched	1991/1995	1992	1994/95	1991	1995
Altitude	785 km	568 km	225 km	300 km	792 km
Radar Bands	C-band	L-band	X/C/L-band	S-band	C-band
Polarizations	VV	HH	HH/VV/VH	HH	HH
Incidence Angle	23°	39°	15-55°	30-60°	20-49° (59°)
Swath Width	100 km	80 km	15-90 km	40 km	50-500 km
Resolution	25 m	18 m	15-30 m	15-30 m	10-100 m
o/b Recorder	no	no	yes	yes	yes

(Source: modified after Li and Raney, 1991, Raney *et al.*, 1990, and Werle, 1992.)

swath centers on incidence angles around 23 degrees. The spatial resolution is 25 m.

The ERS-1 SAR operating time is limited to a maximum of 10 minutes per orbit. Return signals will be digitally processed on-board and transmitted to a series of receiving stations. An on-board data recording system is not available. ERS-1 data for Bangladesh is transmitted to the Thailand Receiving Station near Bangkok; a SAR processing facility is also available in Thailand to transform the radar signal data into actual SAR images. The ERS-1 and ERS-2 mission objectives are both scientific- and application-oriented: to increase the scientific understanding of coastal zones, global ocean processes, and polar ice regions, and to develop and exploit coastal, ocean, and ice applications.

2.4.2 JERS-1

In 1992, Japan launched JERS-1. Its payload includes a SAR operating at L-band with horizontal polarization and a fixed radar incidence angle around 35 degrees (± 3 in.) in mid-range. The

spatial resolution of the JERS-1 SAR is 18 m. Like ESA's ERS missions, the Japanese mission is experimental. JERS-1 SAR data are primarily used in agriculture, forestry, and fisheries, and for monitoring disasters and surveillance of coastal regions. The configuration of the JERS-1 SAR is potentially suitable for flood mapping in Bangladesh. The 80 km-wide image swath, however, necessitates a relatively long revisit period of several weeks in order to obtain complete coverage of Bangladesh. Arrangements for JERS-1 SAR data acquisition over Bangladesh need to be made through regional receiving stations outside the country, such as the one in Thailand.

2.4.3 Shuttle Imaging Radar, SIR-C

In the United States, the National Aeronautic and Space Administration (NASA) and the Jet Propulsion Laboratories (JPL) are using three Space Shuttle missions to conduct the SIR-C experiment. The first two missions were successfully completed in April and September, 1994; the third is scheduled to take place in 1995.

The experiment uses a multi-frequency C- and L-band SAR with a multi-polarization capability (C and L, VV/HH/HV/VH). Also part of the payload is a German-Italian-built X-band SAR with vertical polarization (X-VV). SIR-C allows electronic steering of the antenna beam for data acquisition at incidence angles varying from 15 to 55 degrees. The swath width may range from 15 km to 90 km. The resolution of the SIR-C will be approximately 30 m in low-resolution mode and 15 m in high-resolution mode.

The Shuttle Imaging Radar instrumentation serves as a test bed for U.S.-led SAR satellite missions currently planned for the year 2000 and beyond. Although no data acquisition is planned for Bangladesh, the SIR-C mission results will provide important insights: the first opportunity for simultaneously acquired multi-frequency SAR imagery from space, the first opportunity to use a multi-polarization capability, and acquisition of SAR imagery from space during different seasons.

2.4.4 ALMAZ

In 1991, Russia launched a SAR satellite with the intent of acquiring military and commercial data. The mission, known as ALMAZ, concluded in 1992 and an extensive SAR data archive was opened for commercial use. There are plans to launch a similar SAR satellite, but there is uncertainty about when this will occur and about the data distribution policy for the mission. The ALMAZ SAR operated at S-band (10 cm) with HH polarization. The actual ALMAZ image data sets are 40 km wide and up to 300 km long. The spatial resolution varies between 15 m and 30 m. The ALMAZ SAR used a ground-based optical processor for data output at an image scale of 1:150,000.

2.4.5 RADARSAT

The Canadian RADARSAT is scheduled to be launched in 1995 for a five-year mission. The objective of RADARSAT is to generate SAR data of value for both operational application and

scientific research on ice, oceans, and natural resources. The SAR will operate at C-band with horizontal polarization (C-HH). Unlike previously deployed satellite SAR systems, the RADARSAT SAR is highly flexible in terms of scene illumination, resolution, and revisit capabilities. The SAR will be able to shape and steer the radar beam over a 500 km-wide accessibility swath, which may be extended to include a 200 km-wide experimental swath in far range. The incidence angle geometry may vary accordingly between 20 and 49 degrees for the 500 km-wide swath, and between 49 and 59 degrees for the experimental swath. This will provide daily coverage of Arctic and Antarctic latitudes, coverage of the entire Canadian territory within three days, and global coverage within 16 days. The SAR swath also can be electronically altered in width and spatial resolution (10-55 m) to the specifications of a particular application. The swath choices are illustrated in Figure 2.4.

The RADARSAT data will be processed and formatted on-board to be transmitted either in real-time, or stored on data recorders for later transmission to one of several receiving stations. The main stations will be in Gatineau (Quebec), Prince Albert (Saskatchewan), Fairbanks (Alaska), Europe (UK and Scandinavia), and Asia (Singapore). Canadian companies also have designed "portable" receiving and processing stations as an alternative option for potential users.

The Mission Control Center in Canada will be able to accommodate data requests with a seven-day advance notice; shorter periods may be accepted under exceptional circumstances such as environmental or national emergencies. It is expected that the time interval between acquisition and transmission of SAR data and delivery of the processed SAR product will not exceed four to six hours under optimum conditions. The RADARSAT sensor, orbit, and data-relay configuration appear suitable for satisfying SAR data acquisition requirements likely to be encountered for flood mapping and monitoring in Bangladesh.

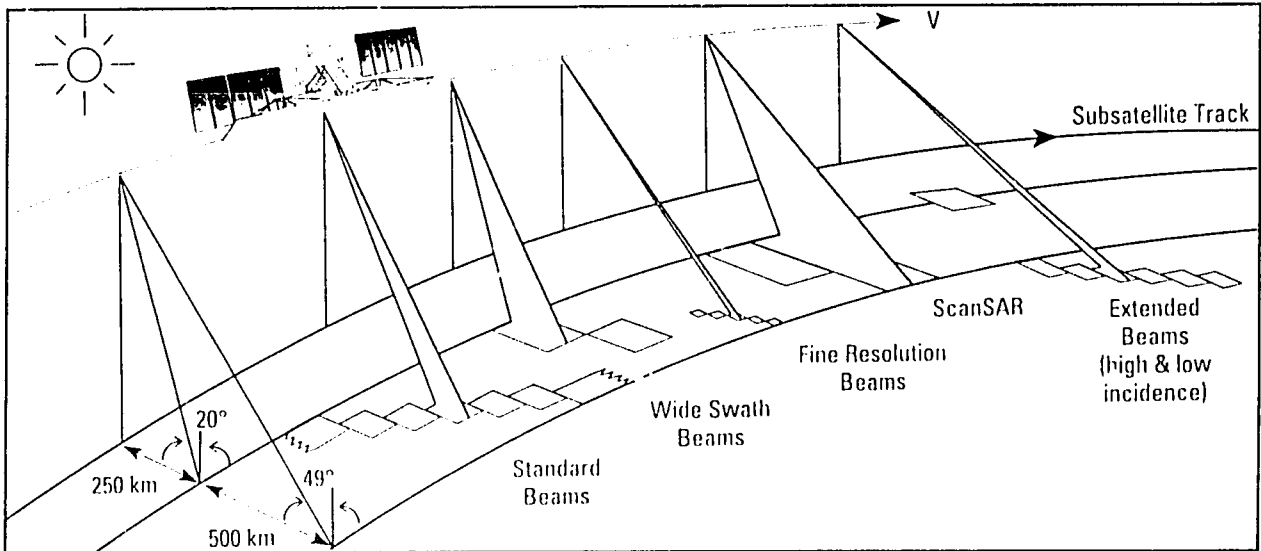


Figure 2.4: RADARSAT SAR Operation Modes
 (Source: RADARSAT Project Office/Canadian Space Agency)

19

CHAPTER 3

REVIEW OF RADAR PROJECTS RELEVANT TO NATURAL RESOURCES IN BANGLADESH

In order to better understand the technology, this study reviewed pertinent literature on international radar remote sensing studies that proved relevant to natural resource issues in Bangladesh. Remote sensing journals, symposia proceedings, handbooks, and project reports were reviewed to find studies covering assessment and management of flooded environments, coastal and marine environments, and general land use analysis.

3.1 Flooded Environments

Several studies indicated that SAR can be used to delineate flood boundaries even when they are obscured by forest or other vegetation.

The only known studies of Bangladesh involved those conducted by Imhoff, *et al.* (1986, 1987, 1990). They analyzed multi-incidence angle SIR-B data of Bangladesh in order to characterize forest canopy and assess radar penetration capabilities. The study found that it was possible to map flood boundaries beneath mangrove vegetation canopies. Varying tide levels were found to have an influence on the generally strong backscattering from mangrove stands. The backscatter from the water surface under the canopy had an overriding effect, and few radar image patterns corresponded to parameters like tree height, stand density, and species composition. Breaches and holes in the natural canopy structure were easily detected.

One of the most comprehensive studies to-date was conducted by Pultz and Leconte (1991) and

Leconte (1989) in Canada. They used airborne C-HH SAR imagery of the 1987 Saint John River flood to demonstrate the potential of RADARSAT (scheduled for launch in 1995; see Section 2.4.5) for flood mapping. The study generated simulated SAR imagery that corresponded to the various operational modes of RADARSAT. Classification accuracy for open water, ice, flooded vegetation, and land classes suggests that RADARSAT can be successfully used to delineate flooded areas, although accuracy is slightly reduced as resolution is degraded and the signal-to-noise ratio is increased. Flood-induced damage may be estimated by combining SAR data with complementary data sets, such as digital cartographic data or other remotely sensed data (Landsat, SPOT). Image analysis results reveal that, regardless of the simulation mode or the noise equivalent selected, the open water area is well delineated.

Radarsat International (1993) conducted a flood assessment exercise using ERS-1 SAR and SPOT multispectral data of the 1993 Mississippi flood in the United States. Within 24 hours of satellite SAR data acquisition, images at a resolution of approximately 25 m were provided to government agencies for monitoring the impact of the flood. Integrated data sets combined the advantages of SAR data—that is to say flood delineation near the peak of the flood—and the usefulness of multispectral visible and infrared data for land use information prior to flood impact. Similar demonstration projects were carried out by European investigators during the 1994 floods along the Rhine and Rhone River in Germany and France. At the regional

level, ERS-1 SAR imagery contained useful information on flood stages and extent.

In China, airborne radars have been used operationally for real-time surveillance of major floods. The radar imagery provided more timely and cost-effective information on flood extent and flood conditions than conventional visible and infrared imagery. During several dozen successful sorties, the displays of both airborne and ground-based reception systems showed clear imagery, which proved useful for regional and national authorities in charge of flood monitoring and prevention (Chen, *et al.*, 1988).

Seasonal flooding occurs frequently in tropical lowlands. Using multi-temporal SEASAT SAR in combination with airborne SAR data, a Guatemala case study carried out by Pope (1988) showed that radar backscatter values of vegetated flooded terrain were at a maximum under small incidence angle illumination.

Investigations of the radar signatures of lowland flooding in temperate climates have led to a general consensus that flooded wetland vegetation produces particularly high returns with increasing vegetation volume and stand height (Krohn, *et al.*, 1981; Ormsby and Blanchard, 1985; Hess, *et al.*, 1990). The enhancement is attributed to multiple scattering mechanisms within the vegetation canopy and the water surface underneath. Airborne and spaceborne L-band data provided particularly strong returns, whereas X-band data revealed only moderate scattering effects mainly related to the vegetation volume. However, low vegetation such as marsh grasses, when flooded, provided higher backscatter at X-band than at L-band.

The analysis of the radar backscatter properties of floodplain vegetation provides an interesting observation at different frequencies. Alluvial forest areas can be clearly identified on SIR-A and SIR-B L-band data (Ford and Da Cunha, 1986). The same forest type could not be separated from surrounding forest areas on airborne X-band SAR data, however. Ford and Casey (1988) reported that it is

possible to distinguish on a map swamp and lowland forest, tidal forest, wetlands, and clear-cut areas. Radar backscatter values for swamp areas were noted to change as a function of incidence angle. SIR-B data were not suitable for discriminating between different forest types within the mountainous interior of Borneo.

There is evidence that floodplain forest and coastal mangrove forest can be mapped accurately because of their distinct radar backscatter signature in comparison with surrounding forest stands. High radar backscatter of mangrove vegetation was observed in relation to environmental conditions such as salinity, topography, soils, and the presence of water or moisture. Using Ka-band airborne radar, the distribution of mangrove vegetation in parts of the eastern Panamanian and NW Colombian coastlines were successfully mapped in the late 1960s for updating and correcting land survey data (MacDonald, *et al.*, 1971; Lewis and MacDonald, 1969; Dellwig, *et al.*, 1978). Similar observations were made during the analysis of X-band radar imagery acquired over coastal regions in Cameroon and Nigeria (Adeniyi, 1985/1986; Lewis, 1977). It was later demonstrated that radar incidence angle variations influence the backscattering behavior of mangroves. It was difficult to differentiate the radar signature of mangrove vegetation from that of other tropical forest types if the incidence angle was greater than 60 degrees.

3.2 Coastal and Marine Environments

Airborne and satellite SAR imagery has been used in a variety of coastal zone studies, primarily in North America and Europe (Radarsat International, 1992), but it also has been used in other coastal regions, including the tropics (Thompson, *et al.*, 1990). In fact, some of the first radar mapping projects were carried out in tropical environments and looked at general land use and geomorphological phenomena (Lewis, 1977). The majority of these investigations fell under research and development, and there is no mention in the literature that SAR is used operationally; topo-

graphic map revision in tropical coastal regions is a notable exception. Study topics include the observation of ocean surface features in shallow coastal waters, potential use of SAR for evaluating erosion and sedimentation of shorelines, identification of aquaculture sites, analysis of intertidal features, flood assessment, and other morphological and cultural features in coastal regions (Werle, 1993). A topic of particular interest has been pollution control, especially oil spill detection.

Compared to imaging and measuring of deep ocean waves by means of SAR, the investigation of near-shore wave and refraction patterns has not stimulated much research. Carter, *et al.* (1988) provided evidence that the majority of requests for wave information during the 1990s have been for positions either relatively close to land, such as on the continental shelf, or on the coast itself. Requests are mainly for short-term forecasts and for information that can be used for the design of offshore structures and shore defenses. In some instances the information is needed for an area or along a track, but in many cases the information requirement is site-specific.

The main problem in obtaining useful data in coastal waters is the considerable change in wave conditions that occurs over relatively short distances because of changes in fetch, bottom topography, currents, and tidal patterns. Airborne and spaceborne SAR data have provided compelling examples of such features, and the prospect of using radar imagery for practical applications in coastal zone engineering and environmental monitoring is considerable. Currently, however, the understanding of SAR imaging mechanisms involved in detecting sandbanks, sand waves, surface expressions of near-shore currents, and patterns of near-shore wave refraction is not clear. The evaluation of bathymetric signatures and their patterns in SAR imagery may assist oceanographers and hydrographers in detecting bottom features and submerged hazards for navigation (Kasischke, *et al.*, 1983). Therefore, SAR imagery can be used as an additional tool for updating nautical and hydrographic charts of coastal areas and as a

reconnaissance tool for coastal engineering and environmental assessment projects.

Radar cannot be used for direct probing of the water column or sea floor because microwaves can penetrate the water surface by only a few centimeters at best. Therefore, SAR can be used only to detect hydrodynamic processes that can be coupled to the bottom topography. Under suitable conditions, such as moderate wind and strong tidal current, these processes modulate the amplitude of the short waves at Bragg wavelength, which is the main contributor to the backscattered microwave energy received by the SAR antenna. While many of the following SAR observations relate to coastal and tidal phenomena, it is important to note that their significant SAR imaging mechanisms may also apply to flow dynamics and bed form assessment of the major river systems in Bangladesh.

Meadows, *et al.* (1980) were able to observe refraction and diffraction of gravity waves, surf zone location, surface currents, and long-period "surf-beats." Outflow patterns of major rivers draining into open water have been detected on radar imagery of the Mississippi delta and the Columbia River (Gaddis and Mouginis-Mark, 1985; Gonzales, *et al.*, 1985).

Koopmans and Wang (1993) examined multi-temporal ERS-1 SAR data of the intertidal zone along the North Sea coast of the Netherlands. Their study provides evidence that spaceborne radar is capable of monitoring tidal activities, including tidal current dynamics and intertidal terrain features.

Griffith, *et al.* (1988) explored the potential of imaging radar for assessing fish stocks. Using airborne SLAR imagery, it was experimentally demonstrated that surface-schooling fish like tuna and jack mackerel can be detected well beyond the range of the usual visual spotting technique. Petit, *et al.* (1992) demonstrated that airborne SAR data can be useful for detecting marine surface life, such as schooling tuna and marine mammals, and fishing gear, such as nets and fish traps. Simulations of

ERS-1 SAR image characteristics also indicated promising results and a unique opportunity to obtain direct information on fishing activities in large survey areas.

The potential of detecting mineral oil spills has received growing attention because of their adverse effects on marine life in coastal waters. Imaging radar data has been used repeatedly as an all-weather surveillance system and for contingency planning purposes (Fingas, *et al.*, 1992). Wahl, *et al.* (1993) presented evidence that radar satellites may become a cost-effective tool for monitoring ship traffic and oil pollution. They evaluated ERS-1 SAR data and confirmed several observations of oil slicks. Difficulties in identifying oil slicks were encountered under high wind conditions.

The detail of information in radar imagery does not equal that obtainable from aerial photographs. Taking coastal zone terrain features as an example, one may summarize the limitations and advantages of radar as follows (MacDonald, *et al.*, 1971; Ellis and Richmond, 1990): SAR data provide a precise enough basis for assessing net changes of the littoral zone in dimensions or shape using multi-temporal data for analyzing morpho-dynamic processes and for updating charts; estimates of sediments deposited as shoals, tidal delta formation, near-shore processes, and sea state may be observed.

3.3 General Land Use

Relatively few attempts have been made to obtain airborne and spaceborne SAR data specifically for agricultural and general land use analyses in the tropics. Studies conducted during the 1970s and early 1980s in South and Central America, Africa, and Southeast Asia commented on the general ability of SLAR and SAR to differentiate between natural vegetation associations, cultivated land, and other land use such as settlements, transportation networks, and related infrastructure. Difficulties were encountered in identifying specific crops. More recent digitally processed SAR coverage

obtained by STAR-1 has proved to be more easily interpreted than the SLAR and SAR imagery on which much of the previous experience was based. ERS-1 SAR data acquisition for tropical land use analysis also has contributed to recent advances in developing this application (ESA 1992/1993). Yet there is little general knowledge regarding the phenological changes of important tropical crops and the related radar backscattering behavior as it changes during the vegetation period. The development of such a knowledge base is important in order to optimize a SAR data acquisition schedule for experimental and operational crop analysis.

SIR-A and SIR-B imagery of South and Southeast Asia have occasionally been used for experimental regional land use studies (Sood, *et al.*, 1985; Imhoff, *et al.*, 1987). In Central India, six major land use categories and 18 subcategories were identified. Pondered water was difficult to delineate against fallow land because of the similarity of their dark radar signature. Land use studies carried out with SIR-B SAR data in Bangladesh toward the end of the monsoon season revealed that immature rice fields with little or no standing crops can be distinguished from mature rice fields that provide larger amounts of radar backscatter. Mature rice and jute fields, however, display similar signatures and therefore cannot be differentiated. Also, in the absence of any contextual information, the tonal signature of turbulent water surfaces may be easily confused with that of agricultural land.

Ahern, *et al.* (1990) reviewed regional and nationwide tropical vegetation surveys carried out by a number of investigators. Major vegetation formations—and to some extent ecological transition and tension zones within the tropics—have been identified, including savanna, dense and open tropical forest, and woodland mosaics. Difficulties were encountered in identifying specific formations in hilly or mountainous terrain. STAR-1 SAR data analysis of several tropical areas, including Australia, Malaysia, Congo, Costa Rica, and Colombia, showed that primary and secondary forest can be differentiated. Also, a variety of forest cover types have been identified (Thompson and Dams, 1990;

Lowry, *et al.*, 1986; Dams, *et al.*, 1987; Wan Ahmed, *et al.*, 1988).

A vegetation survey in Nigeria was able to distinguish between three general categories: farmland, plantations, and agricultural project sites (Trevett, 1986; Adeniyi, 1986; Gelnett, *et al.*, 1978). Land use analyses indicated that agricultural areas can be characterized in terms of farming intensity and a variety of land use mosaics, including farmland with immature forest and farmland with palm forest. Dry season crops provided characteristically high radar signatures, but it was impossible to clearly separate individual crops such as millet, guinea corn and maize, rice, cotton, or groundnuts. Plausible reasons for this include the patchy nature of traditional farming, field separation by hedgerows, mixed cropping, and/or different sowing and harvesting times for a particular crop.

Wagner, *et al.* (1980) conducted a multi-temporal SEASAT SAR study of a test area in Costa Rica. SAR imagery was available for two dates during the wet season within an 18-day period. The result of the investigation is very similar to that obtained previously by means of airborne SAR and SLAR. Larger fields were identified without difficulty, but small lots could not be distinguished from their surroundings. Generally, very high radar backscattering values were measured for sugarcane and forested land, moderate backscatter values corresponded to pasture areas, and low backscatter originated from rice and cotton fields at the early stage of plant growth. Considerable overlap in the mean radar backscatter values was noted for particular crops and land cover types. Changing vegetation conditions, such as rapid plant growth, were observed and found to be related to a transition from bare soil and emerging crops to a closed canopy. Differences in radar response were mainly attributed to vegetation height.

Land use mapping at the 1:250,000 scale can be done using a combination of SAR and optical data (Aschbacher and Lichtenegger, 1990; King, 1985; Lind, 1984; Muenlek and Koopmans, 1983). SAR is highly complementary to conventional remote

sensing methods because of its ability to distinguish between land use categories with similar reflectivity in the visible and/or near infrared portion of the spectrum but different radar backscattering properties. A case study was conducted by an ESA study team in southern Thailand using digitally registered and filtered SIR-A data and multi-spectral SPOT data for digital land use classification. SAR distinguished particularly well between mainly fallow paddy fields and sugar palm plantations. This separation was not possible using SPOT. SAR was also useful to supplement and classify those areas in the SPOT imagery that were affected by cloud cover.

CHAPTER 4

CONSIDERATIONS FOR RADAR PROJECT IMPLEMENTATION IN BANGLADESH

4.1 Project Design

The development of SAR applications for natural resource analysis and environmental monitoring usually proceeds in three stages:

- Research and development studies, including demonstration projects.
- Pilot projects.
- Operational and quasi-operational use of remote sensing data following the successful completion of the pilot project.

Several key elements of modern SAR led to the first two stages of this development process. The most frequently cited potential advantages of radar remote sensing over optical remote sensing in tropical and subtropical regions are:

- Synoptic view of radar.
- Constant illumination direction.
- Rapid data acquisition during the wet season within a matter of days or weeks for entire countries.
- Reliable revisit and repeat coverage using satellite SAR.
- Sensitivity of SAR to surface roughness, moisture, and motion.

Radar remote sensing permits rapid data acquisition regardless of the time of day or the presence of clouds, haze, or fog. This capability ensures that information can be obtained on short notice under most weather conditions. It should be noted, however, that "all-weather" imaging at higher frequencies like X-band (employed by the inter-airborne SAR systems) may be somewhat restricted in the presence of severe rainstorms. This is

important because severe monsoon rainfall could impede X-band SAR data acquisition in Bangladesh during the wet season. SAR imaging at lower frequencies—C-, S-, and L-band—is unaffected by such weather conditions.

The all-weather imaging capabilities of SAR need to be further qualified in terms of the *effects* that weather conditions may have on the surfaces that are being imaged. While SAR data may be acquired under most weather conditions, the imaging process is not *independent* of weather condition. It has been shown, for instance, that some water surface features may not be detected by SAR under certain wind speed conditions. Careful consideration needs to be given to SAR project planning, selection of appropriate imaging parameters, and timing of data acquisition.

The timeliness of data acquisition, or repeat coverage, is an important aspect if radar's use as a mapping tool is to be extended to include monitoring. In the past, airborne radar has been relied upon to provide high-resolution, single-date coverage for tropical or sub-tropical sites or regions site or region. Only in few cases has repeat coverage been acquired for environmental monitoring. Spaceborne radar is eminently suited to this task. The time between data acquisition opportunities is a function of satellite orbit (inclination and altitude), swath width, and to some extent, resolution. Revisit intervals for polar-orbiting spaceborne SAR systems in lower latitudes may range from several days to a few weeks. It is important to establish whether the revisit interval of a particular spaceborne SAR can meet the temporal

resolution requirement for a given application, for example, assessing vegetation growth stages or monitoring flood levels during the monsoon season.

Spaceborne and airborne SAR system flexibility and digital data processing techniques allow high-resolution/small-area coverage as well as low-resolution/large-area coverage. Therefore, data requirements can be efficiently addressed at local, regional, and even sub-continental scales. SAR systems with both high and low resolution modes could lend themselves well to flood mapping and monitoring in Bangladesh because synoptic, nationwide coverage could be obtained effectively and economically at low resolution, while important areas or sites in flood management could be imaged and monitored in greater detail at high resolution. Well-calibrated systems are required for monitoring tasks and quantitative change detection (Curlander and McDonough, 1991; Rancey, *et al.*, 1990).

Satellite SAR can provide different terrain illumination by using different look-directions. Optical remote sensors rely on the sun for scene illumination. The choice of radar look-direction depends on the orbit inclination and, thus, is restricted to two look-directions during ascending and descending passes of the space platform (Leberl, 1990). The imaging geometry of side-looking radar allows for the acquisition of stereoscopic data and base-mapping exercises. Prototype topographic mapping products consist of radar image maps that combine contour information, SAR imagery, and a digital elevation model (DEM). (Mercer and Kirby, 1987; Leberl, 1990).

On several occasions, SAR data acquired by Shuttle Imaging Radar missions were compared to previously acquired airborne imagery. Evidence from test areas in Panama, Colombia, Brazil, and New Guinea suggests that multiple look-angle and multiple look-direction radar imagery is more valuable for terrain mapping than optical imagery obtained at the highest possible spatial resolution. It is important to optimize radar viewing geometry to the local or regional topography. In spaceborne

SAR, the relatively constant scene illumination at a chosen incidence angle configuration was regarded as a major asset. The decreased resolution of spaceborne *versus* airborne sensors does, however, affect mapping and classification accuracy. For instance, drainage patterns in coastal lowlands are detectable on airborne radar imagery, but the narrow channels cannot be detected on SIR-A imagery (Cimino and Elachi, 1982; MacDonald, *et al.*, 1983; Ford and Da Cunha, 1986).

The collection of field data for use in radar image analysis can be challenging in remote areas where there is a lack of logistical support or thick vegetation cover. Bangladesh is no exception, because flooding frequently isolates areas that are otherwise accessible by road.

4.2 Technology Transfer Issues

The transfer of SAR technology and development of potential applications represents a considerable challenge in developing and developed nations alike. Most national, regional, and local projects aim to define aid policy and establish national self-sufficiency in the use of remote sensing technology. Attempts to realize the full potential of SAR in the development context are marked by pitfalls. The successful introduction of SAR technology needs to be based on firm technical knowledge, adequate training, acquisition of the necessary tools and infrastructure, and a clear orientation toward promising applications.

In order to obtain the most useful image data for a given application, modern SAR technology almost exclusively relies on a more-or-less stringent set of digital signal processing requirements in order to transform the data of *radar signal returns* received by the satellite into actual *SAR images*. In the past, SAR signal processors have been located in relatively few North America and European centers that were in a position, technologically and economically, to satisfy and justify the computational demands and data throughput requirements of SAR. Just as dedicated radar signal

processors are now under development for certain "niche" applications and markets, a similar trend is occurring in the digital SAR image analysis domain.

Currently there is a lack of software suitable for SAR image enhancement and analysis; existing software tools developed for optical sensor data analysis, while usable, have proved inadequate for the task. Affordable SAR image analysis tools for PCs recently have been offered by several vendors. In order to fully exploit the information content of SAR imagery for application development, however, technical and professional training is imperative.

Several lessons can be drawn from large, nation-wide radar projects and related technology transfer. An evaluation of the Nigerian NIRAD survey produced the following thoughts (Adeniyi, 1984), which may be applicable to Bangladesh:

- The pace of development should be determined by the host country in order to develop an indigenous capability in the use and application of SAR technology.
- Local personnel and expertise need to be developed in order to acquire knowledge of how to extract information from SAR imagery in accordance with local needs.
- Any major application of new SAR technology should be preceded by a pilot project to ascertain its chances of success and/or develop alternate strategies.
- Many disciplines should participate in major projects rather than selecting just one application area.

4.3 SAR Application Potential in Bangladesh

The following section explores the potential applications of SAR based on the remote sensing data and information requirements of Bangladesh. It focuses on flood mapping and monitoring, coastal zone monitoring, and land use monitoring.

Table 4.1 summarizes the application potential for radar remote sensing in Bangladesh. Primary environmental application potential of radar remote sensing exists in situations where remote sensing by aerial photography and VIR satellite technology is severely restricted because of environmental conditions such as excessive cloud cover. In this case, SAR would be the *only* reliable remote sensing tool for data acquisition, even though the information content of SAR data may be inferior, but adequate, compared to that of VIR data. Thus, SAR would be the remote sensing tool *by default*, particularly in countries like Bangladesh where it has the operational advantage over VIR sensor for wet season environmental monitoring. Depending on satellite orbit and radar sensor parameters, SAR data may be acquired at pre-selected dates and intervals, regardless of cloud cover or time of day.

Primary technical application potential exists in situations where SAR data can provide information that no other remote sensing tool can provide in comparable spectral and spatial detail, areal extent, and frequency of coverage, such as SAR sensitivity to moisture, motion, and roughness. In this case, the information content of SAR data is superior to that of VIR data. Thus, SAR would be the remote sensing tool *of choice* in addition to its operational advantages.

The following are the primary application areas for satellite SAR in Bangladesh: mapping and monitoring of storm surges, river floods, and excessive rain and flash floods; stream flow dynamics; soil moisture assessment; and wind-wave fields in coastal and marine areas.

Secondary application potential exists where SAR data adds value to information derived from a primary remote sensing source. In this case, several remote sensing methods may be exploited synergistically to maximize the amount of information that can be extracted from remote sensing data. By the same token, SAR or VIR data acquired as primary sources of application information may be used in a complementary way by a variety of users or applications by sharing SAR and VIR data sets

Table 4.1 Areas of SAR Application Potential in Bangladesh

Application Area (monsoon season)	Potential in Bangladesh	Stage of Preparation*	Experience in Bangladesh
FLOOD MAPPING/MONITORING			
Coastal floods	SAR/primary	PoC/R&D	demonstrated
River floods	SAR/primary	PoC/R&D/PP	demonstrated
Excessive rain	SAR/primary	PoC/R&D	none
Flash floods	SAR/primary	not proven	none
Stream flow dynamics & riverbed morphology	SAR/primary	PoC/R&D	demonstrated
COASTAL ZONE MONITORING			
Oceanographic feature detection/cyclones (wind/wave conditions)	SAR/Primary	PoC/R&D/PP	none
LAND USE MONITORING			
Wetlands	SAR/primary	PoC/R&D	demonstrated
Forested environments	SAR/primary	PoC/R&D	demonstrated
Soil moisture & drought monitoring	SAR/primary	PoC/R&D	none
Crop assessment	VIR/primary SAR/secondary	PoC/R&D/PP	none
Infrastructure assess- ment (Settlements, roads, railways, embankments)	SAR/secondary VIR/primary	PoC/R&D/PP	none
EARTH SCIENCES			
Assessment of earthquake- related dis- placement using interfer- ometry	SAR/secondary Seismic/primary	PoC/R&D	none

* (PoC = proof-of-concept; R&D = preliminary research and development studies;
PP = pilot project)

(and their acquisition costs). Again, the objective would be to maximize the amount of information that can be extracted from remote sensing data. Candidate areas of secondary application potential in Bangladesh include crop assessment, forest inventory, infrastructure mapping (settlements, roads, railroads, and embankments), terrain analysis, and possibly, earthquake analysis.

4.3.1 Monsoon Season Flood Mapping and Monitoring

The most appropriate SAR sensor parameters for flood mapping under most environmental conditions are: radar wavelength greater than 5 cm (C-band), medium to large incidence angles (>35 degrees), and HH polarization.

For flood monitoring during the monsoon season, when there may be heavy rainfall, the X-band sensors employed by commercially available airborne SARs may be of limited use because the shorter wavelength cannot penetrate heavy rain. C-band and longer wavelengths (S-, L-, and P-band) are immune to this influence.

This study and other investigations of ERS-1 SAR data sets have demonstrated that small incidence angles (<35 degrees) and VV polarization are sensitive to: changes in water surface roughness as a result of wind speed (>5 m/sec), flooded vegetation, and the impact of rain on the water surface. The radar backscatter associated with these situations tends to reduce the contrast between open water and land features and reduce the possibility of successful detection and classification. Vertically polarized microwave energy produces higher radar returns than horizontally polarized energy, particularly at high incidence angles. This also tends to reduce the contrast between open water and land features.

JERS-1 (L-HH) also appears to be suitable for flood mapping. Scene illumination by the JERS-1 SAR exceeds incidence angles of 35 degrees, and its relatively high frequency (L-band) provides good penetration and high radar return capabilities

when detecting partially flooded vegetation. Disadvantages include low repeat cycles (approximately every three weeks) and relatively narrow swath width (80 km). Nonetheless, the JERS-1 SAR may provide information that sensors operating at higher frequencies cannot, such as better discrimination of flooded and nonflooded vegetation.

The ERS-1 and ERS-2 SARs have some limitations for flood mapping, but their monitoring capability may be enhanced if the orbit patterns of the two satellites can be phased to essentially cut the revisit time in half. Thus, a 35-day repeat cycle could be reduced to approximately 18 days using both ERS-1 and ERS-2 sensors for "tethered" data acquisition. The possibility that the ERS-1 and ERS-2 SAR instruments could be used in an interferometric mode has raised additional expectations that they may be usable for earthquake assessment. The use of interferometric SAR for measuring rates of change on the order half the radar wavelengths—approximately three cm in the case of the ERS-1 SAR—and the development of related image products is still in the research and development stage, however.

Based on the simulations, RADARSAT will be suitable for delineating flood boundaries and, in all likelihood, flooded vegetation. C-band RADARSAT SAR will be able to cover 80 percent of Bangladesh and adjacent coastal waters every three days, and it will allow monitoring of dynamic events, including the build-up and recession of a flood (Figure 2.4). Optimum imaging conditions for flooded areas (radar incidence angles greater than 35 degrees), however, may not be obtained as frequently as desired within the 500 km-wide swath of the SAR. Weekly time intervals are considered achievable for assessing flood extent.

All tested RADARSAT SAR modes appear suitable for flood mapping and monitoring. Fine beam mode, with a resolution of 10 m, appears suitable for generating new flood risk maps or updating existing ones because linear features, like roads, are still apparent and may be used as reference fea-

tures for image-to-map registration. ScanSAR mode, particularly the 250 km-wide far-range half of the mode, appears most suitable for delineating the extent of flooding and monitoring major floods at reconnaissance scales. Depending on RADARSAT orbit patterns, a single swath of

4.3.2 Coastal Zone Monitoring

Mapping and monitoring coastal and marine environments during the monsoon and cyclone seasons by means of satellite SAR appears to be a useful addition to weather satellite monitoring.

Table 4.2 Flexibility of RADARSAT SAR System (after Parashar, *et al.*, 1993)

RADARSAT Mode (swath width)	Resolution	Scale	Revisit Period
ScanSAR Wide mode (500 km)	100 m	nation-wide	> 3 days
ScanSAR Half-swath mode (250 km)	50 m	regional	bi-weekly
Standard beam mode (100 km)	25 m	regional	bi-weekly
Fine beam mode (40 km)	10 m	local	> bi-weekly

ScanSAR coverage during both ascending and descending orbits can cover the entire country at a resolution of approximately 100 meters. Key flood areas could be monitored at 35 degrees-plus incidence angles using the RADARSAT imaging modes listed in Table 4.2 (also see Figure 2.4).

Mapping and monitoring river bed morphology throughout the monsoon season appears to be another potential application for satellite SAR. The most dynamic changes in riverbed morphology occur when high current velocities are close to or directly affect river bedforms; this occurs during periods of lower flood levels. In terms of SAR system parameter selection, small incidence angle (20 to 30 degrees) data sets are more suitable than moderate-to-high incidence angle ones for capturing the backscatter associated with expressions of current velocity modification in response to riverbed morphology. The ERS-1 and 2, as well as small incidence angle RADARSAT SAR modes would be most suitable for this potential application.

Satellite SAR potentially could supply data on surface-level oceanographic conditions associated with cyclone activities in the Bay of Bengal.

The 250 km-wide near-range half of the RADARSAT ScanSAR swath appears to be most suitable for synoptic views and for obtaining frequent coverage at the small incidence angles required for detecting ocean surface features. Other SAR sensors, particularly ERS-1 and ERS-2, can also provide valuable data for coastal and oceanographic research and development activities, although their relatively narrow swath width and long revisit interval are less suitable for monitoring tasks.

A key parameter for monitoring coastal environments is the surface wave field and associated currents. Knowledge of the waves and currents is required for: engineering applications (design of coastal structures), waste disposal (marine sewage systems), scientific applications (coastal sea life habitat, sediment transport, and dynamics), and management of such resource-based activities as commercial fisheries and aquaculture. Along the

coast, waves are particularly difficult to measure with existing technology due to the refractive and shoaling effects of shallow water on approaching offshore waves. Satellite-based radar offers the possibility of mapping wave conditions, shoaling, current, and tidal activities over large coastal zones. The mapping capability is particularly valuable right along the coast, where wave conditions change significantly over short distances. Radar-based measurements also offer an all-weather capability, which is particularly critical to engineering design applications, since the largest waves are associated with severe storms.

The capability of incorporating SAR data into coastal zone monitoring activities currently is far from operational in Bangladesh. To make it so will require research and development of applications, skills development, and technological capability.

4.3.3 Land Use Monitoring

There are several noteworthy potential applications of SAR for land use applications in Bangladesh. These include soil moisture analysis during the dry season, agriculture/crop assessment, the analysis of forested environments, and wetland ecology. Satellite SAR can be used as a primary or secondary data source in conjunction with optical satellite data.

4.3.4 Earth Sciences

Several noteworthy potential applications of SAR exist. These include terrain analysis and assessment of earthquake zones. Satellite radar, as a primary or secondary data source, may provide useful structural-geological information for updating and revising existing Bangladesh maps.

CHAPTER 5

APPLICATION STUDY USING RADAR IMAGERY FOR FLOOD MONITORING

This chapter contains a detailed account of the digital SAR image analysis and data integration exercise carried out in support of the radar application study. The study approach and data sets, including ground reference data, are introduced first, followed by a description of the image processing procedures and an assessment of the flood mapping results.

5.1 Approach

With the notable exception of an experimental case study (Imhoff, *et al.*, 1987), airborne and spaceborne SAR have not been used in Bangladesh for natural resource analysis and environmental monitoring. This project represents the first effort to evaluate the usefulness of multi-temporal satellite SAR imagery in Bangladesh. The ability to acquire local and regional SAR data of flooded terrain and adverse weather conditions, and the usefulness of SAR image analysis, have been demonstrated elsewhere by Leconte, *et al.* (1989) and Chen (1988). Based on these North American and Chinese demonstration projects, SAR data distributors see considerable potential for the operational use of satellite SAR imagery for flood mapping and monitoring (Radarsat International Inc., 1993).

Mapping the extent of the 1993 monsoon flooding using radar remote sensing consisted of several steps, including: (1) SAR data acquisition by the European ERS-1 satellite over selected study areas in May, July and August, 1993, and collection of other geographic data sets; (2) design and execution of a ground reference data program; (3) digital

SAR image processing and analysis; (4) evaluation of results for a test area and extent of test results to larger floodplain regions covered by the ERS-1 SAR scenes; and (5) integration of SAR image analysis results with ground reference data and other GIS data sets and assessment of results.

5.1.1 Study and Test Areas

The main study areas coincided with the extent of the ERS-1 SAR scene coverage of the Ganges/Jamuna rivers confluence in central Bangladesh and the Sylhet region in northeastern Bangladesh (see Figures 1.1 -1.3, 1.5). ERS-1 SAR scenes were selected for areas that exhibit floodplain conditions representative of those in Bangladesh during the onset and height of the monsoon season. The main physiographic regions and agronomic practices of the area are described in Figures 1.4 and 1.6.

The Tangail district was selected as a test area for detailed image analyses and GIS data integration (Figure 5.1). The test area is located on the left bank of the Jamuna River and encompasses the Tangail Compartmentalization Pilot Project (CPP), or FAP 20. A schematic profile of flood conditions in the Jamuna River floodplain is presented in Figure 5.2. Much of the land is inundated by rainfall and river water during the monsoon season; the areal extent of flooding is basically defined by topographic features within the floodplain. Flooding of low areas begins with pre-monsoon rainfall in May and June; it reaches a peak in July and August. While rice is the dominant crop, other crops include jute, wheat, mustard, sugarcane and

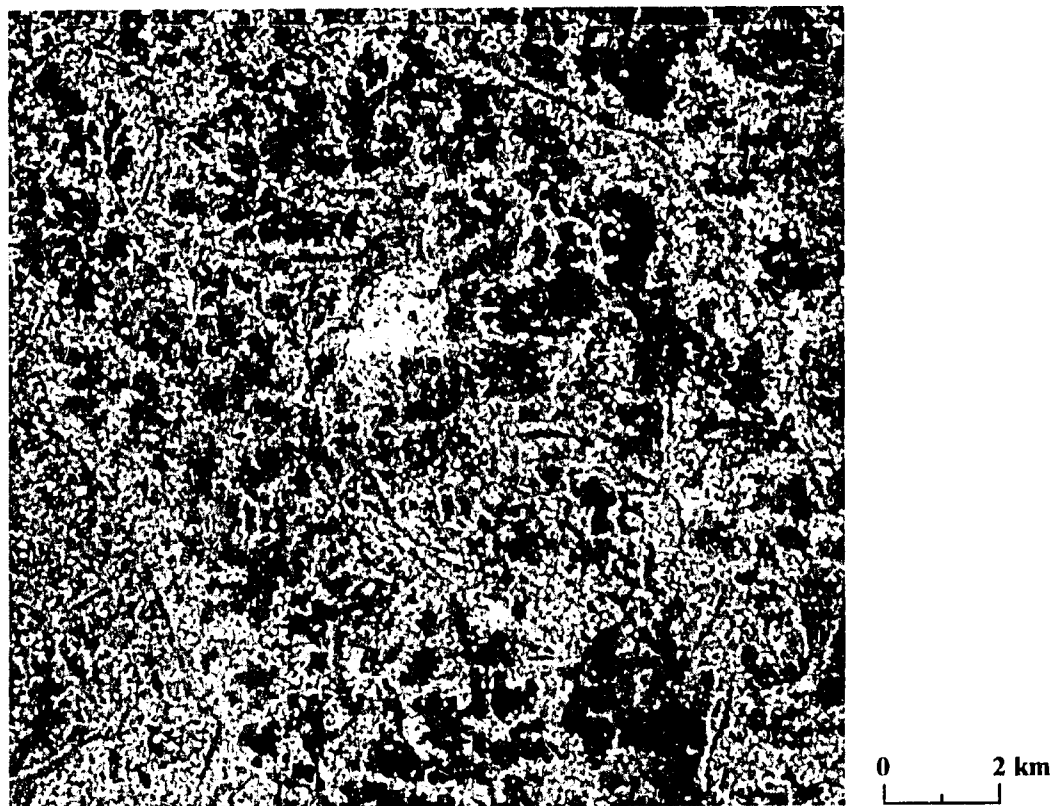


Figure 5.1: ERS-1 SAR Subscene of the Tangail Test Area, July 24, 1993. This 25 m resolution, MAP filtered image covers an area of approximately 15 km by 15 km. The location of this subscene is indicated in Figure 1.2.

pulses. Land use maps for the Tangail district indicate that jute covered 16.5 percent and sugarcane covered 7.5 percent of the agriculturally productive area in 1991/92 (FAP 20, 1992). The fishery is another important source of nutrition and income for the 260,000 people in this area, of whom 60 percent live outside the town of Tangail.

The test area comprises approximately 13,000 hectares, roughly 70 percent of which is cultivable land and 30 percent are homesteads and homestead forests, roads, and permanent water bodies like rivers and *beels*. The Tangail CPP has some flood protection from a low embankment and some means of controlled flooding from inlet sluices; however, the drainage is uncontrolled. There is a provisional division of the Tangail CPP into 16 subcompartments that are formed by roads, rivers,

embankments, or major landscape elements that influence flooding and/or drainage.

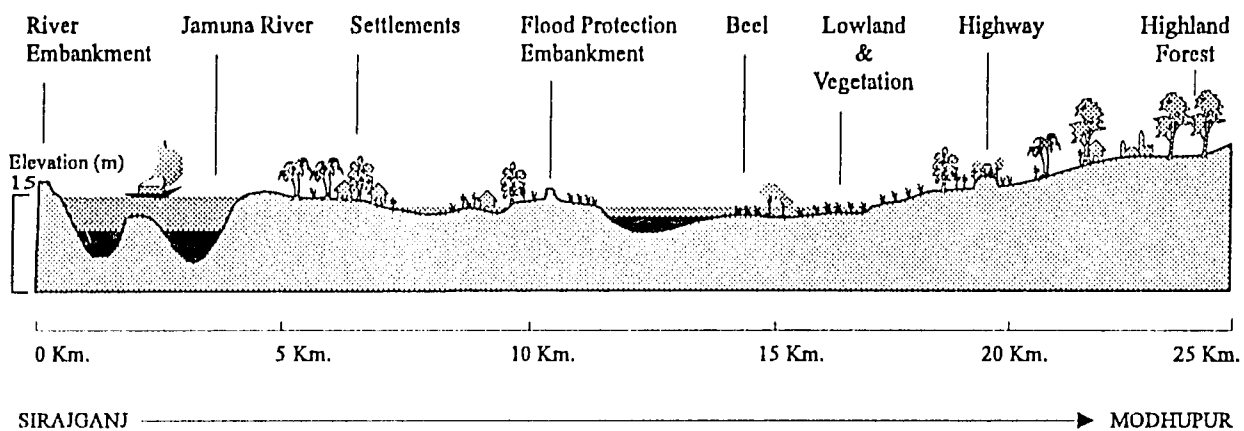
5.2 Data Sets

The primary data used for the pilot study was ERS-1 SAR imagery. Other ancillary data sets, such as Landsat TM and SPOT satellite images, and flood model data and topographic information, also were compiled and used in this study.

5.2.1 ERS-1 SAR Data

The ERS-1 SAR operates at a frequency of 5.3 GHz (C-Band) in vertical transmit and vertical receive antenna polarization (C-VV), and illuminates a 100 km-wide swath to the side of the

33



LEGEND

-  Homestead trees
-  Crops
-  Settlements
-  Monsoon Water Level
-  Dry Season Water Level

Figure 5.2: Schematic Profile of a Typical Landscape in Bangladesh. Included is the Jamuna River, the recent floodplain and Pleistocene upland terraces. Land and flood scape elements are idealized; heights and distances are relative and can vary considerably. In the case of flood levels and terrain, local variations are on the order of a few meters and subtle changes can greatly influence cultivation and land use practices.

satellite nadir track. The radar beam angle of incidence at mid-swath is 23 degrees. The nominal SAR resolution is approximately 25-30 meters in both range and azimuth directions, with 12.5 x 12.5 m pixel spacing in a 100 km by 100 km scene (ESA, 1993).

The ERS-1 satellite can acquire SAR imagery on both descending daytime orbits and ascending nighttime orbits. The SAR data were received at an ERS-1 ground receiving station near Bangkok, Thailand. The FAP 19 image processing and analysis effort concentrated primarily on two scenes that were acquired for an area around the confluence of the Ganges-Brahmaputra/Jamuna rivers in central Bangladesh on July 24, 1993 (orbit 10570/frame 3123) and August 28, 1993 (orbit 11071/frame 3123). The date of the SAR images cover the main flooding period for the floodplains.

Additional image processing was carried out using SAR data acquired in May, 1993 for the Sylhet area.

All images were processed in Germany (D-PAF) as SAR Precision Image (PRI) products (ESA, 1992). These 16-bit images include multi-look processing, geometric correction (slant-to-ground range), and first-order radiometric corrections (antenna elevation gain, antenna pattern, and relative calibration). The data product was generated by using three power-detected looks, over-sampled prior to detection (Vass and Battrick, 1992).

According to records of the Bangladesh Meteorological Department, the following atmospheric conditions generally prevailed during ERS-1 SAR data acquisition for the areas studied. On July 24, 1993, the cloud cover was 100 percent, occasional light precipitation occurred,

34

and variable light winds were recorded; on August 28, 1993, the cloud cover was 100 percent, no precipitation occurred, and there were light southeastern winds at five knots per hour.

5.2.2 Other Satellite Remote Sensing Data

Two frames of Landsat 5 Thematic Mapper imagery also were acquired over central Bangladesh during the dry season in March 1993 and January 1994 (path 138/row 43). In addition, a set of hardcopy 1989, 1:50,000-scale SPOT images covering the areas concerned were used for georeferencing purposes and selecting ground control points. These images were provided to ISPAN by FPCO.

5.2.3 Topographic Map Information and Digital Elevation Model Data

In order to facilitate the ERS-1 SAR data analysis, a GIS database was created using existing GIS data for the Tangail district. For the test area, which covers the Tangail CPP, the GIS database included: major roads; embankments; permanent water bodies; settlements; and biophysical data such as crops, soils, and topography. Map accuracy and quality control was variable because the original data sets came from a variety of sources (FAP 19, 1992).

FAP 19's semi-detailed digital elevation model (DEM) of this area, generated from the Bangladesh Water Development Board (BWDB) 1960s ground survey, were digitized as point elevations at 100 by 300 m and 175 by 175 m point spacing. Digital elevation values were interpolated to a 25m grid pixel (FAP 19, 1993). In addition to these GIS data, more detailed information was compiled for a selected area from a 1:10,000 scale orthophoto that was produced in 1990 by FINNMAP. Surface features digitized from this map included settlements, water bodies, and road networks. Also, a more detailed DEM was generated for this area from the orthophoto's 0.25 m contour lines that were digitized in a "layer-cake" representation and rasterized at a 25-meter resolution cell size.

Figure 5.6 contains sample area of 2 km by 4 km for illustration purposes.

5.2.4 MIKE 11 Flood Model

The flood model result for the Tangail area was collected from the Flood Management Model (FMM) of FAP 25/FPCO in the form of a digital flood depth map. The mathematical flood model was generated using MIKE 11, a one-dimensional hydrodynamic-hydrological model that provides elevations of flood water levels. FAP 25, with the collaboration of FAP 20 (Compartmentalization Pilot Project), set up a detailed FMM (MIKE 11 plus GIS) for the Tangail Compartment Pilot Project Study area in which the river and flood plains were modeled separately (quasi two dimension modeling). The floodplain is more difficult to model than the river because the floodplain it does not follow a defined course; it behaves like a simple storage basin with characteristics which vary with flood levels. Floodplain cells receive, store, and drain flood water, but the FMM model does not consider the conveyance, except via links which model the flow between river and floodplain. A link may be an embankment, a natural levee, or a *khal*.

FAP 25 produced the flood depth and extent maps by the intersecting two surfaces: the water surface generated from the flood model simulation and the land terrain of the same area as derived by a DEM. The digital flood depth maps for July 24 and August 28, 1993, were prepared and rasterized to 25-meter grid cell and provided in GIS format to FAP 19 for further analysis.

5.3 Ground Reference Data

The objective of FAP 19's ground reference data collection program was to correlate ground observations with the radar backscatter responses observed in the SAR imagery. The program involved approximately 60 person-days of field work in May, July, and August 1993. For the scene of central Bangladesh including Ganges/

25

Jamuna river confluence, more than 90 site observations, measurements, and associated polygon data were used as ground reference in the SAR image analysis procedure. In the case of the Sylhet region, data collected from more than 40 sites were used. The results of the ground reference data program for the central Bangladesh scene are contained in Appendix A.

5.3.1 Data Collection Strategies

Ground observations of the area covered by the ERS-1 satellite were recorded systematically on May 28, July 24, and August 28, 1993. The information gathered consisted of general features, degree of flooding, crop or vegetation canopy, geographic position, and reference to any on-ground photographs recorded. Polygons of varying extent representing the areas of data collection were first drawn on hard copy air-photos and satellite images, and later digitized and tagged with a reference identification. The SAR signatures associated with the prevailing land use in those polygon areas were then further analyzed.

5.3.2 Descriptive Parameters

Field data were systematically referenced and coded with each site categorized according to ground cover or water surface characteristics, and degree of flooding. The main categories included settlements, seasonally flooded or inundated crops and other cover types, and water bodies. These categories were further subdivided into urban and rural settlements; sugarcane, jute, rice, weeds, grass, and water hyacinth crops or cover; and river, pond, and *beel* water bodies.

Observation criteria for each site and category included descriptive terms, flood depth, and degree of ground cover or canopy closure. Flood depths were measured or estimated in 10 cm intervals ranging from zero to more than 100 cm of flooding. Ground cover and canopy closure was assessed in percentages at 10 percent intervals.

Location, measurements, weather conditions, and other observations were entered on customized data sheets. In addition to positional information (Geographic Position Systems (GPS) recorded latitude/longitude), 35-mm ground photographs were taken and logged to illustrate flood conditions (see Figure 1.7, Photos A-F).

The field notes were compiled into a comprehensive hierarchical classification and coding scheme that was based on prevalent land, vegetation and flooding conditions. The flexibility of the classification system, shown in Appendix B, proved very useful, as it allowed assessment of ground information at all levels from broad to very detailed. In addition to ground conditions, meteorological conditions were recorded at each site and were correlated with data from the Meteorologica Department.

5.4 SAR Image Processing and GIS Data Integration

This section details the approach and technical procedures of the ERS-1 SAR image analysis and the data integration exercise. The analysis was carried with microcomputers using ARC/INFO, ERDAS, IDRISI, and EarthView software packages.

5.4.1 Strategy and Tools

The SAR image processing and GIS data integration procedure is graphically summarized in Figure 5.3. The approach relies on three major steps: preprocessing, classification, and product generation.

At the *preprocessing* stage, various SAR filter options were introduced and tested with the most effective filter being selected for the entire SAR scene. A comparison of a raw SAR subscene, a resampled SAR subscene, a filtered SAR subscene, and a corresponding Landsat Thematic Mapper (TM) subscene is shown in Figure 5.4. Because of the presence of image noise (speckle), caution is

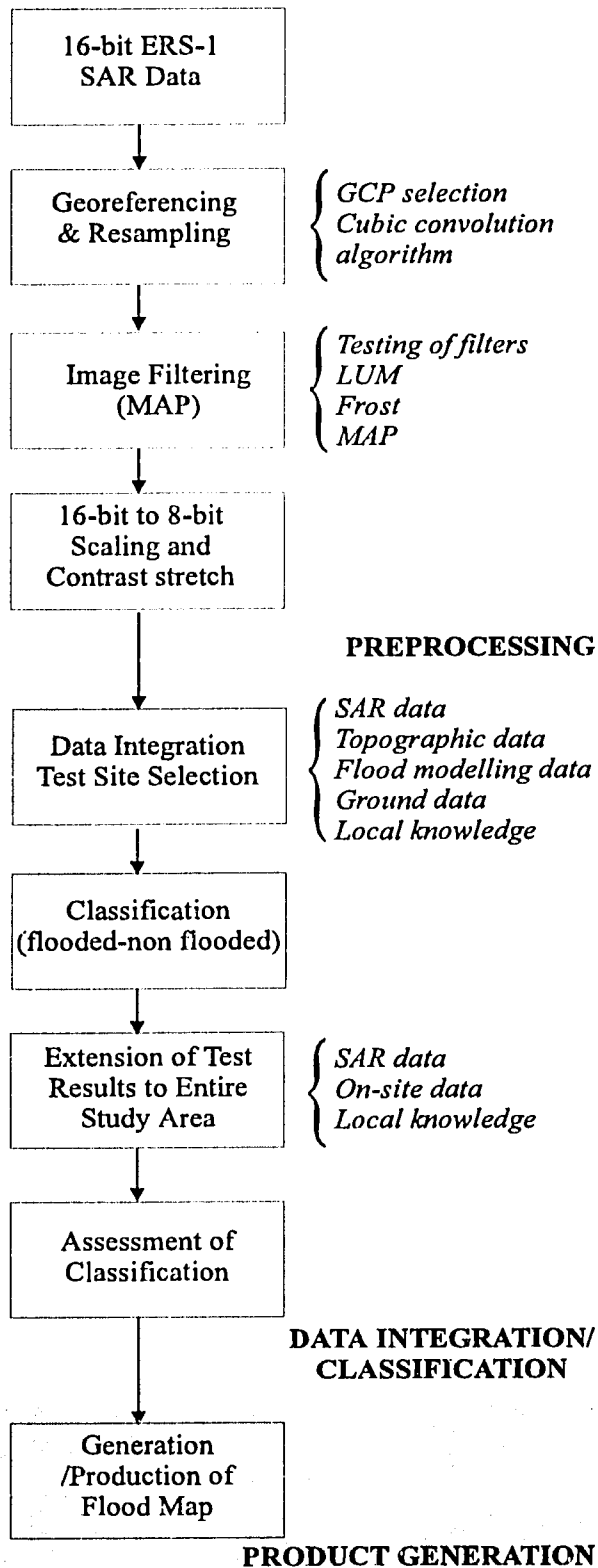


Figure 5.3: Flow Chart of SAR Image Processing Procedure.

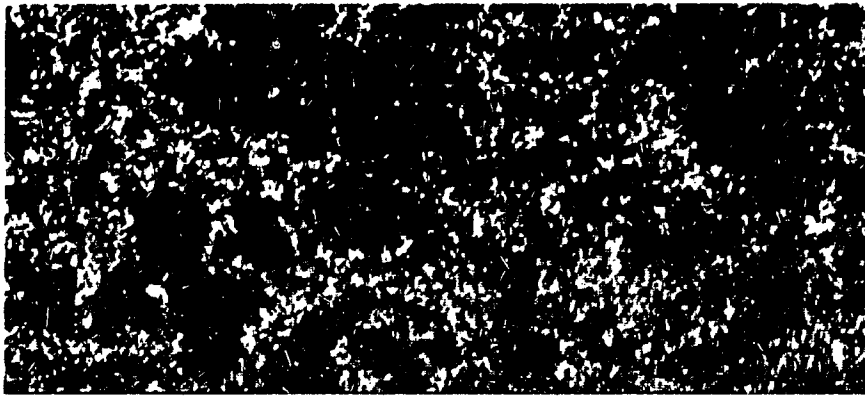
needed when choosing appropriate SAR image processing tools. Procedures and tools that are viable for VIR data analysis often do not work as well with SAR data because speckle statistics tend to produce classification results that compare unfavorably with those obtained for VIR data. Furthermore, VIR data are not affected by noise in the same way as SAR data, and thus produce lower standard deviations during classification.

The strategy for *classification* of the SAR image for flooded and non flooded terrain relied on a stepwise approach. A density slicing technique was chosen as the first step, followed by a computationally more intensive and more refined process to further segregate the density slices. The classification and post-classification steps were carried out for the Tangail test area and then implemented for the entire ERS-1 scene during the next step.

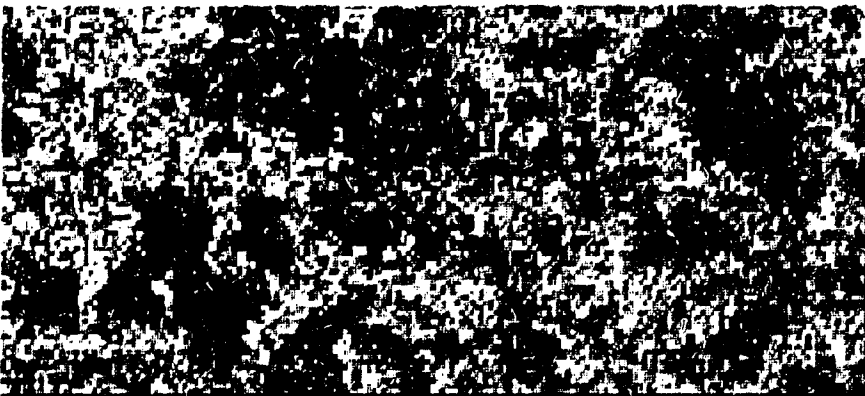
At the *production* stage, a flood map product was generated using data from the entire ERS-1 SAR scene. The classification of flooded and non flooded was restricted to the floodplains in order to avoid confusion with the complex radar signatures of the high velocity water surfaces of the major rivers as well as the hilly terrain not subject to normal monsoon flooding under study.

5.4.2 Geo-referencing and Resampling

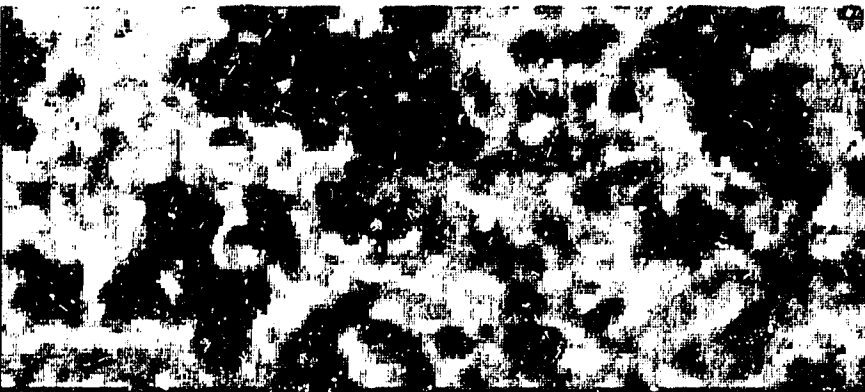
The full ERS-1 precision processed images were read from nine-track computer compatible tape (CCT) into the ERDAS image analysis system. It was necessary to georeference the SAR data in order to integrate ancillary data available in the Transverse Mercator (Everest) projection and for coregistration of SAR images to enable multi-temporal analyses. Ground control points were collected, based on observable features in both the July SAR imagery and 1:50,000-scale SPOT satellite image maps. A first-order transformation (rotation) was applied, and it yielded adequate results because of the flat terrain and the geometric integrity of the SAR images.



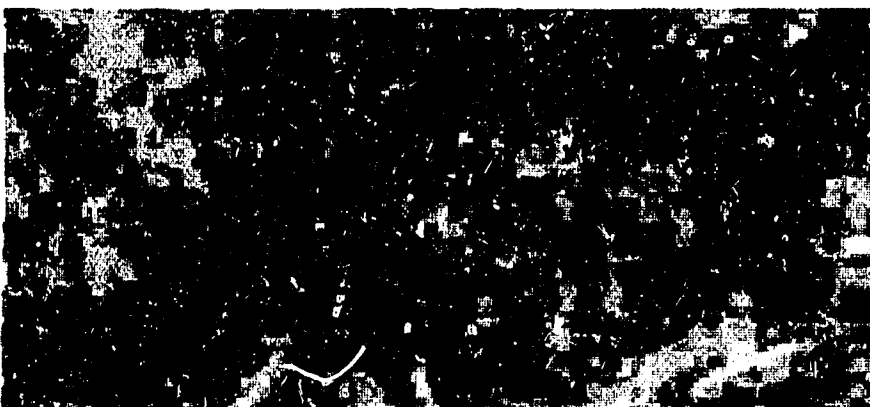
A: A subscene of the August, 1993, monsoon season ERS-1 SAR original, or "raw," image with 12.5 m pixels.



B: The above image resampled to 25 m pixels.



C: The above image after MAP filtering with a 3 by 3 pixel filter size that effectively reduced the amount of image noise, or "speckle," in the image. Filtered SAR imagery tend to produce more reliable classification results than unfiltered image data.



D: A Landsat TM subscene (25 m pixel size) taken in the dry season, January, 1995, and covering the same area as the above SAR images. The Landsat bands displayed are 4, 3 and 2. Note the lack of image noise in the Landsat TM data.



Figure 5.4: Series of SAR Images Showing the Effects of Resampling and Filtering, and a Landsat Image of the Same Area.

During the resampling, the SAR image was block-averaged to a 25 m by 25 m pixel spacing. This reduced speckle and more closely matched the pixel spacing to the actual ground resolution of the ERS-1 SAR data. This procedure also reduced the data volume, a concern when using PC-based image analysis software. A cubic convolution algorithm was used to preserve the statistical relationship (mean and standard deviation) between the input pixel values in the four by four sampling window and the resulting output pixel values. This is a significant point for resampling SAR image data with the imbedded random system noise (speckle).

A three-pixel RMS error occurred from the July ERS-1 image geo-referencing to the SPOT image maps. At 25 m by 25 m this represents a possible error of 75 meters. Once the July SAR scene was geo-referenced, the August SAR image was co-registered by locating observable targets in both images and noting the map coordinates from the July image. This procedure ensured the most accurate relative match between the two images. Less than one pixel RMS (root mean square) error occurred overall from the August ERS-1 image geo-referencing to the July ERS-1 image. This indicates a good relative registration between the two image data sets. The August image was then transformed and block-averaged according to the same procedure applied to the July scene.

5.4.3 Filtering, Scaling, Stretching

During georeferencing and resampling, the 16-bit format data was maintained for both July and August ERS-1 SAR images. A subscene that contained coverage of the Tangail test area was used to determine a suitable filtering procedure. This procedure was then applied to the entire ERS-1 SAR data set.

The SAR imaging process is inherently sensitive to small range variations and produces seemingly random speckle in the data. The speckle degrades image clarity and tends to complicate interpretation and classification. Therefore, SAR image data normally

require specialized filtering procedures to shift the Raleigh-type distribution, caused by the speckle, to a more Gaussian-type of distribution. The unfiltered and filtered histograms from the August image indicate the effects of the filter on the distribution of the data; this is shown in the smoother slopes and narrowing of the brighter regions of the distribution curve (Figure 5.5, top and center). The result of the 16-to-8-bit scaling and stretching is illustrated in the histogram (Figure 5.5, bottom). In the scaled and stretched histogram, the resulting Gaussian-type distribution is evident. The result is a more effective data distribution through the significant portions of the image histogram. This was important for optimizing the spectral separation of the significant SAR targets and related land use classes.

Filtering results were consistent with those reported in other studies that used various filters for assessing filter effectiveness on ERS-1 SAR data and in geoscience investigations (Paudyal and Aschbacher, 1993). The 3 by 3 MAP SAR filter produced the best overall results for the flood mapping application by reducing system speckle and maintaining image sharpness without making a heavy demand on computer processing time. This filter also preserved the spectral character of the darker and the brighter SAR returns--an important aspect when digitally classifying the radar data into flooded and nonflooded areas. Table 5.1 summarizes the filter results.

Median Filter. The median filter enhances an image by replacing each pixel in the file with the median of itself and its neighbors, selected by a filtering window (Lee, *et al.*, 1993). This basic SAR filter reduces a degree of speckle while maintaining some image sharpness. It is best run on high-quality multi-look processed SAR data with well reduced system noise. The ERS-1 SAR data was processed at "three looks." (A "look" refers to a process whereby adjacent pixels were averaged to produce an image of lower resolution, but also of reduced speckle.) The image, therefore, had

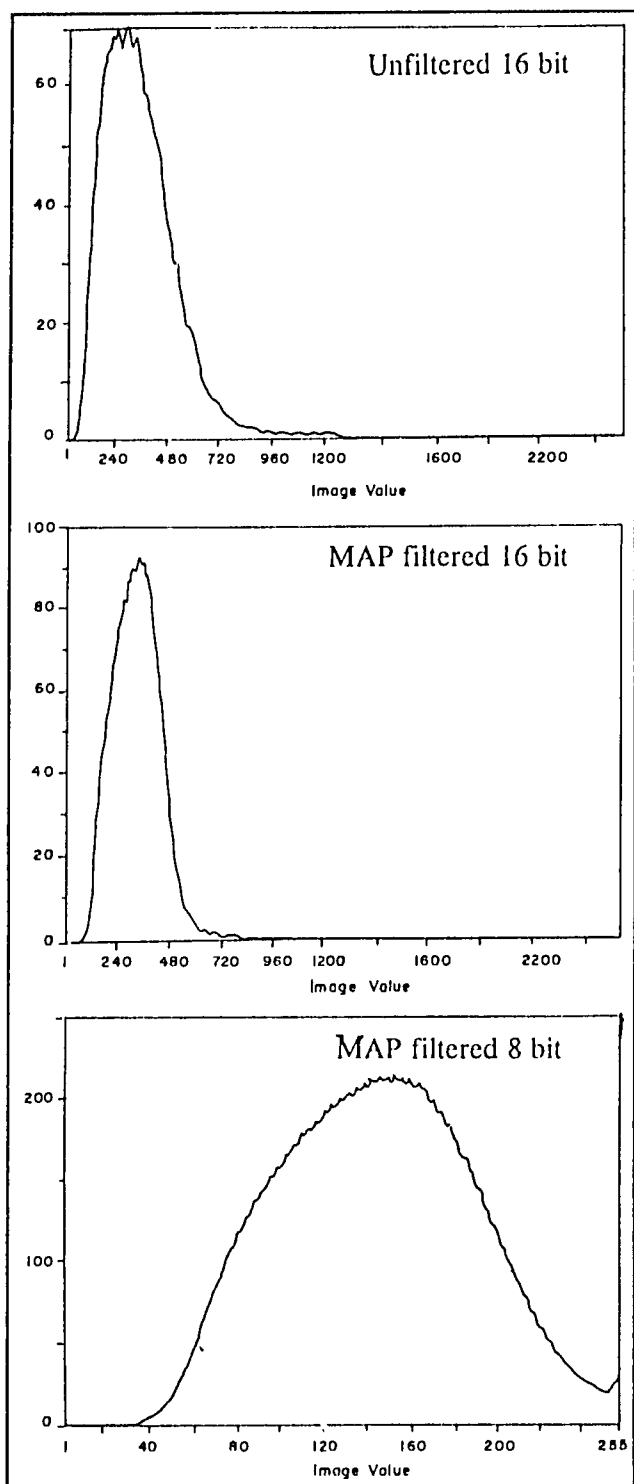


Figure 5.5: Histograms of SAR Data At Various Steps of Processing. Shown are histograms of unfiltered and uncompressed 16-bit SAR data (top); MAP filtered, uncompressed 16-bit SAR data (center); and MAP filtered, compressed, 8-bit SAR data (bottom) for the Tangail test area's August, 1993, image.

moderate system noise, meaning that the median filter only gave average results. A 3 by 3 filter size was used to test this method.

Lower-Upper-Middle (LUM) Filter. LUM filters are rank order-based and are used on data that requires smoothing and image sharpness. Lower-order and upper-order statistics are calculated and compared with the middle sample in the filter window in order to determine the output pixel value. This filter can function as a modified median filter with edge enhancement, depending on the amount of sharpening allowed on the data. The filter requires two user-defined parameters, one for smoothing and one for sharpening (Atlantis Scientific, 1994). Some 5 by 5 LUM filters were passed over the July image, with median filter-type smoothing and varying amounts of sharpening. The output filtered images were evaluated and determined to be of little use in enhancing critical areas of the image. Multi-pass filtering trials with varying smoothing and sharpening factors could eventually produce some useful results, but computer processing requirements and time constraints did not allow for a complete investigation of this filter type.

Frost-Adaptive SAR Filter. The Frost-Adaptive filter uses a minimum mean square error technique to estimate the terrain backscatter for SAR image data. The algorithm uses the local mean and standard deviation calculated from a user-defined window. The filtering is performed on an image area one pixel width smaller than the statistical window (Atlantis Scientific, 1994). A 5 by 5 Frost filter was applied to the July image. This filter produced results similar to the 3 by 3 median filter output and was, therefore, not selected as the best method.

Maximum A Posteriori (MAP) SAR Filter. SAR speckle causes high radiometric variations around the mean SAR image intensity. The MAP filter was designed to reduce the speckle noise component of SAR data, based on a Bayesian approach. The MAP filter takes into account a statistical speckle noise model, a statistical model for the

Table 5.1 Assessment of SAR Filters Used in this Study

Filter	Result	Remarks
Median	Poor-Average	Maintains average tonal edges, limited speckle reduction, and is not suitable for ERS-1 SAR data used in this study.
LUM	Average-Good	Maintains good tonal edges, average speckle reduction, and needs further investigation for SAR.
Frost	Poor-Average	Maintains poor tonal edges, average speckle reduction, and is not suitable for ERS-1 SAR data used in this study.
MAP	Excellent	Maintains best tonal edges while reducing speckle; most suitable for ERS-1 SAR data used in this study.

scene reflectivity (gamma or beta), and the number of independent looks used to generate the SAR image. This filter preserves texture and edges and is statistically and spatially adaptive (Conway, *et al*, 1993). MAP filters with 7 by 7, 5 by 5, and 3 by 3 windows were tested using the gamma probability density function. Results from the 3 by 3 filtering window were visually assessed the most suitable for the flood mapping application.

After filtering, the SAR images were scaled and stretched. Since ERDAS Version 7.4 software does not support advanced SAR processing algorithms, nor does it allow 16-bit data throughput in all tasks, it was necessary to import the image data into the EarthView software package. In order to achieve this, the ERDAS *.lan* files were converted into the IDRISI *.img* format. The IDRISI *.img* is similar to the EarthView *.mff* format in that it has a flat raster binary image file with ASCII header files. After completion of the filtering process, the filtered SAR images were brought back into IDRISI, where they were scaled to 8-bit data through a linear stretch function and converted into ERDAS *.lan* files. For the Tangail test area, the contrast stretch procedure used a 2.5 standard deviation from the mean for the high cut-off value, while maintaining the same low-end value distribution. This produced Gaussian-distributed data through the full 8-bit range for statistical analysis in ERDAS.

Subsequent processing of the entire ERS-1 SAR scene coverage required the use of different cut-off values. Due to the increased standard deviation in the full images compared to the smaller test area, the 16-to-8-bit scaling and linear stretch required lower 16-bit maximum cut-off points. For this reason, both images were scaled and stretched using a 1.5 standard deviation from the mean distribution value in the 16-bit image.

5.4.4 Image Classification

A procedure for discriminating flooded and nonflooded areas was developed using July and August SAR images of the Tangail test area. After much trial and error, a method was chosen that used a simple density slice to segregate the image into two discrete classes and one mixed class. Then, a series of knowledge-based algorithms were applied to the mixed class pixels, resulting in their assignment to one of the two known classes. When results for the test area were considered satisfactory, the classification process was then applied to the entire SAR images.

The classification was based on the principle that the amount of SAR return from standing water is significantly lower than that of soil, vegetation, and other features occurring on dry land. It was

recognized, however, that volume scattering and multiple reflections from vegetation in standing water can create bright SAR return, thus confusing these areas with features on dry land.

The first step of the classification--density slicing--was applied to a SAR subscene of the Tangail test area. Selection of the digital number (DN) range for each density slice involved visual interpretation as well as reference to field information, satellite images and aerial photographs, and use of a DEM of the study area. As shown in Figure 5.6, a single color was assigned to each of three ranges of DN as follows:

- Dark and dark-grey SAR image tones (1-87 DN) were given a blue color and assigned to the class "water."
- Mid-grey SAR image tones (88-118 DN) were given an orange color and assigned to the class "mixed."
- Bright and very bright SAR image tones (119-255) were given a beige color and assigned to the class "nonflooded."

With this simple density slice approach, the water and nonflooded classes were assigned about 75 percent of the test areas for the two dates, and, after considering ancillary information and knowledge of actual conditions in the area, these classifications were determined acceptable. The remaining 25 percent was classified mixed and appeared to contain both flooded and nonflooded features. Most of this mixed class occurred in a transition zone between low-lying flooded areas and the nonflooded, higher elevation agricultural areas and settlements.

To complete the image classification, a procedure was developed to assign each of the mixed class pixels to one of the known classes. This refinement was achieved using ERDAS raster GIS algorithms. The first step in the process identified the distance of each of the mixed class pixels from those classified as water. If the connectivity radius was two pixels or less (50 meters or less on the ground), then the mixed class was assigned to the flooded class; all other pixels were assigned to the

nonflooded class. The two-pixel threshold was decided by testing various search radii and visually assessing the result along with comparison to ground reference data and other relevant information.

After assigning the mixed class pixels, post-classification processing involved smoothing to eliminate the salt-and-pepper appearance of the image and to eliminate small, isolated clumps of both the flooded and nonflooded class. This process began with a 3 by 3 majority filter applied to both classes, followed by an algorithm that counted the number of pixels in each contiguous clump. Clumps with a size of 40 pixels or less (10 ha or less) were eliminated and assigned to the other class. The result of this post-processing was an image of relatively smooth appearance, consisting of flooded and nonflooded classes, each in clumps, or contiguous areas, of 10 ha or greater.

After the classification and post-processing method was accepted for the test area, it was applied to all of the SAR scenes. The following section explains how the accuracy of this classification was assessed.

5.5 SAR Image Processing: Assessment of Results

5.5.1 Flood Maps

The image classification method used in this study yielded a two-class map of flooded and nonflooded areas. This simple result is a representation of a wide range of digital values recorded by the SAR system that are determined by a number of complex, interrelated factors, including: the SAR system parameters, flood and other environmental conditions, and radar backscatter behavior of the various targets under a variety of flooded and nonflooded conditions. The DN thresholds and the post classification processes that developed for the test area to use in differentiating between flooded and nonflooded classes also were used for classifying the three full SAR image data sets.

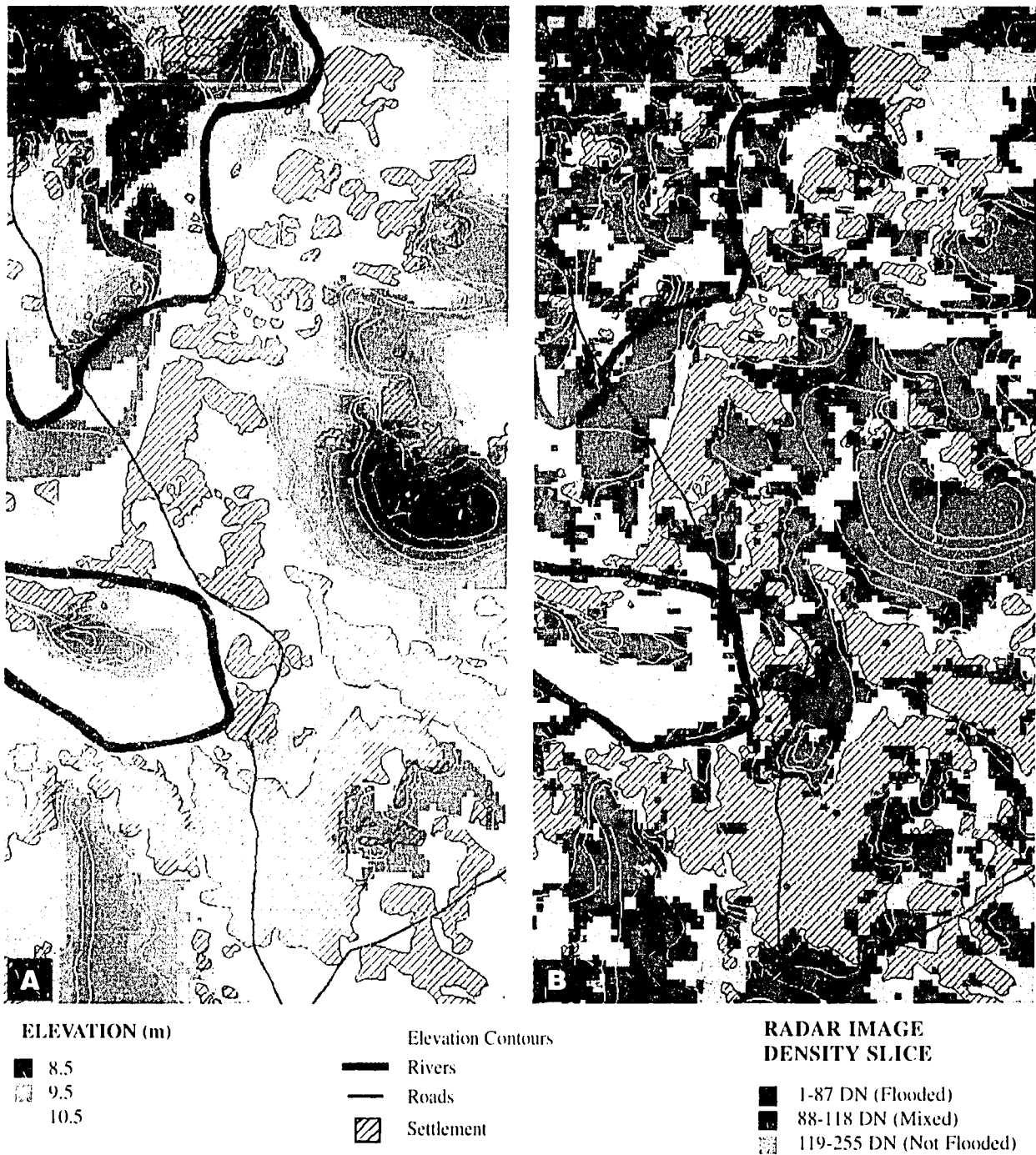


Figure 5.6: Assessment of Radar Image Classification Using Topographic Maps. Examples of thematic GIS maps for a 4 km by 2 km area south of Tangail town showing close correlation of topography with flooded and nonflooded classes, as derived from ERS-1 SAR image analysis.

Map A: GIS map showing topographic contours (in yellow) at 25 cm intervals, as derived from 1:10,000 scale orthophotos prepared by FINNMAP. Higher elevations are in light grey tones and lower elevations, which are more subject to flooding, are shown in dark grays.

Map B: The SAR image for July 24, 1993, combining elevation contour information with a density slice of the SAR digital number (DN). The “mixed” class contains water and land features that cannot be clearly separated.

Because of differences in instrument calibration and preprocessing techniques, it is unlikely that these precise thresholds would be the most suitable for other ERS-1 SAR images acquired for later dates.

The image classification processes were extended from the Tangail test area to the entire SAR coverage area of the July and August scenes of central Bangladesh and for the May scene of the Sylhet region. Visual observation of these scenes had revealed that radar signatures for certain features were quite complex and were likely to yield errors when subjected to the simple classification developed for the typical floodplain area. Signatures of particular concern were associated with rapid flow of the main rivers and with upland and mountainous areas. These areas were excluded from the analysis and, therefore, the resulting flood map products include only the floodplains. Flood maps for the scenes of central Bangladesh, which include the confluence of the Ganges and Brahmaputra/Jamuna rivers, are shown in Figures 5.7 and 5.8.

The flooded and nonflooded classes in Figures 5.7, 5.8 show large continuous areas of flooding throughout the ERS-1 SAR scenes. In the floodplain east of the Jamuna River, the flooding pattern is more irregular with interspersed areas of nonflooded crops and settlements. The overall area of flooding increased slightly from July to August: 48 percent and 53 percent flooded, respectively. Some of the interesting features on these maps include the large beels northwest of the river confluence, and the southern extent of the Brahmaputra Right Embankment (just northwest of the Ganges-Jamuna confluence) where flooded areas are found on the east, unprotected side, and are especially clear in the August image. Also, there are many sinuous features mapped as nonflooded areas that occur alongside the rivers within the floodplain. These features are typical of the settlements and nonflooded, or shallow flooded, cropland on the slightly elevated, natural river levees.

5.5.2 Assessment of SAR Classification Results

In attempting to assess agreement between classified SAR data and ground information or other data sets, it was important to uniformly define flooded land. In the water resources sector of Bangladesh, "flooded" generally refers to areas that are inundated with more than 30 cm of water. Thus, paddy lands that are ponded with, for example, 15 to 30 cm of water would be classified as nonflooded for most local considerations. However, with ERS-1 radar it was not possible to discriminate between shallow and deeper water. Therefore, for this application, flooded areas include any standing water with measurable depth.

Accuracy Assessment: The SAR image classification results were examined by FAP 19 analysts and by persons from several other projects familiar with flood conditions within the study areas. In addition, the classifications were compared with other maps and flood model results and determined to be reasonable and useful. A more quantitative assessment of the SAR image classification then was carried out by comparison with information obtained from the ground surveys, as shown in Tables 5.2 and 5.3.

The information in Tables 5.2 and 5.3 is derived from an overlay of ground reference polygons with the SAR image classification results for both July and August for the central Bangladesh image. The detailed ground reference data, from some 45 observations on a variety of land uses, were simplified into the following four categories: (1) urban, settlement, homestead; (2) nonflooded crops; (3) flooded crops; and, (4) river, floodwater, and beels. These categories were compared with the two-class SAR image classification results, flooded and nonflooded, and presented in a standard classification error matrix format shown in Tables 5.2 and 5.3. Accuracies were calculated for the four separate ground reference categories and an overall classification accuracy was calculated for each of the images. The statistics show a reasonably high overall accuracy: 84 percent for

Table 5.2 Accuracy Assessment of Classification of SAR Image - 24 July 1993

Ground Classification	ERS-1 SAR Classes				
	Flooded (ha)	Nonflooded (ha)	Total (ha)	Percent Accuracy	Percent Omission
Urban, Settlement, Homestead	4	192	196	98	2
Nonflooded Crop	16	75	91	82	18
Flooded Crop	428	130	558	77	23
River, Flood Water, <i>Beels</i>	<u>230</u>	<u>28</u>	<u>258</u>	<u>89</u>	<u>11</u>
Total	678	425	1,103		
Percent Commission	3	37			
Overall Percent Correct	84%				

Table 5.3 Accuracy Assessment of Classification of SAR Image - 28 August 1993

Ground Classification	ERSI-SAR Classes				
	Flooded (ha)	Nonflooded (ha)	Total (ha)	Percent Accuracy	Percent Omission
Urban, Settlement, Homestead	18	173	191	90	10
Nonflooded Crop	50	76	126	60	40
Flooded Crop	397	98	495	80	20
River, Flood Water, <i>Beels</i>	<u>141</u>	<u>16</u>	<u>157</u>	<u>90</u>	<u>10</u>
Total	606	363	969		
Percent Commission	11	31			
Total Percent Correct	81%				

45

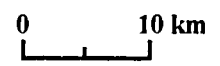
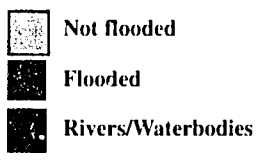
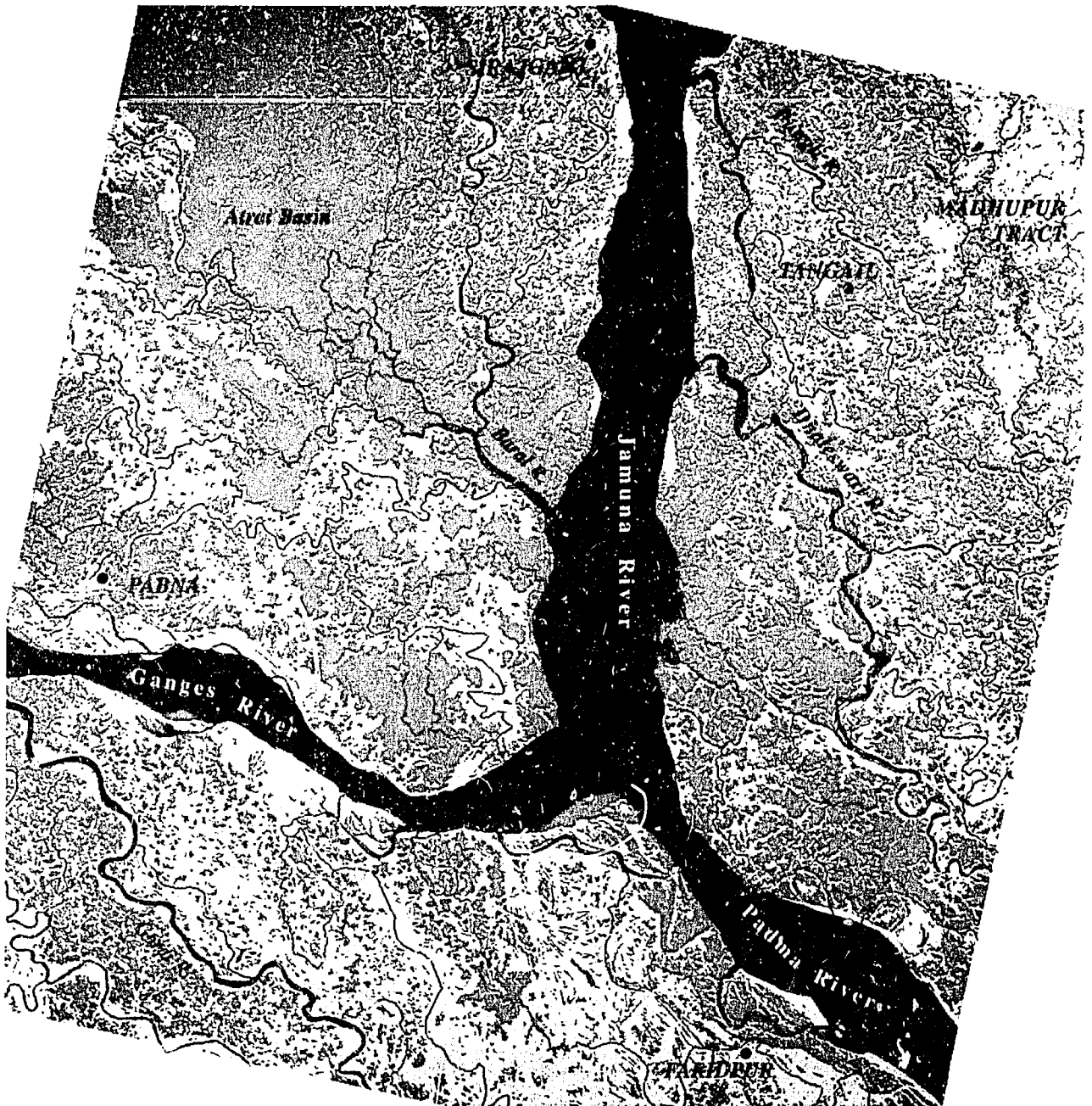


Figure 5.7: Results of ERS-1 SAR Classification for Central Bangladesh Scene of July 24, 1993. Results for the main rivers have been excluded from the classification.

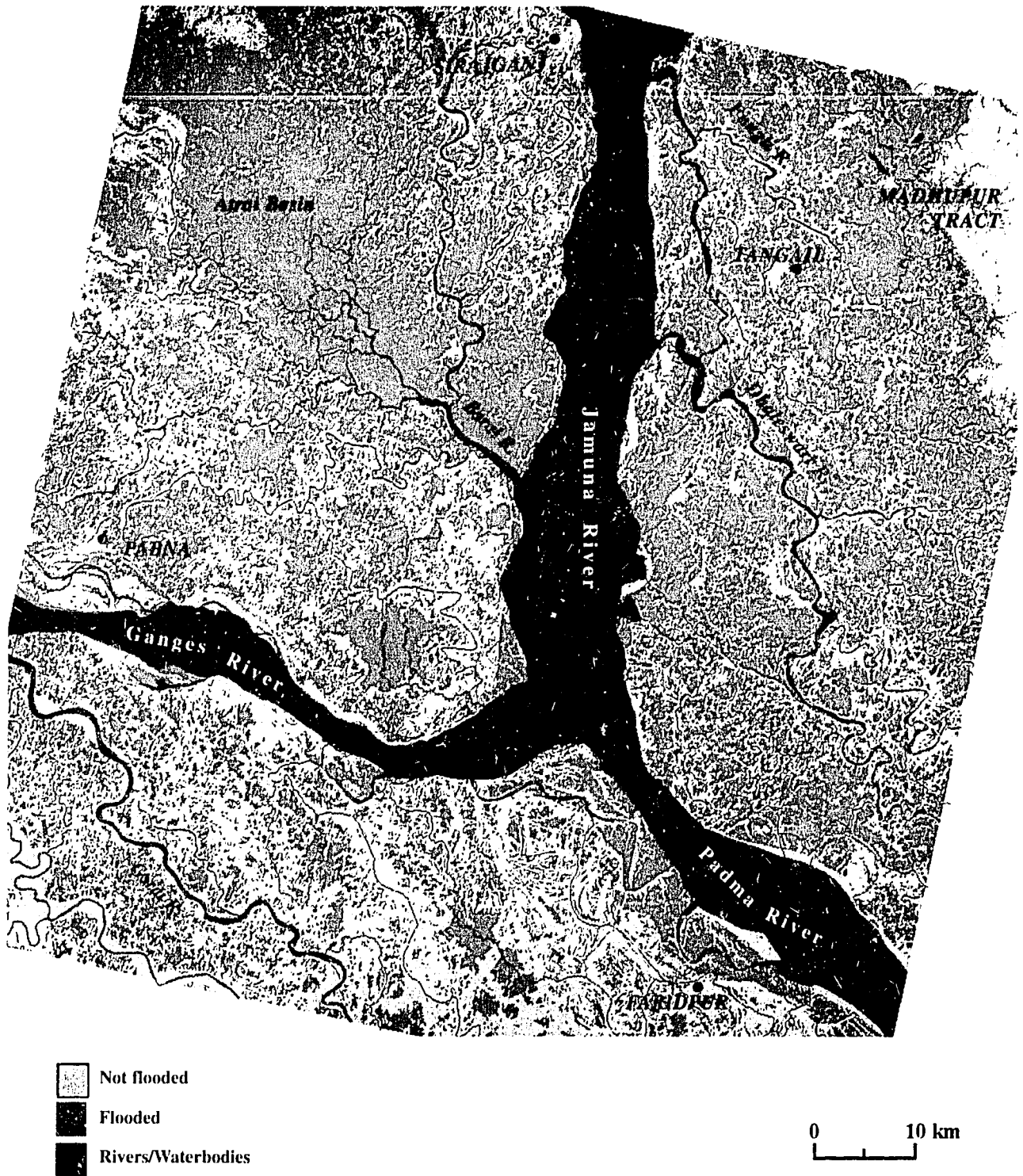


Figure 5.8: Results of ERS-1 SAR Classification for Central Bangladesh Scene of August 28, 1993. Results for the main rivers have been excluded from the classification.

July and 81 percent for August. Agreement of near 90 percent and better was achieved for the settlement and water classes in both images. The lower agreement of the nonflooded crops (82 percent and 60 percent) is most logically attributed to the broad range of SAR signatures for the crops included in the class. The flooded crop category, with 77 percent and 80 percent accuracy for the respective July and August images, also includes a variety of flood water characteristics and a range of crop type, canopy, and condition.

Visual Interpretation: Overall, information on flood extent derived from the SAR data closely agrees with topographic data (see figure 5.6); however, there are some inconsistencies. For example, the nonflooded class is shown in several low lying areas where one would expect to find flooded crops. A possible explanation for this is that some flooded crops, particularly those with dense canopy such as sugarcane and jute, will yield a relatively high radar return, similar to that of nonflooded terrain. An overview of SAR image tone and associated land use is presented in Figure 5.9 and such information may be used as a general interpretation key.

The location of permanent water bodies, such as *beels* and ponds, are well known. Being associated with lower topographic areas, these features expand significantly during flood season and they are often incorporated into the general flooded area. The area corresponding with the dry season extent of these features was correctly identified by SAR as water. However, some smaller ponds were difficult to identify in the SAR image as were some portions of larger water bodies covered with dense surface vegetation such as water hyacinth that can give a brighter SAR return.

The precise location of the flooded/nonflooded boundary can be difficult to determine in the floodplains using single-date SAR imagery alone; use of multi-date SAR images can enhance results considerably (see Section 5.6.4). Settlement areas can be more reliably identified due to their consistently bright signature. Although ground

reference data indicate that vegetation and crops under flooded conditions have a noticeably bright SAR return, the brightness of the signature is relatively less than that of settlements. Nevertheless, some confusion occurred due to the bright signatures from the flooded crops, where the smooth water surface reflected the significant canopy volume scattering back into the canopy, then to the SAR.

Ground reference data suggests that relatively low SAR returns were recorded from water bodies covered with water hyacinth, and therefore, correctly classed as flooded. This was evident in both the July and August images, as indicated in the detailed ground reference data provided in Appendix A. The SAR signature for water hyacinth was, however, noticeably higher than that for open water and flooded paddy.

5.5.3 Ground Reference Data

The design of the ground reference program presented a challenge because of the general uncertainty as to which specific ground parameters the ERS-1 SAR would actually be sensitive. During subsequent evaluation of the ground reference data set, several benefits and shortcomings emerged with regard to both design and execution of the program.

The literature provided some indication of the ground features to observe for a meaningful assessment of the digital SAR imagery. In addition, knowledge of local conditions, especially a familiarity with the cropping calendar and agronomic practices, was essential.

Ground observations and measurements of this study concentrated on land use, water surface characteristics, depth of flooding, and the type and structure of vegetation and crops for the selected sites. These parameters and measurements proved useful, although some difficulties were encountered in accurately referencing their locale and, subsequently, their corresponding SAR signatures. GPS, with a ground accuracy of approximately 80

48

Figure 5.9: Radar Image Signatures Expected for Various Land, Water, and Vegetation Features.

Feature	SAR Signature					Description
	very dark	dark	medium	light	very light	
Open water (low wind conditions)	very dark	dark				Beels, deeply flooded cultivated land, specular radar reflection
Open water (moderate wind)		dark	medium			Open water surface roughened by wind, moderate bragg scattering effects
High velocity river (water surface)		dark	medium	light	very light	High flow velocity and modulation by bottom topography, Bragg scattering
Jute, sugarcane crops (flooded)		dark	medium	light	very light	Standing water surface beneath vegetation canopy, multiple scattering
Rice crops, mature (flooded)		dark	medium	light		Standing water surface beneath vegetation canopy, multiple scattering
Rice, recently transplanted (flooded)	very dark	dark				Very low canopy, open water surface reflections mostly specular
Jute, sugarcane crops (not flooded)			medium	light		Volume and surface scattering effects of dense plant canopy
Rice, mature (not flooded)		dark	medium			Volume and surface scattering effects of dense plant canopy
Other crops (not flooded)		dark	medium	light		Volume and surface scattering effects of plant canopy
Forest (not flooded)			medium	light		Volume and surface scattering effects of dense plant canopy
Rural settlements (not flooded)				light	very light	Corner reflections from houses and volume scatter from homestead forest
Urban Areas (not flooded)					very light	Corner reflections from buildings and other infrastructure

49

meters, was useful in establishing site locations for repeat access and for subsequent cross-referencing of ground data with the ERS-1 SAR imagery and thematic GIS maps.

Due to unexpected logistical problems, not all sites were accessible on multiple dates. In some cases, a site that was easily accessible in July could not be reached in August due to increased flooding, road damage, or bridge or culvert washouts. In these cases, previously arranged boat access would have been particularly useful.

Because of the floodplain's highly fragmented land, vegetation, and flood conditions, it was difficult to locate relatively large, homogeneous sites for data collection. Instead, the ground reference polygons were of various sizes, some relatively small considering the ERS-1 SAR ground resolution of 25 m per pixel. A more useful result could have been attained from a standardized polygon, or sampling window, of at least several pixels in both x- and y- dimensions to account for locational errors and radar speckle effects.

Ideally, the collection of local ground reference data should be supplemented by information on the spatial context in which it is collected. In this study, 35 mm photographs were taken from the ground at each site. A better perspective would be from low altitude, oblique aerial photography that could be used for spatial and contextual cross-reference; however, it is difficult to obtain government clearance for collecting them in Bangladesh.

5.6 Assessment and Use of the SAR Flood Map

5.6.1 Comparing SAR with Flood Model Results

The SAR classification results were compared with results of the hydrological model, the FMM. The GIS maps in Figure 5.10 and 5.11 compare the areal coverage of flooded and nonflooded terrain in the Tangail test area, as indicated by SAR and

FMM analysis for the same dates in July and August, 1993. For those dates, results show 67 percent and 73 percent agreement, respectively, for both flooded and nonflooded classes between the two methods. The FMM analysis showed an increase in inundated area, from 57 percent in July to 65 percent in August. Similarly, the classified radar images show a 39 percent to 49 percent increase in land flooded for the same dates; this increased flooding from July to August is consistent with observation of the Tangail area in normal flood years.

The location of areas of both agreement and disagreement between the two sources, shown in Figure 5.10 and 5.11, can be revealing. For example, there is a cluster of dark red areas that the radar classified as flooded and the FMM as not flooded in the southeast region of the figures for both the July and August dates. Since most of the clustered dark red area falls within a single "cell" or modeling unit of the FMM, the consistent radar result between the two dates suggests that the elevation of the modeled water surface may be too low for this area. Another example is the crescent shaped lake, just north of Tangail town which was erroneously shown as nonflooded on the July radar image. It is likely that wind created a roughened surface on the large open water body on the day of the July radar satellite overpass, causing backscatter in the SAR return which resulted in the misclassification. Comparisons such as these can yield useful information and potentially improve both the radar and the FMM analysis tools.

An analysis was made of radar results for each 10 decimeter depth increment of the flooded area predicted by the FMM. The plot of flood depth and area coverage, shown in Figure 5.12, takes an interesting, but not unexpected form: relative agreement is highest at greater flood depths, and disagreement is strongest where flood depths are low. This trend is consistent for both the July and August dates, although overall agreement is significantly higher for the August date.

The analysis for July indicates that 58 percent of the water extent projected by the flood management model occurred where the SAR also identified water; disagreement existed for 42 percent. This significant discrepancy is improved for August where agreement between the FMM and SAR flood classification methods was 69 percent. Such an increase in agreement between the two dates is not unexpected; from examination of the curve in Figure 5.12, the FMM prediction of some 1,000 ha more flooded area in August than in July is accompanied by an increase in the average depth of flooding. Thus, the FMM results show flooding in August which is deeper and more extensive than that in July.

5.6.2 Change Detection

Multi-date SAR imagery can be used to quantify changes in the flood scenario over time. Figure 5.13 is a map showing changes in flood extent between July and August, 1993. The map was produced by overlaying classified SAR images of July and August using GIS. The net increase in flood extent was found to be about 10 percent of the total area of the Tangail CPP. As expected, most of the areas of change are found along margins of areas which are flooded on both dates.

5.6.3 Comparing Classification with Land-Type Map

A comparison was made between the radar classes and the flood inundation land-type map for an area of 62,237 ha east of the Jamuna River, including the Tangail test area. The land-type map was prepared by FAP 19 using GIS manipulation of a DEM and reconnaissance soil maps obtained from the FAP 19 national-level database. As detailed in a separate report (FAP 19, 1995), the digital land-type map represents flooding during a "normal" monsoon flood season. The land type classification follows the MPO flood depth classification scheme where F0, F1, F2, etc., are used to denote flood depth and other characteristics.

The flood inundation land-type map is relatively coarse and was designed for use and analysis at a regional or national level. In addition, the soils and topographic data layers are outdated for some areas, since they are derived from 1960s surveys. Nevertheless, a comparison of the flood depth classes with the SAR classification results yielded some useful information, as shown in Table 5.4. The results are similar to the comparison of SAR with the Flood Management Model: as the flood depth class increases there is increasing agreement with the flooded category of the SAR classification. For the flooded land type classes, the range of agreement is from 61 percent for F1 land to 95 percent for the deeply flooded F3F4 land. The Master Plan Organization (MPO) defines the F0 class as "flood free," with a flood depth of 0-0.3 m. From the perspective of SAR, any ground area of the F0 land type with standing water would be considered flooded; in this comparison, some 44 percent of the F0 land area was classified as flooded by the SAR and 66 percent as nonflooded. Since the landtype map does not segregate the nonflooded area, no conclusion can be drawn from a comparison with the SAR result for the F0 class.

5.6.4 Multi-temporal Display and Analysis

The multi-temporal satellite radar data was used to produce a composite SAR image product for assessing changes between the two images at both the local and regional scale. As shown in Figure 5.14, the July and August 1993 SAR data were merged into a composite image for an area northwest of the confluence of the Ganges and Jamuna rivers. This composite was produced by displaying separate images, and a ratio of the images, in separate color planes of the image processing system, as follows:

<u>Color plane</u>	<u>Display</u>
Red	July SAR Image
Green	August SAR Image
Blue	August/July (the ratio for the two dates)

Table 5.4 Comparison of SAR Classification With Land Type

Land Type	Flood Depth (m)	ERS-1 SAR Classes			
		Total Area (ha)	Nonflooded Area (ha)	Flooded	
				Area (ha)	Percentage
F ₀	0-0.3	20,841	11,568	9,273	44
F ₁	0.3-0.9	31,056	12,083	18,973	61
F ₂	0.9-1.8	9,216	1,891	7,325	79
F ₃ F ₄	> 1.8	1,124	55	1,069	95

The resulting image and its color renditions provide an effective display of change. In the composite image (Figure 5.14c), areas in light blue color have low SAR returns in the July image and high returns in the August image. From the ground survey results of this study, and discussions with others familiar with the area, the light blue color probably represents areas of transplanted *aman* (paddy) that are flooded in both July and August; the higher canopy cover in August yields a brighter SAR return. Dark blue areas represent water in July that gave brighter returns in August, probably due to the backscatter effect of low-density crops with standing water underneath, such as transplanted or broadcast *aman*. Orange areas most likely represent crops that became flooded in August. The yellow/beige color appears to correspond to areas of nonflooded crops, levees, and settlements with homestead forests.

5.6.5 Merger of SAR Image with Landsat TM

Figure 5.15 shows a composite of the classified SAR image of August 1993 and two bands from the Landsat TM image of January 1994. The radar flooded class is displayed in the red plane with Landsat TM bands 4 and 2 displayed in the green and blue color planes, respectively.

<u>Color plane</u>	<u>Display</u>
Red	August 1993 SAR Flooded Class
Green	Landsat TM Band 4 (near infrared)
Blue	Landsat TM Band 2 (visible green)

For the floodplain in the composite image, the dark green areas correspond to forest cover in both the monsoon SAR image and the dry season Landsat TM image. The medium green areas were classified as nonflooded in the monsoon and included both cropped and fallow lands in January. The red and pink areas were flooded in the monsoon and were mostly fallow in January. The bright yellow color corresponds with areas flooded in August, but were under a full vegetation canopy in January.

Because the ERS-1 SAR classification was not reliable for high-flow river channels, the dry season extent of the Jamuna River channels were used in place of the SAR information in the red image plane. This explains the bright red color for the river channels, which helps when interpreting the composite image for the chars (riverain islands). Within the chars, the white, pink, red, and yellow areas are flooded in August while green areas are

- 52 -

not. The dark grey areas gave very bright returns in the August SAR image, hence they were classified as nonflooded; these are probably areas of catkin grass or jute that, in reality, may or may not have been flooded in the monsoon. In the following January Landsat image, these same areas gave signatures of vegetated land, probably grass. The blue color was classified as nonflooded in the SAR image, but much of this may correspond with the bright SAR signature of high velocity floodwater in August; thus, interpretation of the blue color is unreliable.

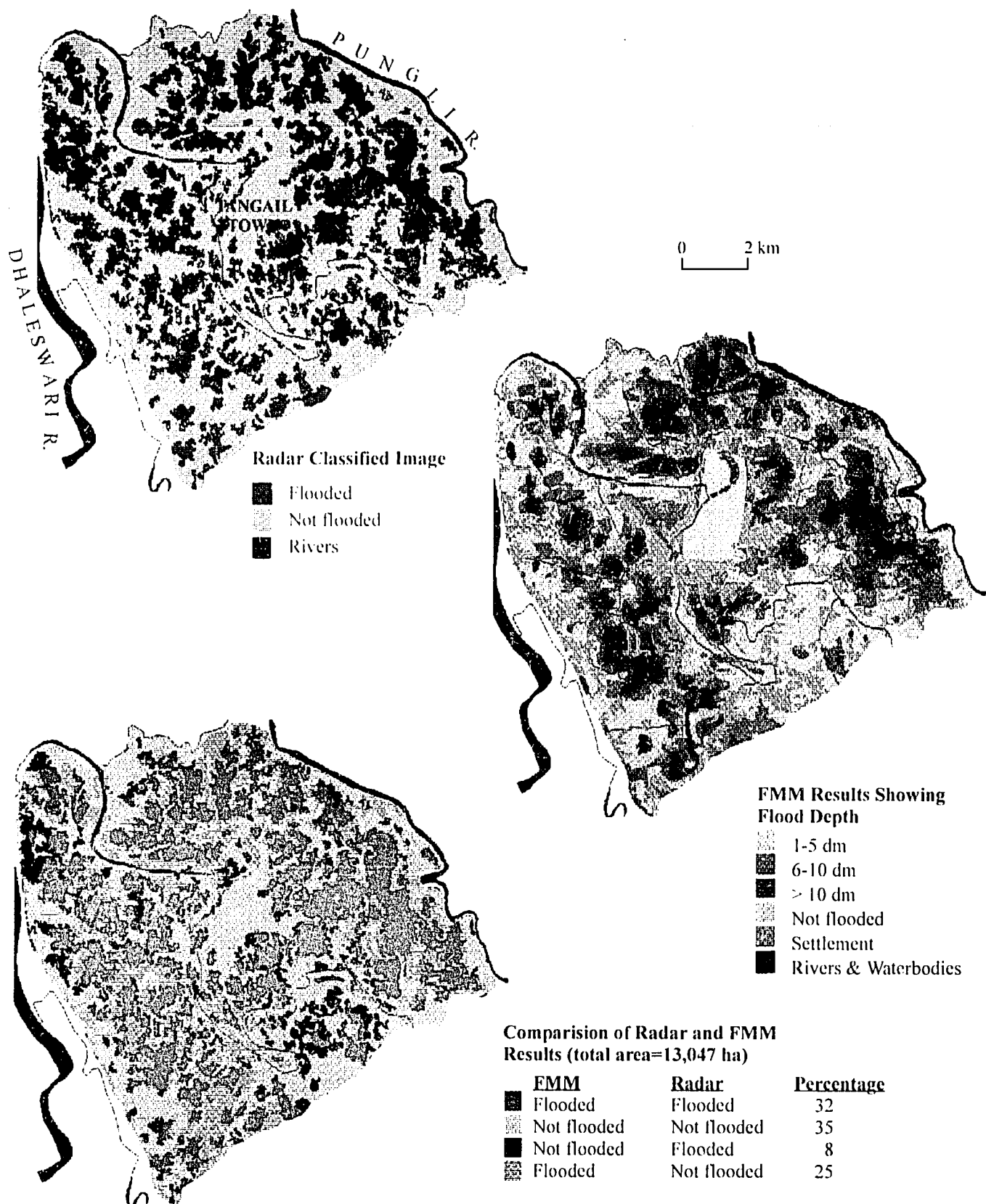


Figure 5.10: Comparison of Results from the Flood Management Model and SAR Image Classification for July 24, 1993.

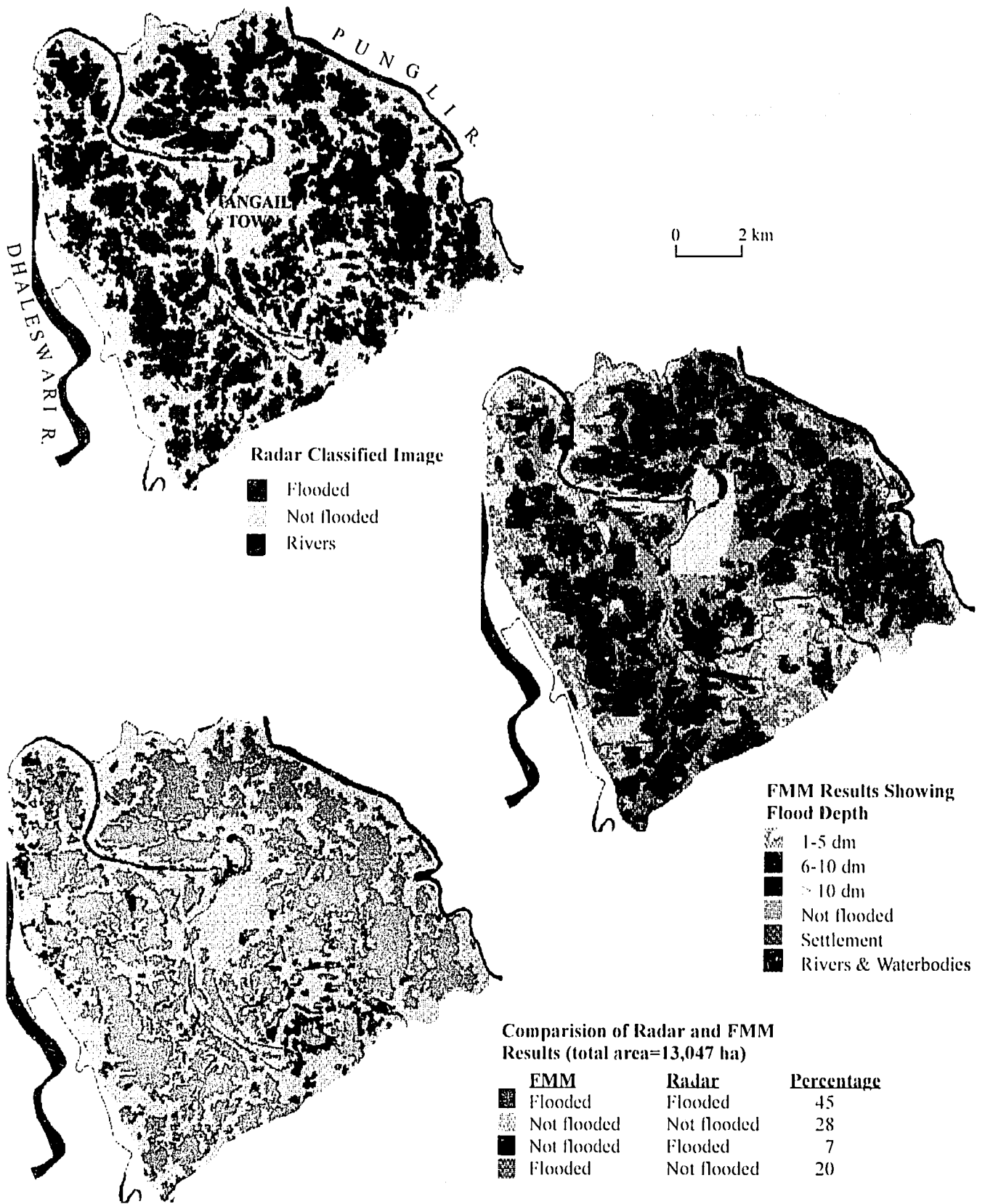
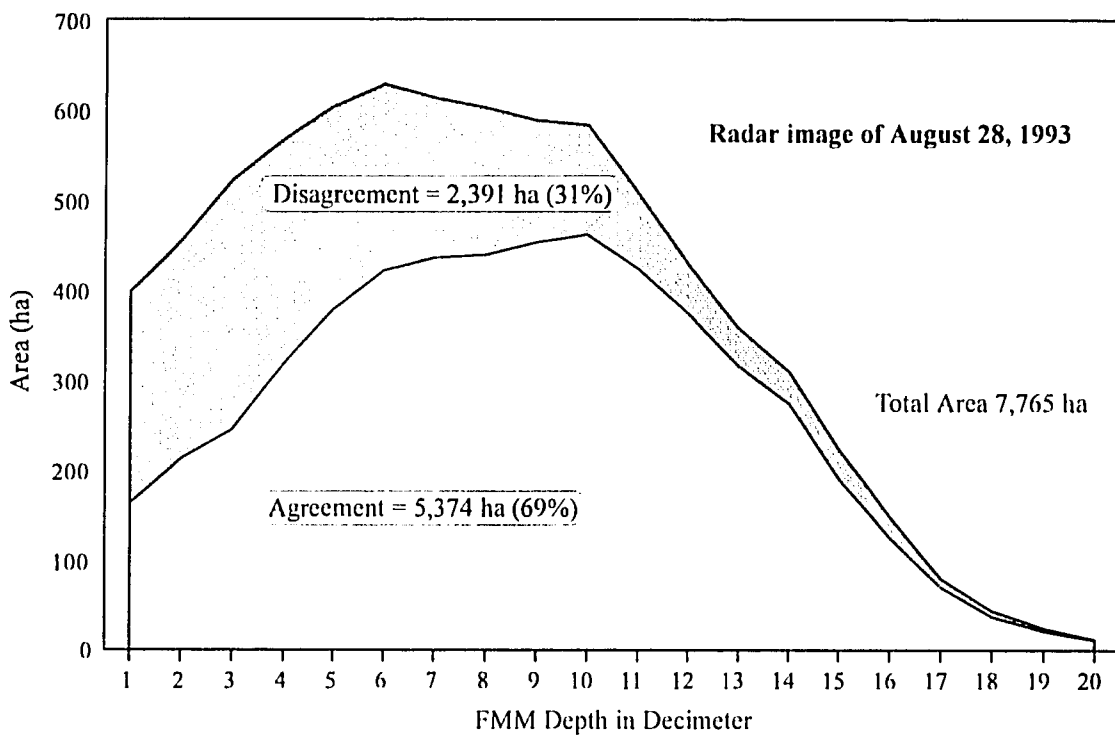
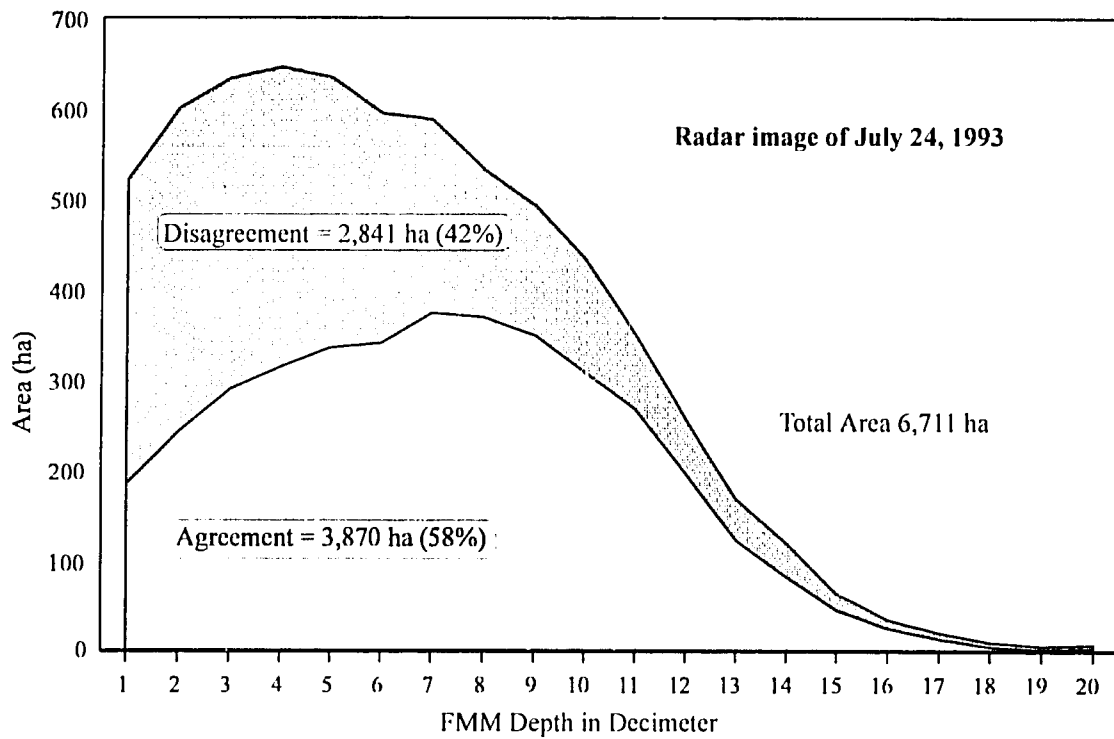
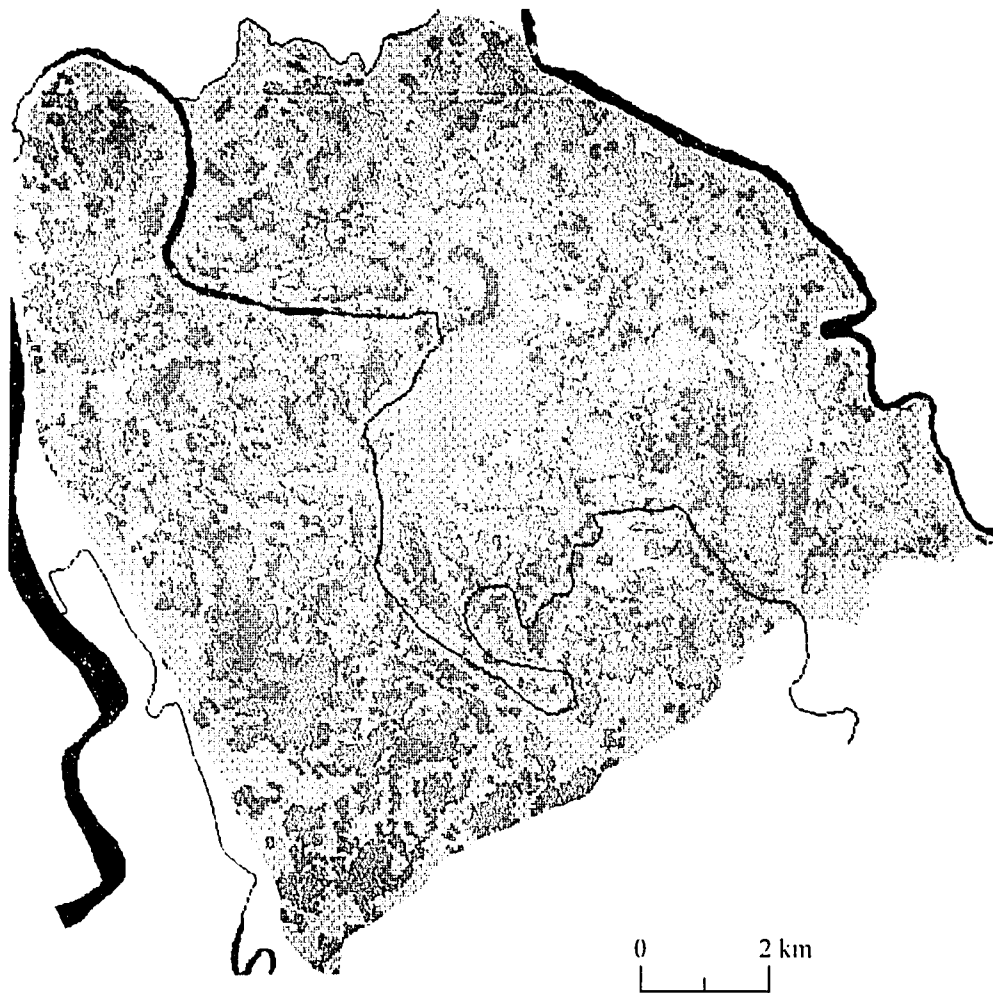


Figure 5.11: Comparison of Results from the Flood Management Model and SAR Image Classification for August 28, 1993.



Radar, Flooded (Agreement)
 Radar, Non-Flooded (Disagreement)

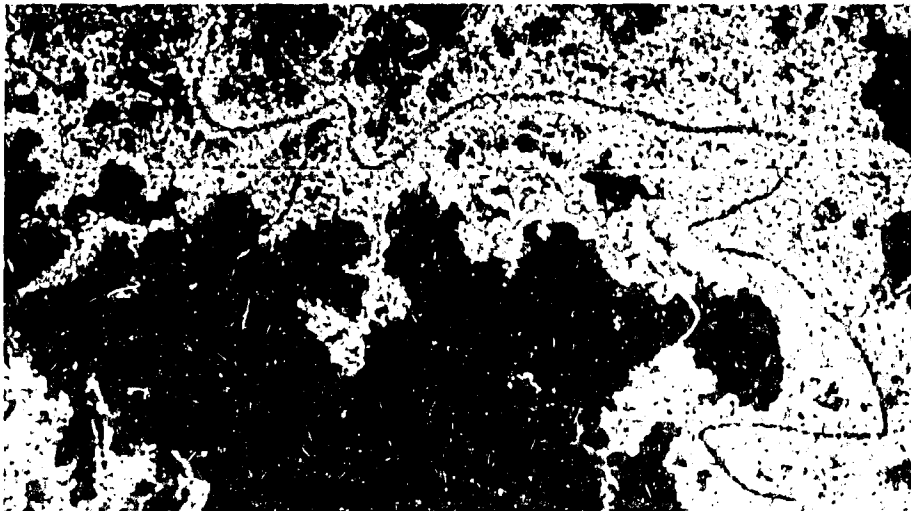
Figure 5.12: Comparison of SAR Classification Results with Flooded Areas Predicted by the Flood Management Model. Results are for the Tangail test area for both July and August, 1993.



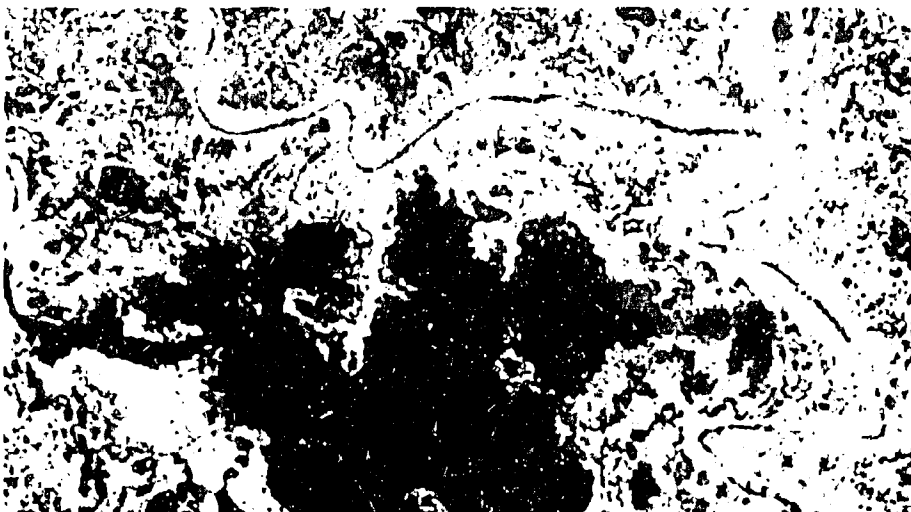
Flood Scenerio (total area = 13,047 ha)

	July	August	Percentage
○	Flooded	Not flooded	6
■	Flooded	Flooded	35
■	Not flooded	Flooded	17
■	Not flooded	Not flooded	42
■	Rivers	Rivers	

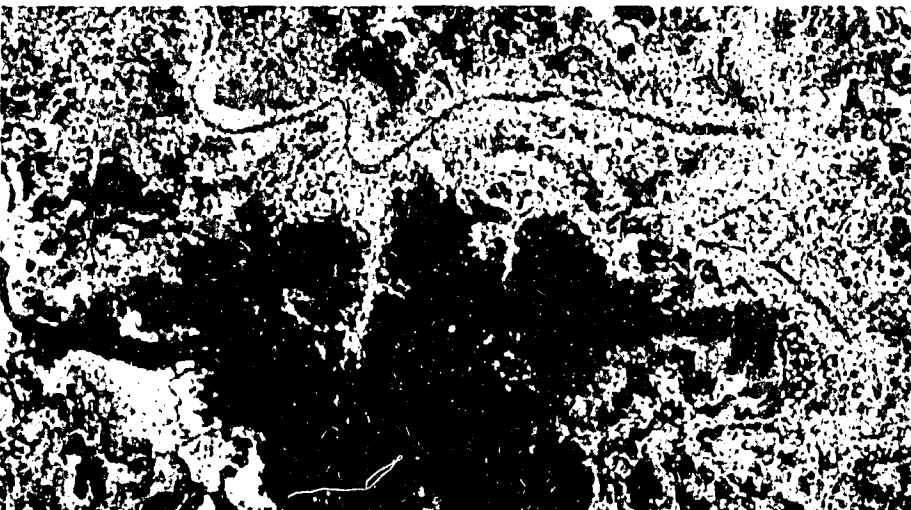
Figure 5.13: Change Detection Map of Different Flood Levels in July and August, 1993. The flood scenario was developed from SAR image analysis of the two dates for the Tangail test area.



A: SAR subscene, MAP filtered, of July, 1993.



B: SAR subscene, MAP filtered, of August, 1993.



C: A composite image of the above SAR subscenes. The July and August subscenes are displayed in the red and green color planes of the image processing system, respectively. A ratio image (August/July) is displayed in the blue plane.

0 2 km

 A simple horizontal scale bar with a vertical tick at the 0 mark and another at the 2 km mark.

Figure 5.14: Multi-temporal ERS-1 SAR Data Set and Change Detection Map. The location of these images, shown in Figure 1.2 is northwest of the confluence of the Ganges and Jamuna rivers. The large open water surface of *Gajna Beel* appears dark. Note the change in the extent of the open water surface from July to August as a result of increased flooding and vegetation growth along the margins of the water.



0 5 km

Figure 5.15: Merger of Radar Classification Results with Landsat TM Data. The radar flooded class for August, 1993, is shown in the red plane, and Landsat TM bands 4 and 2 from January 1994, are displayed in the green and blue planes, respectively.

CHAPTER 6

CONCLUSIONS AND RECOMMENDATIONS

6.1 SAR Technology

Although radar remote sensing satellites have been operating since the early 1990s, satellite-based SAR technology has received little attention in Bangladesh. This FAP 19 radar project, which began in 1993, is the first to explore the application potential of satellite-based SAR for natural resource assessment and environmental monitoring in Bangladesh.

SAR technology offers high-resolution imaging capability for acquiring information through the persistent monsoon cloud cover of Bangladesh and for both day and night data acquisition. This operational advantage can be fully exploited during the monsoon season to monitor dynamic environmental processes.

Radar data can be acquired from satellite-based systems at specified time intervals. Applying radar image analysis to these data can provide vital information for mapping and monitoring flood extent, studying river morphology and dynamics, monitoring coastlines, providing information for damage assessment following a disaster, and monitoring land use. This project's review of current literature on SAR application development in subtropical environments confirms that imaging radar can provide valuable information for these applications.

Satellite SAR data covering Bangladesh are currently available from experimental sensor systems on board the European ERS-1 and the Japanese JERS-1. Limited archival SAR data also are available from the Russian ALMAZ and SIR-B missions

of the United States. In late 1995, another ERS satellite is planned for launch as well as the new Canadian RADARSAT satellite, which, with its variety of incidence angles, viewing and resolutions modes, will allow for the observation of Bangladesh flood conditions every three to five days.

Availability of SAR imagery and its resolution could become crucial in the operation of radar remote sensing for resource management and environmental monitoring applications which require timely and frequent information. When the planned SAR satellites are added to the those currently operational, there will be an opportunity for a variety of applications in Bangladesh. However, acquisition of data for a particular project will require planning with the satellite operators and processing facilities, especially in the near future. This point is emphasized by the experience of this project, which required a substantial effort for obtaining the processed data, not all of which has been delivered.

6.2 Application for Flood Monitoring

This project has demonstrated how multi-temporal satellite SAR imagery can be useful for mapping and monitoring a monsoon flood in Bangladesh. In addition, various methods were explored for increasing the utility of the radar data by combining it with VIR satellite imagery, hydrologic models and other digital information. It is believed that satellite radar technology, especially when combined with GIS, mathematical modelling and other

techniques, has enormous potential for understanding, monitoring and predicting changes in the complex hydrology of Bangladesh's floodplains.

The radar image analysis techniques used in this project were developed for delineating flooded and nonflooded areas. The 3 by 3 MAP SAR filtering method produced the best overall results for the flood mapping application by reducing system speckle of raw SAR 16-bit data and maintaining image sharpness without making a heavy demand on computer processing time. For classifying the radar images, simple density slicing yielded useful information with minimal processing time. A refinement of the level slice required application of knowledge-based algorithms, and yielded an improved result. The final classification results provided a relatively high agreement with ground reference data, in excess of 80 percent.

There are more sophisticated SAR image analysis tools available, such as textural classifiers and image segmentation. These are conceptually more advanced and computationally more demanding than the techniques used in this study, and should be introduced at future stages of SAR application development in Bangladesh.

In this project, ground reference data proved to be essential for radar image interpretations and for verifying the classification results. The ground reference data collection campaign, carried out on the day of each ERS-1 SAR data acquisition, was based on a sound methodology. However, the field experience revealed problems with repeated site access, mapping of precise site locations, and configuration of sample polygons. For future programs, a more rigorous program of selection and documentation of site locations is recommended.

One of the most promising applications of satellite SAR imagery in Bangladesh is in verifying and improving the flood models currently in use. Comparison of the FMM maps and classified ERS-1 data showed agreement of 61 and 70 percent. Although more ground data is needed to fully

assess this comparison, it appears that for certain areas the radar data could be used directly for adjusting water elevations in the flood model. As the radar processing techniques are more fully developed, other applications are expected to be developed for the model setup and for presentation of results.

This study has taken an important first step in exploring the use of satellite-based SAR technology. Much has been learned about the potential applications; however, as noted above and elsewhere in this report, there are shortcomings to this study which follow-on projects could address. In order to optimize SAR data acquisition and the information that can be retrieved by SAR image analysis, future projects should consider environmental factors such as crop calendars, flood cycles, atmospheric and ground surface conditions. A well designed, comprehensive ground data collection program should be orchestrated. In addition, radar-specific factors such as SAR system parameters, satellite orbit parameters, and SAR data product availability should be considered. This is particularly important when considering the new radar satellites, scheduled for launch in late 1995, and the possibilities for developing operational use of SAR data from these sources.

6.3 Awareness and Institutional Needs

Information on the application potential for SAR technology in Bangladesh is limited. Few organizations outside the scientific research and development domain are familiar with SAR. Consequently, the capability to incorporate SAR data into flood monitoring activities, land use analysis, and coastal zone management is limited in Bangladesh. Achievement of this capability will require substantial technical and logistical support, training, and technology transfer.

To fully realize the application potential of this new technology for natural resource management and environmental monitoring in Bangladesh, the following are essential:

- sound knowledge of SAR system capabilities, satellite orbit parameters, and limitations on their operational use;
- specialized image processing and analysis software and training;
- knowledge of SAR application potential and its limitations.

To achieve this potential, strengthening of one or more Bangladesh institutions could be undertaken. This would include building up of the knowledge base through acquisition of key resource materials, such as textbooks, training manuals, and other SAR application literature and illustration materials. SAR data should be available to remote sensing scientists and applications specialists for further development of appropriate algorithms and visual analysis techniques.

For operational use of satellite-based SAR, the availability of satellite data coverage needs to be considered in terms of areal extent, spatial resolution, temporal resolution, and single or multiple sensor coverage. SAR information products should be adequately defined prior to implementation of an operational program. Data acquisition and processing streams need to be in place, including quality control provisions. The mode and format of product delivery should also be established in order to ensure continual use.

62-

REFERENCES CITED

- Adeniyi, P.O. 1984. Some lessons of the Nigerian radar project (NIRAD). *Atti. 24 Convegno Int. le Sullo Spazio*, Rome, Italy, 125-135.
- Adeniyi, P.O. 1986. A preliminary assessment of the probable impacts of the Lagos State (Nigeria) regional master plan (1980-2000). *Applied Geography*, No. 6: 223-240.
- Ahern, F.J., R.K. Raney, R.V. Dams, and D. Werle. 1990. A review of remote sensing for tropical forest management to define possible RADARSAT contributions. *Proceedings International Symposium on Primary Data Acquisition/International Archives of Photogrammetry and Remote Sensing*. Vol. 28, Part 1: 141-157.
- Aschbacher, J. and J. Lichtenegger. 1990. Complementary nature of SAR and optical data: a case study in the tropics. *ESA Earth Observation Quarterly*, No. 31: 4-8.
- Atlantis Scientific. 1994. *EarthView User's Guide, Version 4.0*. Atlantis Scientific Systems Group, Inc., Ottawa, Ontario, Canada.
- Atlantis Scientific. 1994. *EarthView SAR Application Module: User's Guide and Reference Manual, Version 4.0*. Atlantis Scientific Systems Group, Inc., Ottawa, Ontario, Canada.
- Bangladesh Meteorological Department. 1993. Weather conditions recorded for the Tangail, Atrai, and Sylhet regions for July 24, 1993, and August 28, 1993. Unpublished notes. Dhaka, Bangladesh.
- Carter, D.T.J., P.G. Challenor, and M.A. Srokosz. 1988. Satellite remote sensing and wave studies into the 1990s. *International Journal of Remote Sensing*, Vol. 9, No. 10/11: 1, 835-1,846.
- Carter, D.T.J., P.G. Challenor, and M.A. Srokosz. 1988. Satellite remote sensing and wave studies into the 1990s. *International Journal of Remote Sensing*, Vol. 9, No. 10/11: 1,835-1,846.
- Chen, J., Y. Chen, P. Duan, and Y. Ni. 1988. Application of RAR for flood surveillance and terrain investigation in North China and East China. *Proceedings of the 9th Asian Conference on Remote Sensing*, Bangkok.
- Cimino, J.B. and C. Elachi. 1982. Shuttle Imaging Radar—A (SIR-A) experiment. Jet Propulsion Laboratory, Pasadena, California. JPL Publishing, 82-77.
- Conway, J.A., H. De Groof, and A.J. Sieber. 1993. A Suite of Tools for Information Extraction from ERS-1 SAR Data. *Proceedings First ERS-1 Symposium—Space at the Service of Our Environment*, Cannes, France, ESA, Paris, France, SP-359, Vol 1: 679-684.
- Curlander, J. and R.N. McDonough. 1991. *Synthetic Aperture Radar—systems and signal processing*. J. Wiley and Sons, New York.
- Dellwig, L.F., J.E. Bare, and R. Gelnett. 1978. SLAR—for clear as well as cloudy weather. *Proceedings of the International ISPRS Symposium*. Freiburg/Br., Germany, 1, 527-1,546.
- Ellis, J.M. and D.A. Richmond. 1990. Mapping the coastal plain of the Congo with airborne digital radar. *Proceedings of the 8th Thematic Conference on Geologic Remote Sensing Exploration, Engineering and Environment*, Denver, Colorado, USA, 87-100.
- ESA. 1992. *ERS-1 SAR.PRI Product CCT Format*. EARTHNET Program Office, ESA, Italy.

- ESA. 1993. ERS-1: 500 Days in Orbit. ESA Public Relations, Paris, France.
- ESCAP/SPARRSO. 1989. Remote Sensing for flood plain mapping and flood monitoring. ESCAP/UNDP (RAS86/141) Bangkok, Thailand. Dhaka, Bangladesh, Workshop Report ST/ESCAP/848: 182.
- FAP 19 GIS. 1992. GIS Atlas for Tangail Area Study. Technical Report, ISPAN/USAID, Dhaka, Bangladesh.
- FAP 19 GIS. 1993. Classification of Flood Depth and Extent Using GIS and MIKE 11. Technical Report, ISPAN/USAID, Dhaka, Bangladesh.
- FAP 19 GIS. 1995. The Bangladesh National Level GIS Database. ISPAN/USAID, Dhaka, Bangladesh.
- FAP 20, 1992, Tangail CPP Interim Report, Annex 2/Agriculture.
- Fingas, M., M. Fruhwirth, and L. Gamble. 1992. Oil spill remote sensing sensors and aircraft. Proceedings from the 15th Arctic and Marine Spill Program Technical Seminar, Edmonton, Alberta, Canada, 407-425.
- Ford, J.P. and F.F. Sabins. 1986. Satellite radars for geologic mapping in tropical regions. Proceedings of the 5th Thematic Conference on Remote Sensing for Exploration Geology, Reno, Nevada, USA.
- Ford, J.P. and R. Da Cunha. 1986. Shuttle radar images for geologic mapping in tropical rainforest. Proceedings of the 4th Thematic Conference on Remote Sensing for Exploration Geology, San Francisco, California, USA, 669-676.
- Ford, J.P., J.B. Cimino, B. Holt, and M.R. Ruzek. 1986. Shuttle imaging radar views Earth from Challenger: The SIR-B experiment. JPL Publ. 86-10, Jet Propulsion Laboratory, Pasadena, California, USA.
- Ford, J.P. and D.J. Casey. 1988. Shuttle radar mapping with diverse incidence angles in the rainforest of Borneo. *International Journal of Remote Sensing*, Vol. 9, No. 5: 927-943.
- Gaddis, L.R. and P.J. Mougini-Mark. 1985. Mississippi River outflow patterns seen by SEASAT radar. *Geology*, Vol. 13: 227-230.
- Gelnett, R.H., L.F. Dellwig, and J.E. Bare. 1978. Increased visibility from the invisible—a comparison of radar and LANDSAT in tropical environments. Proceedings of the 12th International Symposium on Remote Sensing of the Environment, Manila, Philippines, Vol. 3: 2,205-2,216.
- Gonzales, F.I., E.D. Cokelet, J.F.R. Gower, and M.R. Mulherm. 1985. SLAR and in-situ observations of wave-current interaction on the Columbia River bar in the ocean surface. Toba, Y. and H. Mitsuyasu (eds.), Reidel Publishing Company, 301-303.
- Griffith, F.B., V.D. Lyne, G.P. Harris, and J.S. Parslow. 1988. Detecting surface schooling fish using a sideways looking airborne radar. Proceedings from the UN/ESA workshop on Microwave remote sensing technology, Bangkok, Thailand.
- Imhoff, M.L. and D.G. Gesch. 1990. The derivation of a sub-canopy digital terrain model of a flooded forest using synthetic aperture radar. *Photogrammetric Engineering and Remote Sensing*, Vol. 56, No. 8: 1,155-1,162.
- Imhoff, M.L., C.H. Story, M.H. Vermillion, F. Khan, and F. Polcyn. 1986. Forest canopy characterization and vegetation penetration assessment with spaceborne radar. *IEEE Trans. Geoscience & Remote Sensing*, Vol. GE-24, No. 4: 535-541.

64

- Imhoff, M.L., C. Vermillion, M.H. Story, A.M. Choudhury, A. Gafoor, and F. Polcyn. 1987. Monsoon flood boundary delineation and damage assessment using spaceborne imaging radar and Landsat data. *Photogrammetric Engineering and Remote Sensing*, Vol. 54, No. 4: 405-413.
- Kasischke, E.S., R.A. Shuchman, D.R. Lyzenga, and G.A. Meadows. 1983. Detection of bottom features on seasat synthetic aperture radar imagery. *Photogrammetric Engineering and Remote Sensing*, Vol. 49, No. 9: 1,341-1,353.
- King, R.B. 1985. Comparison of SLAR, SIR, and Landsat imagery for mapping land systems in Kalimantan, Indonesia. *Proceedings of the International Conference of the Remote Sensing Society/Center for Earth Resources Management*, London, 381-390.
- Leberl, F.W. 1990. *Radargrammetric Image Processing*. Artech House, Inc., Norwood, Massachusetts, USA.
- Lecote, R. and T.J. Pultz. 1991. Evaluation of the potential of RADARSAT for flood mapping using simulated satellite SAR imagery. *Canadian Journal of Remote Sensing*, Vol. 17, No. 3: 241-249.
- Lee, J.S., P. Dewaele, P. Wambacq, A. Oosterlinck, and I. Jurkevich. 1993. Speckle Filtering of Synthetic Aperture Radar. *Harwood Academic Publishers, Remote Sensing Reviews*, Vol 8: 93-109.
- Lewis, A.J. 1977. Coastal mapping with radar. *Geoscience and Man*, Vol. 18: 239-247.
- Lind, A. 1984. An analysis of spaceborne imaging radar—Songkhla Barrier, South Thailand. *Photointerpretation*, 84-5/2,3.
- Lowry, R.T., Vaneck, and R.V. Dams. 1986. SAR imagery for forest management. *IGARSS/86 Proceedings*, Zurich, Switzerland, 901-906.
- MacDonald, H.C. 1969. Geologic evaluation of radar imagery from Dairen Province, Panama. *Modern Geology*, Vol. 1: 1-63.
- MacDonald, H.C., A.J. Lewis, and R.S. Wing. 1971. Mapping and landform analysis of coastal regions with radar. *Geological Society of America Bulletin*, Vol. 82: 345-358.
- MacDonald, H., W.P. Waite, V.H. Kaupp, V.H., L.C. Bridges, and M. Storm. 1983. Evaluation of SIR-A space radar for geologic interpretation: United States, Panama, Colombia, and New Guinea, Final Report. JPL Contract No. 964940, University of Arkansas Remote Sensing Laboratory Tech. Report 83-2, Fayetteville, Arkansas, USA.
- Meadows, G.A., E.S. Kasischke, and R.A. Shuchman. 1980. SAR observations of coastal zone conditions. *Proceedings from the 14th International Symposium on Remote Sensing of Environment*, San Jose, Costa Rica, Vol. II: 845-863.
- Mercer, J.B. and M.E. Kirby. 1987. Topographic mapping using STAR-1 radar data. *Geocarto International*, No. 3: 39-42.
- Muenlek, S.T. and B.N. Koopmans. 1983. The Shuttle Imaging Radar over south peninsula Thailand. *ITC Journal*, 258-269.
- Ormsby, J., B. Blanchard, and A. Blanchard. 1985. Detection of lowland flooding using active microwave systems. *Photogrammetric Engineering & Remote Sensing*, Vol. 51, No. 3: 317-328.
- Parashar, S., E. Langham, J. McNally, and S. Ahmed. 1993. RADARSAT mission requirements and concepts. *Canadian Journal of Remote Sensing*, (Special RADARSAT Issue), Vol. 19, No. 4: 280-288.
- Paudyal, D.R. and J. Aschbacher. 1993. Evaluation and Performance Tests of Selected SAR

- speckle Filters. Proceedings, International Symposium "Operationalization of Remote Sensing", ITC Enschede, The Netherlands, 89-96.
- Petit, M., J.M. Stretta, H. Farrugio, and A. Wadsworth. 1992. Synthetic aperture radar imagery of sea surface life and fishing activities. *IEEE Trans., Geosciences Remote Sensing*, Vol. 30, No. 5: 1,085-1,089.
- Pope, K.O. (1988), Radar remote sensing of seasonal inundation in the Bajos near El Mirador, Peten, Guatemala, in: Dahlin, B.H. (ed.) *Human Ecological studies at El Mirador*, New World Archaeological Foundation Publications, Provo, Utah, USA.
- Pultz, T.J., R. Leconte, L. St.Laurent, and L. Peters. 1991. Flood mapping with airborne SAR imagery. *Canadian Water Resources Journal*.
- Radarsat International Inc. 1993. Radar satellite tracks Mississippi River flood. *Reflections*, Ottawa, Canada.
- Radarsat International. 1992. Catalogue of recent radar research related to Canada's RADARSAT. Main Volume, Radarsat International, Ottawa.
- Raney, R.K./APL. 1994. Radar basics—Introduction to synthetic aperture radar remote sensing. CCRS/GlobeSAR/RSI. Geomatics Canada, Ottawa, 75.
- Raney, R.K./APL (formerly CCRS), in: CCRS/GlobeSAR/RSI. 1994. *RADAR BASICS: Introduction to Synthetic Aperture Radar Remote Sensing*. Geomatics Canada, Ottawa, Canada.
- Raney, R.K., F.J. Ahern, R.V. Dams & D. Werle (1990) A review of radar remote sensing for tropical forest management, UN/FAO/ESA Microwave Workshop, INPE, Brazil, Nov. 19-23.
- Sood, R.K., N.S. Mehta, and A.S. Rajawat. 1985. Evaluation of SIR-B images over parts of Indian region. Indian Space Research Organization, Bangalore, India, TR-48-85.
- Sood, R.K., N.S. Mehta, V.D. Bhate, and S.B. Sharma. 1985. A comparative evaluation of SIR-A, Landsat MSS and RBV data covering parts of Central India. Indian Space Research Organization, Bangalore, India, TR-48-85.
- Thompson, M.D. and R.V. Dams. 1990. Forest and land cover mapping from SAR: A summary of recent tropical studies. Proceedings of the 23rd International Symposium of Remote Sensing of the Environment, Bangkok, Thailand/ERIM, Michigan, USA.
- Trevett, J.W. (1986), *Imaging radar for resource surveys*, London, New York.
- Ulaby, F.T., R.K. Moore, and A.K. Fung. 1981, 1982, 1986. *Microwave Remote Sensing: Active and Passive*. Addison-Wesley, Reading, Massachusetts, USA, vol. I-III.
- Vass, P., B. Battrock, (editors), 1992. *ESA ERS-1 Product Specification*; ESA Publications, ESTEC, Noordwijk, The Netherlands.
- Wagner, T.W. 1980. The nature of spaceborne (SEASAT) radar data of developing countries: A Costa Rican case study. Proceeding from the 14th International Symposium on Remote Sensing of Environment, San Jose, Costa Rica.
- Wahl, T., K. Dildhuset, and A.Skoelv. 1993. Ship traffic monitoring and oil spill detection using ERS-1. Proceeding from the International Symposium Operationalization of Remote Sensing, ITC Enschede, The Netherlands, Vol. 5: 97-106.

Wan Ahmed, W.Y., F. MacCullum, R.V. Dams, S.B. Mokhtar, and H.O. Cheah. 1988. Landsat MSS, SPOT and SAR for tropical forestry applications in Malaysia. Proceedings of the 9th Asian Conference on Remote Sensing, Bangkok, Thailand, Q-23/1-8.

Werle, D. 1992. Second edition of radar remote sensing: A training manual. Dendron Resource Surveys, Canada Centre for Remote Sensing/RADARSAT International, Ottawa, Canada.

Werle, D. (ed.). 1993. Radar remote sensing imagery of coastal regions on CD-ROM. CD-ROM and User Guide, AERDE Environmental Research, Halifax, Nova Scotia.

OTHER REFERENCES

- Adams, R.E.W., W.E. Brown, and T.P. Culbert. 1981. Radar mapping, archaeology, and ancient Maya land use. *Science*, Vol. 213: 1,457-1,463.
- Adeniyi, P.O. 1984. Land use and land cover in Nigeria: an appraisal of the Nigerian radar project. *The Nigerian Geographical Journal* 27, Vol. 1 and 2.
- Akam, B., R. Dean, M. Sartori, R. Lowry, and B. Mercer. 1988. An integrated radar imaging system for the STAR-2 aircraft. *Proceedings of the 1988 IEEE Radar Conference*, 28-32.
- Alam, S., S.D. Shamsuddin, and M. Kamal. 1992. A geomorphological approach to flood zoning using remote sensing techniques, pp. 70-79 in: Elahi, K.M., A.H.M. Raihan Sharif, and A.K.M. Abul Kalam (eds.). 1992. *Bangladesh: Geography, Environment and Development*, Bangladesh National Geographic Association, Dhaka.
- Alam, S. and A.H.M. Raihan Sharif. 1992. Remote sensing and GIS for geographical research in Bangladesh, pp. 287-296 in: Elahi, K.M., A.H.M. Raihan Sharif, and A.K.M. Abul Kalam (eds.). 1992. *Bangladesh: Geography, Environment and Development*, Bangladesh National Geographic Association, Dhaka.
- Banyard, S.G. 1979. Radar: Interpretation based on photo-truth keys. *ITC Journal*, 267-276.
- Brazilian Ministry of Mines and Resources. Various Years. *Projecto RADAM BRAZIL, levantamentos de recursos naturais, Brazilia/Rio de Janeiro*.
- Bullock, B.L. 1987. Radar applications in remote sensing: An airborne remote sensing case history. *Proceedings of the 21st International Symposium on Remote Sensing of the Environment*, Ann Arbor, Michigan.
- Calla, O.P.N. 1984. Development of microwave sensors for remote sensing applications—An Indian experience. *Atti. 24 Convegno Int. lo Sullo Spazio*, Rome, Italy, 249-266.
- Catt, P. 1990. Side-looking airborne radar (SLAR) imagery for terrain mapping in the humid tropics. *Proceedings of the 5th Australian Remote Sensing Conference*, Perth, 495-503.
- Chen, J., Y. Chen, P. Duan, and Y. Ni. 1988. Application of RAR for flood surveillance and terrain investigation in North China and East China. *Proceedings of the 9th Asian Conference on Remote Sensing*, Bangkok.
- Churchill, P.M., A. Horne, and R. Kessler. 1985. A review of radar analyses of woodland. *EARSel Workshop Proceedings*, ESA SP-227, 25-32.
- Dans, R.V., D. Flett, M.D. Thompson, and M. Lieberman. 1987. SAR image analysis for Costa Rican tropical forestry applications. *SELPER/II Simposio Latino Americano Sobre Sensores Remotos*, Bogota, Colombia, 22-28.
- De Molina, I. and C. Molina. 1989. The use of high resolution radar imagery in forest inventories in tropical forests of Cativo (prioria copai-fera). *Proceedings of the 1989 SELPER Conference*, Buenos Aires, Argentina.
- De Molina, G.I and L.C. Molina. 1986. The use of SLAR and SIR-A images for the classification of forest types in the tropics, Mimeo.
- De Molina, I., L. Mosquera, M. Molina, and R. Deagostini. 1973. SLAR in the mapping of humid tropical forests of Columbia. *Proceed-*

- ings of the 1st Panamerican Symposium on Remote Sensing, Panama City, 231-272.
- Dekker, F., H. Balkwill, A. Slater, R. Herner, and W. Kampschuur. 1989. Hydrocarbon exploration through remote sensing and fieldwork in the onshore Eastern Papuan Fold Belt, Gulf Province, Papua New Guinea. Proceedings 7th Thematic Conference on Remote Sensing for Exploration Geology, Calgary, Alberta, Vol. I: 65-80.
- Denyer, N., R.K. Raney, and N. Shepherd. 1993. The RADARSAT SAR data processing facility. Canadian Journal of Remote Sensing (Special RADARSAT Issue), Vol. 19, No. 4: 311-316.
- Eden, M.J. and J.T. Perry (eds.). 1986. Remote sensing and tropical land management. John Wiley, London, New York, Sydney, Toronto.
- Elachi, C. 1988. Spaceborne radar remote sensing: applications and techniques. IEEE Press, New York.
- Ellis, J.M. and F.D. Pruett. 1986. Application of SAR to southern Papua New Guinea Fold Belt exploration. Proceedings of the 5th Thematic Conference on Remote Sensing for Exploration Geology, Reno, Nevada, USA, 15-34.
- Ellis, J.M. and L.L. Dekker. 1988. Petroleum exploration with airborne radar (SAR) and geologic field work, Sinu Basin of NW Colombia. Proceedings of the 6th Thematic Conference on Remote Sensing for Exploration Geology, Houston, Texas, 79-89.
- ERDAS. 1990. Field Guide, Version 7.4. ERDAS Inc., Atlanta, Georgia, USA.
- Fagbami, A. and A. Fapohunda. 1986. SLAR imagery for soil mapping and regional planning in western Nigeria, pp. 55-77, in: Eden, M.J. and J.T. Perry (eds.). 1986. Remote sensing and tropical land management. John Wiley, London, New York, Sydney, Toronto.
- FAP 19 GIS. 1993. Area-Elevation Curves for BWDB Southwest Regional Projects. Technical Note 3, ISPAN/USAID, Dhaka, Bangladesh.
- FAP 19 GIS. 1993. Tangail Area Digital Elevation Model. Technical Note 6, ISPAN/USAID, Dhaka, Bangladesh.
- Ford, J.P., J.B. Cimino, and C. Elachi. 1983. Space Shuttle Columbia views the World with imaging radar: The SIR-A experiment. JPL Publishers 82-95, Jet Propulsion Laboratory, Pasadena, California.
- Furley, P.A. 1986. Radar surveys for resource evaluation in Brazil: an illustration from Rondonia, pp. 79-99 In: Eden, M.J. and J.T. Perry (eds.). Remote sensing and tropical land management. John Wiley, London, New York, Sydney, Toronto.
- Gardner, J.V. 1982. Utility of SLR in hydrocarbon exploration: An appraisal based on case histories. Proceedings of the 2nd Thematic Conference on Remote Sensing for Exploration Geology, Fort Worth, Texas, 191-198.
- Gower, J.F.R., P.W. Vachon, and H. Edel. 1993. Ocean applications of RADARSAT. Canadian Journal of Remote Sensing, Vol 19, No. 4: 372-383.
- Granath, J.W., K.A. Soofi, and J.B. Mercer. 1990. Application of SAR in structural modeling of the Central Ranges Thrust Belt, Irian Jaya, Indonesia. Proceedings of the 8th Thematic Conference on Geologic Remote Sensing Exploration, Engineering and Environment, Denver, Colorado, USA, 105-116.
- Grant, D.F., D.R. Inkster, and R.T. Lowry. 1986. The application of STAR-1 synthetic aperture radar in tropical environments. Unpublished paper, Intera Technologies, Calgary, Alberta, Canada.

- Harris, J., T.K. Hirose, and R. Murray. 1989. The IHS transform for the integration of radar data with other remotely sensed data. *Journal of Photogrammetric Engineering and Remote Sensing*, Vol. 56, No. 12: 1,631-1,641.
- Herner, R.R. 1985. The Gabon Basin: Its regional setting with respect to onshore basement tectonic elements as interpreted from side-looking airborne radar imagery. *Proceedings of the 4th Thematic Conference on Remote Sensing for Exploration Geology*, San Francisco, California, USA, 31-47.
- Hess, L.A., J.M. Melack, and D.S. Simonett. 1990. Radar detection of flooding beneath the forest canopy: A review, *International Journal of Remote Sensing*, Vol. 11, No. 7: 1,313-1,325.
- Hoffer, R.M and K.S. Lee. 1989. Forest change classification using SEASAT and SIR-B satellite SAR data. *IGARSS 1989 Symposium Proceedings*, Vancouver, Vol. 3: 1,372-1,375.
- Jet Propulsion Laboratory. 1980. *Radar geology: An assessment*. JPL Publishers, 80-61, Pasadena, California, 513.
- Koopmans, B.N. 1986. Satellite radar interpretation of the Bintuni Basin area, Eastern Vogelkop Peninsula, West Irian, Indonesia. *Geologie en Mijnbouw*, 65, 197-204.
- Koopmans, B.N. 1983. Side-looking radar—A tool for geological surveys. *Remote Sensing Reviews*, Vol. 1: 19-69.
- Koopmans, B.N. 1979. Description of radar imagery in the SLAR sample collection. *ITC Training Manual*, International Institute for Aerial Survey and Earth Sciences, Enschede, The Netherlands.
- Krohn, M.D., N.M. Milton, and D.B. Segal. 1983. SEASAT SAR response to lowland vegetation types in eastern Maryland and Virginia. *Journal of Geophysical Research*, Vol. 88, No. C3: 1,937-1,952.
- Li, F. and R.K. Raney (eds.). 1991. *Spaceborne radars for Earth and planetary observation*. *Proceedings of the IEEE, Special Section*, Vol. 79, No. 6: 773-880.
- Mercer, J.B. 1989. A new airborne SAR for ice reconnaissance operations. *Proceedings of the IGARSS, Vancouver, Canada*, 6.
- Nezry, E., E. Mougin, A. Lopez, J.P. Gastellu-Etchegorry, and Y. Laumonier. 1993. Tropical vegetation mapping with combined visible and SAR spaceborne data. *International Journal of Remote Sensing*: 2, 165-2, 184.
- Parkin, D. 1990. A new image for the Ericsson side looking airborne radar. *Proceedings of the 5th Australian Remote Sensing Conference*, Perth, 724-727.
- Parry, D.E. & J.W. Trevett (1979), Mapping Nigeria's vegetation from radar, *Geographical Journal* 145, No. 2: 265-281.
- Raney, R.K., K.F. Link & R.P. da Cunha (1990) Radar processing, RADARSAT, and technology transfer issues, *Proceedings of the International Symposium on Primary Data Acquisition/International Archives of Photogrammetry and Remote Sensing*, Vol. 28, Part1, 221-227.
- Rebillard, P. & T. Dixon (1984) Geologic interpretation of SEASAT SAR imagery near the Rio Lacuntum, Mexico, in Teleki, P. & V. Weber (eds.) *Remote sensing for geological mapping*, *Proceedings IUGS/UNESCO Seminar*, New Orleans, USA, IUGS Publ. No. 18: 129-142.
- Ringrose, S.M. & P. Large (1983) The Comparative value of LANDSAT print and digitized data and radar imagery for ecological land classification in the humid tropics, *Canadian*

- Journal of Remote Sensing, Vol. 9, No. 1: 45-60.
- Sabins, F.F. (1983) Geologic interpretation of Space Shuttle radar images of Indonesia, American Association of Petroleum Geology Bulletin, Vol. 67, No. 11: 2076-2099.
- Sader, S.A., T.A. Stone & A.T. Joyce (1990) Remote sensing of tropical forests: An overview of research and applications using non-photographic sensors, Photogrammetric Engineering & Remote Sensing, Vol. 56, No. 10: 1343-1351.
- Sicco-Smit (1978) SLAR for forest type classification in a semi-deciduous tropical region, ITC Journal, 1978-3: 385-401.
- Sicco-Smit, G. (1980), SLAR mosaic interpretation for forestry purposes, Proceedings of the 14th Congress International Society of Photogrammetry, Hamburg, Germany.
- Simonett, D.S., A.H. Strahler, G.Q. Sun & Y. Wang (1987) "Radar forest modelling: Potentials, problems, approaches, models," Proceedings of the 13th Annual Conference of the Remote Sensing Society, University of Nottingham, September 1987, 256-270.
- Soofi, K. & F. Payot (1990) Acquisition and processing of synthetic aperture radar (SAR) for Conoco, Proceedings of the 8th Thematic Conference on Geologic Remote Sensing Exploration, Engineering and Environment, Denver, Colorado, USA, 59-85.
- Southworth, C.S. (1984) Structural and hydrogeologic applications of remote sensing data, eastern Yucatan Peninsula, Mexico, In: Beck, B. (1984) Sinkholes: Their geology, engineering and environmental impact, Proceedings of the 1st Multi-disciplinary Conference on Sinkholes, Orlando, Florida, USA, 59-64.
- Specter, C.N. & R.K. Raney (1990) The Ever-Green Plan for monitoring and management of tropical forests, Proceedings of the International Symposium on Primary Data Acquisition/International Archives of Photogrammetry and Remote Sensing, Vol. 28, Part 1: 158-165.
- Stone, T.A., G.M. Woodwell & R.A. Houghton (1989), Tropical deforestation in Pará, Brazil: Analysis with Landsat and Shuttle Imaging Radar, IGARSS '89 Symposium Proceedings, Vancouver, Vol. 1:192-195.
- Stone, T.A. & G.M. Woodwell (1988) SIR-A analysis of land use in Amazonia, International Journal of Remote Sensing, Vol. 9, No. 1: 95-105.
- Wadge, G. & T.H. Dixon (1984) a geological interpretation of SEASAT SAR imagery of Jamaica, Journal of Geology, Vol. 92: 561-581.
- Werle, D. (1989) Potential application of imaging radar for monitoring depletion of tropical forests, Proceedings of the IGARSS '89/12th Canadian Symposium on Remote Sensing, Vancouver, BC, Canada, Vol. III: 1383-1386.
- Werle, D. (1990) Radar remote sensing for application in forestry—A literature review for investigators and potential users of SAR data in Canada, CCRS Report, 45.
- Werle, D. (1991) Spaceborne SAR observations of a high-tidal estuary and its mangrove vegetation: Ord River-Cambridge Gulf, NW Australia, Proceedings of the 14th Canadian Symposium on Remote Sensing, Calgary, Alberta, 465-469.
- Werle, D., 1988. Radar Remote Sensing: A Training Manual; Dendron Resource Surveys Ltd., Ottawa, Ontario, Canada.

11

Zhang, C.B. (1988) A synthetic aperture radar with multichannel and multipolarization, Proceedings IGARSS'88, Vol. 1: 331-333, Edinburgh, Scotland.

APPENDIX A (1 of 6)

Ground Reference Information and Accuracy Assessment of Classification

central Bangladesh ERS-1 SAR Images

Ref No	Class Code	Flood Depth	Canopy %	Croptype	Remarks	July				August			
						Flooded	Not Flooded	Total	%Correct	Flooded	Not Flooded	Total	%Correct
150	1100	0	0	--	urban						18.7	18.7	100%
150	1100	0	0	--	urban		18.7	18.7	100%				
151	1100	0	0	--	urban						25.2	25.2	100%
151	1100	0	0	--	urban		25.2	25.2	100%				
152	2210	0	0	--	settlement					1.0	20.9	21.9	95%
152	2210	0	0	--	settlement	1.4	20.5	21.9	94%				
153	2210	0	0	--	settlement	0.4	12.6	13.0	97%				
153	2210	0	0	--	settlement					0.6	12.4	13.0	96%
154	2210	0	0	--	settlement					0.3	13.6	13.9	98%
154	2210	0	0	--	settlement		13.9	13.9	100%				
155	2210	0	0	--	settlement		20.4	20.4	100%				
155	2210	0	0	--	settlement						20.4	20.4	100%
156	2210	0	0	--	settlement		23.1	23.1	100%				
157	2210	0	0	--	settlement					0.1	19.1	19.3	99%
157	2210	0	0	--	settlement	0.1	19.1	19.3	99%				
158	2210	0	0	--	settlement					0.1	15.6	15.6	100%
158	2210	0	0	--	settlement		15.6	15.6	100%				
URBAN / SETTLEMENTS						JULY: 99%				AUG: 98%			
9	2210	0	>60	trees	homestead					3.4	3.4	6.8	50%
9	2210	0	>60	trees	homestead	0.3	6.5	6.8	96%				
204	2220	0	--	mixed	homestead	2.0	16.8	18.8	89%				
217	2210	0	>60	trees	homestead					12.2	23.6	35.7	66%
WOODED HOMESTEADS						JULY: 93%				AUG: 58%			

13

APPENDIX A (2 of 6)

Ground Reference Information and Accuracy Assessment of Classification
central Bangladesh ERS-1 SAR Images

Ref No	Class Code	Flood Depth	Canopy %	Crop/Type	Remarks	July				August			
						Flooded	Not Flooded	Total	%Correct	Flooded	No. Flooded	Total	%Correct
111	2533	0	70-100	sugarcane	dry soil					5.3	1.2	6.4	18%
112	2533	0	70-100	sugarcane	dry soil		7.6	7.6	100%				
113	2533	0	70-100	sugarcane	dry soil	1.6	3.8	5.4	70%				
SUGARCANE (DRY)						JULY: 85%				AUG: 18%			
13	2633	0	70-100	sugarcane	moist soil	0.1	34.1	34.2	100%				
190	2633	0	70-100	sugarcane	moist soil					4.6	9.3	13.9	67%
111	2633	0	70-100	sugarcane	moist soil	0.4	6.1	6.4	94%				
201	2633	0	70-100	sugarcane	moist soil		3.3	3.3	100%				
219	2633	0	70-100	sugarcane	moist soil					0.5	32.5	33.0	98%
SUGARCANE (MOIST)						JULY: 98%				AUG: 83%			
209	2632	0	70-100	jute	moist soil		10.8	10.8	100%				
JUTE (MOIST)						JULY: 100%							
103	3532	30-90	70-100	jute	flooded	2.0	4.9	6.9	29%				
103	3532									1.9	5.0	6.9	28%
JUTE (DEEP)						JULY: 29%				AUG: 28%			
106	3632	>90	70-100	jute	flooded	16.7	5.5	22.2	75%				
JUTE (VERY DEEP)						JULY: 75%							
110	2611	0	0-30	sparse paddy	moist soil					1.4	4.6	6.0	77%
122	2611	0	0-30	sparse paddy	moist soil					13.4	1.8	15.2	12%
203A	2611	0	0-30	sparse paddy	moist soil	8.2	4.6	12.8	36%				
SPARSE RICE (MOIST)						JULY: 36%				AUG: 44%			

APPENDIX A (3 of 6)

Ground Reference Information and Accuracy Assessment of Classification
central Bangladesh ERS-1 SAR Images

Ref No	Class Code	Flood Depth	Canopy %	Croptype	Remarks	July				August			
						Flooded	Not Flooded	Total	%Correct	Flooded	Not Flooded	Total	%Correct
7	3411	1-30	0-30	sparse paddy	flooded	4.0		4.0	100%				
102	2711	1-30	0-30	sparse paddy	<10cm					2.1	3.6	5.7	63%
110	2711	1-30	0-30	sparse paddy	<5cm	3.7	2.3	6.0	61%				
117	3411	1-30	0-30	sparse paddy	flooded					14.2	1.5	15.7	90%
121	2711	1-30	0-30	sparse paddy	ponded					10.3		10.3	0%
123	3411	1-30	0-30	sparse paddy	flooded					40.1	24.5	64.6	62%
205A	3411	1-30	0-30	sparse paddy	flooded	9.5		9.5	100%				
207A	3411	1-30	0-30	sparse paddy	flooded	94.0	0.6	94.6	99%				
213	3411	1-30	0-30	sparse paddy	flooded	42.1	27.6	69.7	60%				
SPARSE RICE (SHALLOW)						JULY: 84%				AUG: 54%			
101	3511	30-90	0-30	sparse paddy	flooded	5.6		5.6	100%				
SPARSE RICE (DEEP)						JULY: 100%							
107	3611	>90	0-30	sparse paddy	flooded	13.9	7.1	21.0	66%				
124	3600	>90	0	empty paddy	flooded, fallow					42.0		42.0	100%
221	4219	W	0-30	sparse paddy	deep aman					40.8		40.8	100%
SPARSE RICE (VERY DEEP)						JULY: 66%				AUG: 100%			
2053	2521	0	30-70	intermed paddy	dry soil					3.9	4.4	8.3	53%
MEDIUM RICE (DRY)										AUG: 53%			
216	2621	0	30-70	intermed paddy	moist soil					21.1	21.8	42.9	51%
MEDIUM RICE (MOIST)										AUG: 51%			

APPENDIX A (4 of 6)

Ground Reference Information and Accuracy Assessment of Classification
central Bangladesh ERS-1 SAR Images

Ref. No.	Class Code	Flood Depth	Canopy %	Crop type	Remarks	July				August			
						Flooded	Not Flooded	Total	%Correct	Flooded	Not Flooded	Total	%Correct
7	3421	1-30	30-70	intermed paddy	flooded					2.6	1.4	4.0	64%
115	2721	1-30	30-70	intermed paddy	10-20cm					4.8	1.1	5.9	19%
125	3421	1-30	30-70	intermed paddy	flooded					5.8	9.1	14.9	39%
MEDIUM RICE (SHALLOW)										AUG:		41%	
206A	3521	30-90	30-70	intermed paddy	flooded	52.7	20.6	73.3	72%				
206B	3521	30-90	30-70	intermed paddy	flooded					64.4	6.2	70.6	91%
MEDIUM RICE (DEEP)						JULY: 72%				AUG:		91%	
191	3621	>90	30-70	intermed paddy	flooded					30.6	7.3	37.8	81%
MEDIUM RICE (VERY DEEP)										AUG:		81%	
203B	2731	1-30	70-100	mature paddy	20cm					8.1	4.4	12.5	35%
207B	3431	1-30	70-100	mature paddy	flooded					91.6	0.4	92.0	100%
MATURE RICE (SHALLOW)										AUG:		67%	
2	3531	30-90	70-100	mature paddy	flooded	46.3	49.4	95.7	48%				
16	3531	30-90	70-100	mature paddy	flooded					9.2	1.9	11.1	83%
MATURE RICE (DEEP)						JULY: 48%				AUG:		83%	
10	3631	>90	70-100	mature paddy	flooded	10.1		10.1	100%				
215	3631	>90	70-100	mature paddy	flooded					30.4	0.1	30.6	100%
218	3631	>90	70-100	mature paddy	flooded					7.1	14.9	22.1	32%
MATURE RICE (VERY DEEP)						JULY: 100%				AUG:		66%	

✓

APPENDIX A (5 of 6)

Ground Reference Information and Accuracy Assessment of Classification
central Bangladesh ERS-1 SAR Images

Ref No	Class Code	Flood Depth	Canopy %	Croptype	Remarks	July				August			
						Flooded	Not	Total	%Correct	Flooded	Not	Total	%Correct
104	3222	30-90	0-30	weed,grass,mixed	flooded	7.7		7.7	100%				
116	3212	30-90	0-30	weed,grass,mixed	flooded	76.6		76.6	100%				
					WEEDS (DEEP)		JULY:		100%				
6	3312	>90	0-30	weed,grass,mixed	flooded	3.6	5.8	9.4	38%				
6	3312	>90	0-30	weed,grass,mixed	flooded					3.9	5.4	9.4	42%
18	3312	>90	0-30	weed,grass,mixed	flooded					4.3	11.5	15.8	27%
105	4312	W	0-30	weed,grass,mixed	ponds	3.1	0.8	3.9	79%				
118	4412	W	0-30	vegetation	marshy land					2.9	3.7	6.6	44%
					WEEDS (VERY DEEP)		JULY:		40%		AUG:		38%
115	3112	1-30	0-30	weed,grass	seasonal flooded	5.375	0.5	5.9	91%				
108	2719	1-30	0-30	other	15cm water,grass	8.8	0.8	9.6	92%				
					SPARSE GRASS (SHALLOW)		JULY:		92%				
15	3619	>90	0-30	other	grass, water 5-6 m	19.9		19.9	100%				
212B	3312	>90	0-30	grass	flooded					65.9		65.9	100%
					SPARSE GRASS (VERY DEEP)		JULY:		100%		AUG:		100%
102	2629	0	30-70	other	moist soil, grass	1.8	3.9	5.7	68%				
					MEDIUM GRASS (MOIST)		JULY:		68%				
114	2639	0	70-100	other	moist soil, grass	3.6	1.3	4.9	27%				
					DENSE GRASS (MOIST)		JULY:		27%				
109	3221	30-90	30-70	hyacinth	flooded	4.4	5.3	9.7	45%				
119	4331	W	30-70	hyacinth						1.1	1.7	2.8	40%
					SCATTERED WATER HYACINTH		JULY:		45%		AUG:		40%

11

APPENDIX A (5 of 6)

Ground Reference Information and Accuracy Assessment of Classification
central Bangladeshi ERS-1 SAR Images

Ref. No	Class Code	Flood Depth	Canopy %	Crop type	Remarks	July			August				
						Flooded	Not	Total % Correct	Flooded	Not	Total % Correct		
8	3331	>90	70-100	hyacinth	flooded	6.7		6.7	100%				
17	4331	W	70-100	hyacinth	ponds					3.4	2.3	5.6	60%
208	4231	R	70-100	hyacinth	river		3.9	3.9	0%				
DENSE WATER HYACINTH						JULY:			AUG:			60%	
1	4120	R	0	--	river/khal:turbid	0.4	9.1	9.5	5%				
192	4120	R	0	--	river/khal:turbid					2.6	4.1	6.7	38%
193	4120	R	0	--	river/khal:turbid					2.4	0.4	2.8	86%
14	4120	R	0	--	river/khal:turbid	2.3	6.8	9.1	25%				
105	4300	W	0	--	ponded					3.1	0.9	3.9	78%
202	4200	W	0	--	beel	421.3		421.3	100%				
194	4100	R	0	--	river					4.3	2.3	6.6	65%
210	4110	R	0	--	river	3.9	2.5	6.4	61%				
211	4110	R	0	--	river	15.4	0.1	15.5	99%				
195	4210	R	0	--	river					14.2	0.9	15.1	94%
212A	4200	W	0	--	beel	68.4	0.4	68.8	99%				
214	4120	R	0	--	river	36.3	4.4	40.6	89%				
220	4200	W	0	--	beel					24.3		24.3	100%
OPEN WATER						JULY:			AUG:			77%	

13

Level 1	Level 2	Level 3	Level 4
	2700 INUNDATED (Water Depth 1-30 cm)	2630 CANOPY 70-100%	2631 PADDY 2632 JUTE 2633 SUGARCANE 2639 OTHERS
		2710 CANOPY 0-30%	2711 PADDY 2712 JUTE 2713 SUGARCANE 2719 OTHERS
		2720 CANOPY 30-70%	2721 PADDY 2722 JUTE 2723 SUGARCANE 2729 OTHERS
		2730 CANOPY 70-100%	2731 PADDY 2732 JUTE 2733 SUGARCANE 2739 OTHERS
3000 SEASONAL FLOODED LAND	3000 WITH VEGE. FLOOD DEPTH (1-30 cm)	3110 CANOPY 0-30%	3111 HYACINTH 3112 WEED GRASS MIXED 3119 OTHER
		3120 CANOPY 30-70%	3121 HYACINTH 3122 WEED GRASS MIXED 3229 OTHER
		3130 CANOPY 70-100%	3131 HYACINTH 3132 WEED GRASS MIXED 3139 OTHER
	3200 WITH VEGE. FLOOD DEPTH (30-90 cm)	3210 CANOPY 0-30%	3211 HYACINTH 3212 WEED GRASS MIXED 3219 OTHER
		3220 CANOPY 30-70%	3221 HYACINTH 3222 WEED GRASS MIXED 3229 OTHER
		3230 CANOPY 70-100%	3231 HYACINTH 3232 WEED GRASS MIXED 3239 OTHER

APPENDIX B

CLASSIFICATION FOR MONSOON SEASON RADAR GROUND REFERENCE INFORMATION

Level 1	Level 2	Level 3	Level 4
1000 INFRASTRUCTURE	1100 URBAN 1200 ROAD 1300 RAIL 1400 EMBANKMENT 1500 CANAL		
2000 NON-FLOODED LAND	2100 FOREST (canopy > 30%)	2110 CLOSED (cp > 60%) 2120 OPEN (cp 30-60%)	
	2200 HOMESTEAD	2210 TREES (cp > 60%) 2220 MIXED	
	2300 BARE SOIL (With 0-10% vege canopy)	2310 DRY	2311 LOAM/CLAY 2312 SAND
		2320 MOIST	2321 LOAM/CLAY 2322 SAND
		2330 SATURATED	
		2340 PONDED (1-30 cm)	
	2400 PASTURE/GRASS (canopy 30-80%, short, grazed)		
	2500 CROPS (Dry Soil)	2510 CANOPY 0-30%	2511 PADDY 2512 JUTE 2513 SUGARCANE 2519 OTHERS
		2520 CANOPY 30-70%	2521 PADDY 2522 JUTE 2523 SUGARCANE 2529 OTHERS
		2530 CANOPY 70-100%	2531 PADDY 2532 JUTE 2533 SUGARCANE 2539 OTHERS
	2600 CROPS (Moist Soil)	2610 CANOPY 0-30%	2611 PADDY 2612 JUTE 2613 SUGARCANE 2619 OTHERS
		2620 CANOPY 30-70%	2621 PADDY 2622 JUTE 2623 SUGARCANE 2629 OTHERS

Level 1	Level 2	Level 3	Level 4
	3300 WITH VEGE. FLOOD DEPTH (> 90 cm)	3310 CANOPY 0-30%	3311 HYACINTH 3312 WEED GRASS MIXED 3319 OTHER
		3320 CANOPY 30-70%	3321 HYACINTH 3322 WEED GRASS MIXED 3329 OTHER
		3330 CANOPY 70-100%	3331 HYACINTH 3332 WEED GRASS MIXED 3339 OTHER
	3400 WITH VEGE. FLOOD DEPTH (1-30 cm)	3410 CANOPY 0-30%	3411 PADY 3412 JUTE 3413 SUGARCANE 3419 OTHER
		3420 CANOPY 30-70%	3421 PADY 3422 JUTE 3423 SUGARCANE 3429 OTHER
		3430 CANOPY 70-100%	3431 PADY 3432 JUTE 3433 SUGARCANE 3439 OTHER
	3500 WITH VEGE. FLOOD DEPTH (30-90 cm)	3510 CANOPY 0-30%	3511 PADY 3512 JUTE 3513 SUGARCANE 3519 OTHER
		3520 CANOPY 30-70%	3521 PADY 3522 JUTE 3523 SUGARCANE 3529 OTHER
			3530 CANOPY 70-100%
	3600 WITH VEGE. FLOOD DEPTH (> 90 cm)	3610 CANOPY 0-30%	3611 PADY 3612 JUTE 3613 SUGARCANE 3619 OTHER

Level 1	Level 2	Level 3	Level 4
		3620 CANOPY 30-70%	3621 PADY 3622 JUTE 3623 SUGARCANE 3629 OTHER
		3630 CANOPY 70-100%	3631 PADY 3632 JUTE 3633 SUGARCANE 3639 OTHER
	3700 FOREST		
4000 WATER (Permanent)	4100 RIVER/KHAL	4110 CLEAR	
		4120 TURBID	
	4200 BEEL	4210 VEGE CP < 30%	4211 HYACINTH 4212 WEED GRASS MIXED 4219 OTHER
		4220 VEGE CP 30-70%	4221 HYACINTH 4222 WEED GRASS MIXED 4229 OTHER
		4230 VEGE CP 70-100%	4231 HYACINTH 4232 WEED GRASS MIXED 4239 OTHER
	4300 PONDS	4310 VEGE CP 0-30%	4311 HYACINTH 4312 WEED GRASS MIXED 4319 OTHER
		4320 VEGE CP 30-70%	4321 HYACINTH 4322 WEED GRASS MIXED 4329 OTHER
		4330 VEGE CP 70-100%	4331 HYACINTH 4332 WEED GRASS MIXED 4339 OTHER

Level 1	Level 2	Level 3	Level 4
	4400 MARSH LAND	4410 VEGE CP 0-30%	4411 HYACINTH 4412 WEED GRASS MIXED 4419 OTHER
		4420 VEGE CP 30-70%	4421 HYACINTH 4422 WEED GRASS MIXED 4429 OTHER
		4330 VEGE CP 70-100%	4431 HYACINTH 4432 WEED GRASS MIXED 4439 OTHER

82